NTNU – Trondheim
Norwegian University of
Science and Technology

Spin-Motive Forces and Coulomb Interaction in a Ferromagnetic Wire

Sverre Aamodt Gulbrandsen

MSc in Physics
Submission date: May 2015
Supervisor: Arne Brataas, IFY

Norwegian University of Science and Technology
Department of Physics

Abstract

In metallic ferromagnets, external voltages induce charge and spin-polarized currents. Additionally, there can be magnetization dynamics, where the magnetic moments precess in time in response to external magnetic fields. The exchange interaction strongly couples the spin-polarized currents with the magnetization dynamics. In this way, external voltages can induce magnetization dynamics or, vice versa, external magnetic fields can induce currents.

In ferromagnets, the long-range dipole interaction leads to the formation of magnetic domains, regions of aligned magnetic moments. In between the magnetic domains, there are domain walls, where the magnetization gradually varies. Such domain walls move in response to external magnetic fields. Previous studies have shown that a moving domain wall in ferromagnets generates a spin-motive force on the conduction electrons. In turn, the spin-motive force generates currents. Experimentally, the spin-motive induced currents have been detected.

So far, research in this field has neglected the ubiquitous Coulomb interaction between the electrons. The central question we address is how Coulomb interaction between electrons affects the transport of the electrons subject to the spin-motive forces.

To study this question, we first reproduce the known results of spin-motive forces when the magnetic domain wall is of the Neel type. The moving domain wall generates a spin-polarized electric current. We discuss its Berry's phase origin. Beyond previous studies, we find that the Coulomb interaction between the electrons leads to the screening of the spin-motive induced accumulated charges. The screening takes within the Thomas-Fermi screening length, which is very short in high-density metals. While screening strongly modifies the accumulated charges in the ferromagnets, the domain wall motion induced currents remains unaffected due to current conservation.

Sammendrag

I ferromagnetiske metaller vil påtrykte spenninger indusere ladnings- og spinnpolariserte strømmer. I tillegg kan det oppstå magnetiseringsdynamikk, der magnetiske momenter preseserer i tid som en respons til eksterne magnetiske felt. Den magnetiske vekselvirkningen i ferromagneter kobler spinnpolariserte strømmer til magnetiseringsdynamikken. På dette viset kan eksterne spenninger indusere magnetiseringsdynamikk, mens det ved hjelp av den motsatte prosessen kan induseres eletriske strømmer fra magnetiseringsdynamikk.

I ferromagneter fører den magnetiske dipol-vekselvirkningen til at det dannes magnetiske domener, som er områder der de magnetiske momentene peker i en felles retning. Innimellom de magnetiske domenene er det domenevegger, der magnetiseringsretningen varierer gradvis fra retningen i et domene til retningen i det neste domenet. Slike domenevegger kan flytte på seg, som en respons til eksterne magnetiske felt. Tidligere forskning har vist at domenevegger som flytter på seg i ferromagneter genererer en spinnmotorisk kraft på ledningselektronene. Videre genererer den spinnmotoriske kraften en elektrisk strøm, og denne strømmen er blitt målt eksperimentelt.

Så langt har forskningen på dette feltet sett bort ifra Coulomb-vekselvirkningen mellom ledningselektronene. Hovedproblemet vi prøver å finne et svar på er hvordan Coulomb-vekselvirkningen endrer transporten av ledningselektroner som påvirkes av den spinnmotoriske kraften.

For å finne et svar på dette spørsmålet har vi først reprodusert de kjente ligningene for den spinnmotoriske kraften når domeneveggen er av Neel-type. Resultatet er at en domenevegg som beveger seg genererer en spinnpolarisert elektrisk strøm. Videre diskuterer vi hvordan den spinnmotoriske kraften er relatert til en kvantemekanisk Berry-fase.

Av ny kunnskap finner vi at Coulomb-vekselvirkningen mellom ledningselektronene fører til en skjerming av de akkumulerte ladningene, som er blitt indusert av den spinnmotoriske kraften. Denne skjermingen er effektiv på en lengdeskala tilsvarende Thomas-Fermis skjermingslengde, som er veldig kort i metaller med høy elektrontetthet. Selv om skjermingen modifiserer ladningsopphopningen i ferromagneter i stor grad, så påvirkes ikke den elektriske spinnpolariserte strømmen, generert fra magnetiseringsdynamikken, på grunn av strømbevarelse.

Ved å sammenligne typiske diffusjonstider med tiden domeneveggen bruker på å flytte seg, ser vi at vår antagelse om en dynamisk likevekt er anvendbar, spesielt for domenevegger som beveger seg sakte.

Preface

This master thesis concludes the work for the degree Master of Science in Physics at Norwegian University of Science and Technology, submitted in the spring of 2015. The work has been done under supervision and with guidance from professor Arne Brataas at the Department of Physics.

I would like to thank my supervisor professor Arne Brataas for all his help during this process. The meetings have been very valuable and encouraging, and I have learned something new every week. I am looking forward to working with Arne in the future.

The work in sections 3, 4 and 5.1 has been done in cooperation with Snorre Rist, who wrote his thesis in the spring of 2014. Our discussions were very helpful and enjoyable. The work done by Snorre in his thesis led to a crucial turning-point, where we found out that it was better to utilize the Boltzmann transport equation rather than using a mean-field perturbative approach.

Even though the results are not very spectacular, I have certainly learned a lot.

Contents

1 Introduction

Spintronics, or spin-electronics, is the physics of magnetoelectronics in systems where the electron spin plays a crucial role. Electrons are fermions with a spin magnetic moment, which affects the magnetization in materials. The improvement of nano-fabrication methods in the last decades have led to new physics, where the combination of spin, magnetization and other quantum-mechanical phenomena has interesting and useful effects.

In 1985 Johnson and Silsbee where the first to show how charge and spin couples in transport across the interface between a ferromagnet (FM) and a paramagnet [1]. Their work proposed a method to measure the spin-transport as an electric voltage.

An important experimental discovery was of the Giant Magnetoresistance (GMR), which the group of Fert et al. [2] and Grünberg et al. [3] measured independently in 1988 and 1989 respectively. The GMR-effect was first studied for currents in the plane (CIP) of multilayers of ferromagnetic and normal metallic materials. The measured resistance ranged between minimal and maximal values by changing the relative orientation between the magnetization directions in different layers, with external fields. This effect is a consequence of spin-dependent scattering at the interfaces. Fert and Grünberg received the Nobel Prize in 2007 for the discovery of the GMR [4], and GMR-based read heads have led to improved hard disk drives.

1.1 Spin-Transfer Torque

The spin-transfer torque (STT) is the torque on a magnetization due to the transfer of spin-angular momentum from a spin-current. The STT was proposed theoretically in 1996 by the independent work of Slonczewski [5] and Berger [6]. Their calculations indicated that a spin-polarized current perpendicular to the planes (CPP) of ferromagnet-normal-metal multilayers can reorient the magnetization in one of the ferromagnetic layers, if the current density is large. The group of Tsoi et al. measured in 1998 the current and voltage in Cu/Co-layers [7], and the resulting changes in resistance indicated current-driven magnetization excitations via the GMR-effect.

Consider a spin-polarized current entering a ferromagnet with uniform magnetization and a strong exchange interaction. When an electron enters the ferromagnet, its spin magnetic moment then aligns with the magnetization in the ferromagnet. The spin magnetic moment is thus changed for the outgoing electron compared to its initial magnetic moment. The change of angular momentum in the spin-current is transfered to the magnetization, which is described as a torque. The STT acts in the plane of the incident and outgoing electron moment-directions. From symmetry there is also a torque (called the field-like torque) in the plane perpendicular to the plane of the STT, as discussed in Ref. [8].

The physical explanation for the STT acting on a continuously varying magnetization is similar as in the case of uniformly magnetized ferromagnets. In an

adiabatic limit the electron magnetic moment continuously aligns itself with the magnetization as the electron moves inside the ferromagnet. The change of angular momentum from rotating the electron spin is transferred to the magnetization. The STT acting on a continuously varying magnetization is described theoretically in Ref. [9].

The current densities required to generate spin-transfer torques of any significance also generate competing torques from Oersted fields. By decreasing the system-size the STT can dominate over the Oersted field torques [10]. With better methods to construct nano-structures, Myers et al. created ferromagnetic-layered nanopillars (Co/Cu/Co) in 1999 [11], and they were able to fully reverse the magnetization direction in one of the layers by injecting a spin-polarized current.

Magnetic switching based on STT can be more efficient than magnetic switching with Oersted fields, which is used in information storage today. One important improvement is lower switching-currents and more dense devices. Thermal heating is minimized in small nano-structures, which also prevents information loss due to thermal oscillations. Non-volatile random access memory based on STT (STT-RAM) is currently under development by several companies [12].

1.2 Spin-Motive Force and Spin-Pumping

The reciprocal phenomenon of the STT is spin-pumping. Spin-pumping is the emission of a spin-current due to magnetization dynamics, and the theory behind this process was established by the work of Tserkovnyak et al. in Refs. [13] and [14]. On a fundamental level, the STT and spin-pumping are equivalent reciprocal processes, which is proved by Brataas et al. by using the Onsager reciprocity relations and assuming linear response [15].

The relationship between STT and spin-pumping was demonstrated in a groundbreaking experiment done by Kajiwara et al. in 2009 [16]. By using a magnetic insulator sandwiched between platinum films, they were able to transfer spin angular momentum over a macroscopic distance. The experiment is explained as follows. A spin-polarized current in the first metal-layer transfers angular momentum to the magnetic insulator via the spin Hall effect [17], i.e. a spin current flows in the direction perpendicular to the charge flow. These magnetization excitations travel across the insulator as a spin wave, and by the inverse Hall effect the angular momentum is transferred to the last metal-layer, inducing an electric current via spin-pumping.

The process of spin-pumping can be viewed as a consequence of spin-motive forces acting on conduction electrons, due to time-dependent dynamics of a magnetization. The spin-motive force was first described by Volovik in 1987 in terms of effective electric and magnetic fields [18], which tend to push on and/or bend the path of electrons with opposite spins in opposite directions. The work by Yang and Beach et al. shows that the spin-motive force is related to gauge-invariant Berry-curvature fields [19].

1.3 Motivation

The motivation for studying the spin-motive force is the interesting connection between the spin-transfer torque and spin-pumping. The combination of STT and spin-pumping can be used to connect electrical signals with pure spin-signals in new spintronics-devices. By understanding all these phenomena we pave the way for a new field of electronics, where information is transfered and stored via pure spin-currents, with no flow of electric charges.

While the spin-motive force is a relatively new concept, the additional contribution from the Coulomb interaction between conduction electrons is not well understood. We expect that the Coulomb interaction is important in ferromagnets with high electron density.

2 Basic Theory of Ferromagnetism

This section describes some useful concepts related to magnetism and how these ideas can be used to model the transport of electrons in a ferromagnetic metal wire. The inclusions of the electron spin and ferromagnetic exchange energy require a quantum mechanical treatment. Since it is difficult to make a full many-body quantum mechanical description, it will be necessary to use statistical physics and make some semi-classical assumptions. The physical aspects of these assumptions are discussed, together with the limitations they have for the model.

2.1 Magnetism and Magnetic Moment

The classical treatment of electromagnetism is described by Maxwell's equations and the Lorentz force law. The movement of charges, such as a current in a coil, induces a magnetic field, and one can define the magnetic field, $\vec{B}$, from the measured force exerted on a moving charge, subject to this field. This force, called the Lorentz Force, $\vec{F}_{\mathrm{L}}$, is defined (in SI-units) as

$$\vec{F}_{\mathrm{L}} = q\left(\vec{E} + \vec{v} \times \vec{B}\right), \tag{2.1}$$

where q is the charge of the particle, $\vec{E}$ is an electric field and $\vec{v}$ is the velocity [20].

If magnets are placed in a magnetic field, they are affected by a magnetic torque, $\vec{\tau}_{\mathrm{M}}$, which tends to align the magnets parallel with the applied magnetic field. This torque defines the magnetic moment, $\vec{\mu}$, from

$$\vec{\tau}_{\mathrm{M}} = \vec{\mu} \times \vec{B}, \tag{2.2}$$

where the magnetic moment is measured in units of J/T [21]. The magnetic potential energy associated with a magnetic moment in a magnetic field is

$$E_{\mathrm{M}} = -\vec{\mu} \cdot \vec{B}, \tag{2.3}$$

which has lowest value when $\vec{\mu}$ is parallel with $\vec{B}$ [22]. A classical example of a magnetic moment is a compass, where the compass needle has lowest energy when it is aligned with the magnetic field lines of the Earth.

2.1.1 Spin Magnetic Moment

Elementary particles also have a spin magnetic moment, which generates and interacts with magnetic fields. A measurement of the spin magnetic moment gives quantized values, in agreement with quantum mechanics. The spin magnetic moment of the electron, $\vec{\mu}_e$, is defined as

$$\vec{\mu}_e = -g_e \frac{e}{2m_e} \vec{S}, \tag{2.4}$$

where $g_e > 0$ is the g-factor, e is the elementary charge, m_e the mass of the electron and $\vec{S}$ the spin quantum operator [23]. Since the electron is a spin-1/2

particle, a measurement of $\vec{S}$ along some chosen quantization axis will give two distinct values, either $+\hbar/2$ or $-\hbar/2$, in terms of the reduced Planck constant, $\hbar = 6.58211928(15) \cdot 10^{-22}$ MeV s [24]. From Eq. (2.4) it is clear that the electron spin points in the opposite direction of its spin magnetic moment.

In the following, the g-factor is approximated by $g_e \approx 2$, which is the value obtained by solving the Dirac equation for free electrons. See Ref. [24] for corrections to this value, which can be computed from quantum electrodynamics. With $g_e = 2$ the electron spin magnetic moment is written in terms of the Bohr magneton, μ_{B}, such that

$$\vec{\mu}_e = -\mu_{\mathrm{B}}\vec{\sigma}, \tag{2.5}$$

where the Bohr magneton is defined as

$$\mu_{\mathrm{B}} = \frac{e\hbar}{2m_e}, \tag{2.6}$$

and $\vec{S} = (\hbar/2)\vec{\sigma}$. The operator $\vec{\sigma}$ is a two-by-two spin-matrix acting on two-dimensional spinors, and it satisfies the eigenvalue equation

$$\vec{\sigma} \cdot \hat{n}|\chi_\pm\rangle = \pm|\chi_\pm\rangle, \tag{2.7}$$

for some unit vector, $\hat{n}$, and eigenspinor $|\chi_\pm\rangle$. The sign $\pm$ corresponds to spin up and spin down respectively. Eq. (2.7) means physically that a measurement of $\vec{S}$ along the direction $\hat{n}$ gives the expectation value $\langle\chi_\pm|\vec{S} \cdot \hat{n}|\chi_\pm\rangle = \pm\frac{\hbar}{2}$.

The spin space for electrons is in the following represented by a unit matrix, $\hat{1}$, and the Pauli spin matrices, $\vec{\sigma} = \sigma_x\hat{x} + \sigma_y\hat{y} + \sigma_z\hat{z}$, defined as

$$\sigma_x = \begin{pmatrix} 0 & 1 \\ 1 & 0 \end{pmatrix}, \qquad \sigma_y = \begin{pmatrix} 0 & -i \\ i & 0 \end{pmatrix}, \qquad \sigma_z = \begin{pmatrix} 1 & 0 \\ 0 & -1 \end{pmatrix}, \tag{2.8}$$

and these four matrices create a basis which spans the whole spin space.

2.1.2 Magnetization and Ferromagnetic Exchange Energy

Magnetic materials are classified according to how they respond to an external magnetic field. An applied magnetic field affects the collection of magnetic moments in the material. The internal magnetization, $\vec{M}$, of a material consists of the sum of all these magnetic moments, where electrons, ions and molecules in the material can contribute to the internal magnetization. If the internal magnetization points in the opposite direction of the external magnetic field, the material is diamagnetic. If $\vec{M}$ points along the external magnetic field, the material is paramagnetic.

A ferromagnet is special since it can have a non-zero magnetization when there are no external magnetic fields. This is due to the exchange interaction between identical fermions, which is a consequence of the Pauli exclusion principle. The internal magnetization of a ferromagnet depends on the history of the applied external magnetic fields. The remaining magnetization when the external fields are turned

off is called the saturation magnetization, with symbol $\vec{M}_s$. Ferromagnetism occurs below a material-dependent critical temperature (Curie-temperature), which can be high, e.g. 1400 K for Co [25].

The Pauli exclusion principle states that two identical fermions can not occupy a state with the same location in space and the same spin [23]. For electrons localized to the lattice sites, the wavefunctions for neighboring electrons overlaps if the distance between ions are small enough. If two electrons at nearby lattice sites are in the same spin state, the spatial part of their wavefunctions is separated, due to the Pauli exclusion principle. This reduces the electrostatic energy between the electrons, such that parallel spins between neighboring localized electrons are energetically favored. This mechanism is called the ferromagnetic exchange interaction, and it is the main contribution to ferromagnetism.

2.1.3 Ferromagnetic Domains

If all the internal magnetic moments in a bulk ferromagnet points in the same direction, the total magnetization sets up a large magnetic field, which stores magnetostatic potential energy. To reduce the net magnetization, many ferromagnets are divided into domains with different magnetic orientations, where the magnetization is uniform within each domain. Between domains there are domain walls, where the magnetization direction rotates from one direction to another. The domain wall length, λ_w, is usually in the order of 10-100 nm [26]. Two types of domain walls are sketched in Fig. 1, i.e. Bloch and Neel-type domain walls.

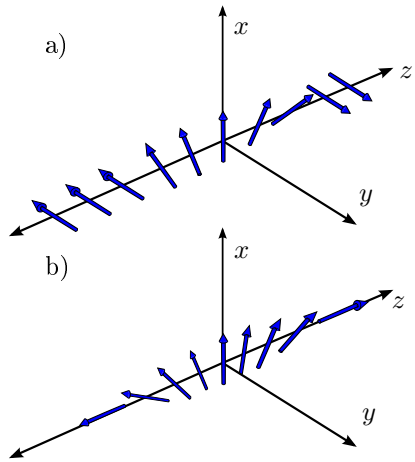

Figure 1: a) 180° Bloch-type domain wall. The local magnetization direction varies from $-\hat{y}$ (left domain) to $+\hat{y}$ (right domain) by rotating 180° around the $\hat{z}$-axis.
b) 180° Neel-type domain wall. The magnetization direction rotates 180° around the $\hat{y}$-axis from $-\hat{z}$ (left domain) to $+\hat{z}$ (right domain).

2.2 s-d-Model of the Ferromagnetic Domain Wall

In the *s-d*-model of a ferromagnetic metal domain wall the conduction electrons are treated as a free electron gas moving in the vicinity of a varying effective magnetization, $\vec{M}(\vec{r},t)$ [15]. The magnetization is assumed to be generated by the nearest neighbor exchange interaction of a large number of *d*-orbital electrons, which are localized to the lattice sites. It is also assumed that the magnetization vector has constant length, given by the saturation magnetization, such that $\vec{M}(\vec{r},t) = M_s\vec{m}(\vec{r},t)$, where $\vec{m}$ gives the direction of the internal magnetization and $|\vec{m}| = 1$.

In an adiabatic approximation, the spins of the conduction electrons follow the direction of the local magnetization, $\vec{m}$, as they move inside the ferromagnet, due to a high exchange energy. The magnetic potential energy for a conduction electron will therefore be approximated by the term $-\frac{1}{2}\Delta_{\text{ex}}\vec{\sigma}\cdot\vec{m}$. This is a mean-field approximation to the exchange energy, Δ_{ex}, which in other terms can be written as

$$\Delta_{\text{ex}} = \hbar J M_{\text{s}}, \tag{2.9}$$

where $J > 0$ is the angular momentum density [27].

The contribution to the magnetization from the free *s*-orbital conduction electrons are not taken into account, since the number of localized *d*-spins are much larger, and the total magnetic moment is close to $\vec{m}$ when conduction spins follow parallel or anti-parallel to the local magnetization. The Zeeman-splitting of electron energies, $\Delta E_{\text{Z}} \sim \mu_{\text{B}}B_0$, due to the applied external field, B_0, is ignored, because the exchange energy is assumed to be much larger than the Zeeman-splitting from a weak external field [28].

The conduction electrons are filled according to the Pauli principle, from the bottom of the spin-dependent conduction band energy, ε_s^0, up to the Fermi energy, ε_{F}. It is assumed a parabolic energy dispersion relation for the electrons, such that the one-electron total energy, $\varepsilon_{k,s}$, is

$$\varepsilon_{k,s} = \frac{\hbar^2k^2}{2m} + \varepsilon_s^0, \tag{2.10}$$

where the spin-dependent band offset, $\varepsilon_s^0 = \varepsilon_{\text{cb}} \mp (1/2)\Delta_{\text{ex}}$, consists of a constant conduction band energy, ε_{cb}, and a spin-dependent term, $\mp(1/2)\Delta_{\text{ex}}$, as a result of the magnetic potential energy due to the magnetic exchange field.

The convention used in the following is that spin up ($\uparrow$ or $+$) corresponds to the lowest magnetic potential energy:$-(1/2)\Delta_{\text{ex}}$, while spin down ($\downarrow$ or $-$) has the highest potential energy: $+(1/2)\Delta_{\text{ex}}$. Spin up is called majority spin, and spin down is called minority spin, since there will be a higher number of spin up conduction electrons when $\Delta_{\text{ex}} > 0$. The exchange energy can thus be written as

$$\Delta_{\text{ex}} = \varepsilon_-^0 - \varepsilon_+^0. \tag{2.11}$$

The dispersion relation and filling of conduction electrons is shown in Fig. 2.

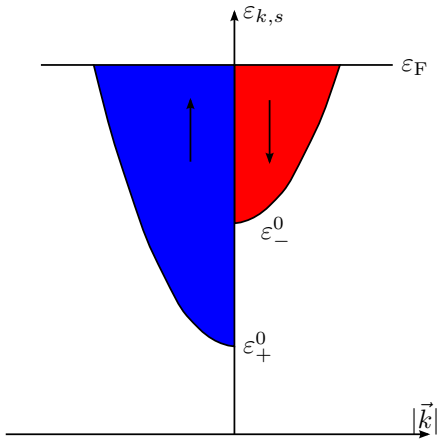

Figure 2: Total energy, $\varepsilon_{k,s}$, as a function of k for conduction electrons with a parabolic dispersion relation. Majority spin is represented by blue and drawn on the left side for comparison with minority spin in red. Electrons are filled from the lowest energy at the band offset up to the Fermi energy ε_{F}. Unequal band offsets, ε_s^0, for electrons of different spin species lead to a higher number of available states with spin up at the Fermi energy, in our convention.

2.2.1 Fermi-Dirac Distribution Function

To model the transport of a large number of particles, it is useful to incorporate statistical mechanics. The Fermi-Dirac distribution function, $f_{\mathrm{FD}}(\varepsilon_{k,s}-\mu_0)$, is the mean number of fermions in an energy-state with total energy, $\varepsilon_{k,s}$, and spin, s, for a system in thermodynamic equilibrium. The quantity μ_0 is the total chemical potential, which is an energy defined such that the total particle number density is calculated by summing the Fermi-Dirac distribution (FD-distribution) over all possible energy- and spin states.

The FD-distribution is defined [29] as

$$f_{\mathrm{FD}}(\varepsilon_{k,s}-\mu_0) = \frac{1}{e^{\beta(\varepsilon_{k,s}-\mu_0)}+1}, \tag{2.12}$$

where $\beta = 1/(k_{\mathrm{B}}T)$, with temperature, T, and the Boltzmann constant, $k_{\mathrm{B}} = 8.6173324(78)\cdot 10^{-5}\mathrm{eV\ K^{-1}}$ [24]. A temperature is only defined at points in equilibrium. At absolute zero temperature, $T = 0$ K, the total chemical potential is equal to the Fermi energy, i.e. $\mu_0(T=0) = \varepsilon_{\mathrm{F}}$.

The number of particles per volume for a system in equilibrium, n^0, is found by summing the FD-distribution over all possible states:

$$n^0 = \sum_s \sum_{\vec{k}} \frac{1}{e^{\beta(\varepsilon_{k,s}-\mu_0)}+1}, \tag{2.13}$$

such that a system with volume, $\mathcal{V}$, where all points are in equilibrium, has a total number of particles, N^0, given by $N^0 = \mathcal{V}n^0$.

In order to do the summation over momentum states, we assume that the $\vec{k}$-states lie so close to each other in momentum space, that they form a quasi-continuum. This approximation is appropriate for metals with a high number of conduction electrons. In this limit the summation is replaced by an integral, such that, in three dimensional space, $\sum_{\vec{k}} \to \int \frac{d^3k}{(2\pi)^3}$.

To avoid difficult integrals, all momentum-integrations of distribution functions and related quantities are done at zero temperature, $T = 0$. This is a good approximation for low-temperature electron transport in a metal, since the conduction electrons contributing to transport have an energy within $k_\mathrm{B}T$ of the Fermi energy, and metals are, from definition, such that at $T = 0$, only an infinitesimal energy is required to excite an electron from a populated state at ε_F to an unpopulated state.

At zero temperature, the FD-distribution can be written in terms of the Heaviside Theta function, $\Theta(k)$, such that the equilibrium number density of electrons with spin s is

$$\begin{aligned} n_s^0 &= \int \frac{d^3k}{(2\pi)^3} f_\mathrm{FD}(\varepsilon_{k,s} - \mu_0) = \int \frac{d^3k}{(2\pi)^3} \Theta(k)\Theta\left(\varepsilon_F - \varepsilon_s^0 - \frac{\hbar^2k^2}{2m}\right) \\ &= \frac{1}{(2\pi)^3} \int_0^{2\pi} d\phi \int_0^{\pi} \sin\theta d\theta \int_0^{k_{\mathrm{F}_s}} k^2 dk \\ &= \frac{1}{6\pi^2} k_{\mathrm{F}_s}^3, \end{aligned} \tag{2.14}$$

where the Fermi wave-vector, k_{F_s}, is defined from the Fermi energy and the band offset, such that

$$k_{\mathrm{F}_s} = \frac{1}{\hbar}\sqrt{2m\left(\varepsilon_\mathrm{F} - \varepsilon_s^0\right)}. \tag{2.15}$$

With the spin convention used in Eq. (2.11) then $k_{\mathrm{F}_+} > k_{\mathrm{F}_-}$, which also states that the Fermi velocity, v_{F_s}, is bigger for spin up electrons than for spin down electrons.

2.2.2 Density of States

The density of states (DOS), $d_s(\varepsilon)$, is the number of available particle states per volume at an energy infinitesimally close to ε. In three dimensions and a parabolic dispersion the DOS is proportional to the length of the electrons wave vector, $|\vec{k}| = k$.

An important quantity is the density of states at the Fermi energy, $d_s(\varepsilon_\mathrm{F})$. Some relevant results in the following is written in terms of the DOS at the Fermi energy, which makes it possible to compare the results with similar calculations for systems of other dimensions, e.g. 0-dimensional quantum dots, 1-dimensional quantum wires or 2-dimensional quantum wells.

In three dimensions and zero temperature the DOS at the Fermi energy is

$$\begin{aligned} d_s(\varepsilon_F) &= \int \frac{d^3k}{(2\pi)^3}\left(-\frac{f_{\mathrm{FD}}(\varepsilon_{k,s}-\mu_0)}{\partial\varepsilon_{k,s}}\right) \\ &= \frac{1}{(2\pi)^3}\int_0^{2\pi} d\phi \int_0^{\pi} \sin\theta d\theta \int_0^{\infty} k^2 dk \delta\left(\varepsilon_{\mathrm{F}} - \varepsilon_s^0 - \frac{\hbar^2k^2}{2m}\right) \\ &= \frac{1}{2\pi^2}\int_0^{\infty} k^2 dk \frac{m}{\hbar^2 k}\delta\left(k - k_{\mathrm{F}_s}\right) \\ &= \frac{2m}{(2\pi\hbar)^2} k_{\mathrm{F}_s}, \end{aligned} \tag{2.16}$$

where k_{F_s} is given by Eq. (2.15) for conduction electrons in a ferromagnet, and it was used that the derivative of the FD-distribution at $T = 0$ is (minus) a delta function.

Since $k_{\mathrm{F}_+} > k_{\mathrm{F}_-}$ then $d_+(\varepsilon_{\mathrm{F}}) > d_-(\varepsilon_{\mathrm{F}})$, which means that there is a higher number of available states with majority spin than minority spin, at the Fermi energy. This is important for creating spin-polarized currents.

3 Magnetization Dynamics

This section shows how to model the magnetization dynamics of a domain wall subject to a weak external magnetic field. The calculations are based on and similar to the methods and work done by Brataas et al. in Ref. [30], with the difference that we calculate the dynamics of a tail-to-tail Neel-type domain wall, which involves some modifications compared to the dynamics of the head-to-head configuration calculated in Ref. [30].

3.1 Landau-Lifshitz-Gilbert Equation

The magnetization dynamics is described by the Landau-Lifshitz-Gilbert (LLG) equation [31] which reads

$$\dot{\vec{m}} = \gamma\mu_0\vec{H}_{\text{eff}} \times \vec{m} + \alpha\vec{m} \times \dot{\vec{m}}, \tag{3.1}$$

and the resulting effects on the magnetization direction are shown in Fig. 3. Here the effective magnetic field, $\mu_0\vec{H}_{\text{eff}}(\vec{r}) = -\delta U/\delta\vec{M}(\vec{r})$, is dictated by the magnetic free energy, $U = U[\vec{M}(\vec{r})]$, which is a functional of the magnetization. The first term on the RHS of Eq. (3.1) leads to precession of the magnetization direction around the effective magnetic field. The gyromagnetic ratio is $\gamma = g_e\mu_{\text{B}}/\hbar$, where $g_e \approx 2$ is the g-factor and μ_{B} is the Bohr magneton in Eq. (2.6).

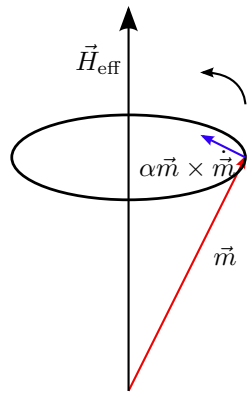

Figure 3: The magnetization direction, $\vec{m}$, precesses around the effective magnetic field, $\vec{H}_{\text{eff}}$. The damping term, $\alpha\vec{m} \times \dot{\vec{m}}$, is a torque which slowly moves the magnetization direction towards alignment with the effective magnetic field.

The second term on the RHS of Eq. (3.1) describes the damping of the system, which in general is written in terms of a tensor, $\alpha_{ij}[\vec{m}]$, with functional dependence on the magnetization. In many materials it is reasonable to assume that the damping is isotropic, local and independent of $\vec{m}$, such that α is a constant. It is also assumed a small damping, thus $\alpha \ll 1$, e.g. in permalloy $\alpha \approx 0.01$ [32].

An approximate approach to this problem is to introduce a set of collective coordinates, $\{\xi_i\}$, such that the magnetization direction is a functional $\vec{m}[\vec{r},t] = \vec{m}[\vec{r},\xi_1(t),...,\xi_n(t)]$. The assumption is that in the adiabatic approximation much of the magnetic structure is unchanged as time evolves, such that the ξ_i's describe the collective movement of the magnetization. In the limit where the number, n, of collective coordinates goes to infinity, the solution is exact. The time derivative of the magnetization is thus

$$\frac{d\vec{m}}{dt} = \frac{\partial \vec{m}}{\partial \xi_i}\dot{\xi}_i, \tag{3.2}$$

with implicit summation over i.

In terms of the collective coordinates, the equations of motion are derived in App. A.1 from the LLG Eq. (3.1), which are

$$F_i - \Gamma_{ij}\dot{\xi}_j + G_{ij}\dot{\xi}_j = 0, \tag{3.3}$$

where F_i is the generalized force, G_{ij} is an antisymmetric gyrotropic tensor and Γ_{ij} is a symmetric tensor, which contributes to damping. By integrating over the sample volume, these terms are given by

$$F_i = -\int dV \frac{\delta U}{\delta \vec{m}} \cdot \frac{\partial \vec{m}}{\partial \xi_i} = -\frac{\partial U}{\partial \xi_i}, \tag{3.4}$$

$$\Gamma_{ij} = \alpha J \int dV \frac{\partial \vec{m}}{\partial \xi_i} \cdot \frac{\partial \vec{m}}{\partial \xi_j}, \tag{3.5}$$

$$G_{ij} = J \int dV \vec{m} \cdot \left(\frac{\partial \vec{m}}{\partial \xi_i} \times \frac{\partial \vec{m}}{\partial \xi_j} \right), \tag{3.6}$$

with $J = M_\mathrm{s}/\gamma$ as the angular momentum density.

3.2 Tail-to-Tail Neel-Type Domain Wall in a Cylindrical Wire

Consider the special case of an infinite cylindrical wire aligned with the z-axis, subject to an external magnetic field, $\vec{B}_0 = B_0\hat{z}$. The magnetic free energy, U, associated with the magnetization dynamics is described by

$$U = M_\mathrm{s}\mathcal{A} \int dz \varphi(z), \tag{3.7}$$

where $\mathcal{A}$ is the cross section of the wire, and the integral is taken over the energy density, φ, along the z-axis [30].

The energy density is on the form

$$\varphi(z) = \frac{A_\mathrm{ex.s}}{2} \left| \frac{\partial \vec{m}}{\partial z} \right|^2 - B_0 m_z + \frac{K_1}{2}(1 - m_z^2) + \frac{K_2}{2} m_x^2, \tag{3.8}$$

where $A_\mathrm{ex.s}$ is the stiffness of the exchange energy and K_1 is a constant describing the anisotropy energy along the wire. The anisotropy in the transverse direction

of the wire is modeled by the term with the K_2 constant.

In the case of a Neel-type domain wall in a wire, one choice of collective coordinates is $\xi_1(t) = r_{\rm w}(t)$ which gives the middle position of the wall, the polar angle of the wall $\xi_2(t) = \phi_{\rm w}(t)$, and the width of the wall, $\xi_3(t) = \lambda_{\rm w}(t)$. The magnetization direction is in spherical coordinates $\vec{m}(z) = (\sin\theta_{\rm w}\cos\phi_{\rm w}, \sin\theta_{\rm w}\sin\phi_{\rm w}, \cos\theta_{\rm w})$.

It is shown in App. A.2 how to find the solution which minimizes the energy in Eq. (3.7) for a Neel-type domain wall with a tail-to-tail configuration. This type of domain wall is shown in Figs. 1 and 4. The solution is

$$\cos\theta_{\rm w} = \tanh\frac{z - r_{\rm w}}{\lambda_{\rm w}}, \tag{3.9}$$

or equivalently

$$\frac{1}{\sin\theta_{\rm w}} = \cosh\frac{z - r_{\rm w}}{\lambda_{\rm w}}, \tag{3.10}$$

where the constraints are that the magnetization points away from the domain wall at both endpoints. This solution satisfies the constraints since $m_z = \cos\theta_{\rm w}$ approaches ± 1 as z goes to $\pm$ infinity.

From the solution in Eq. (3.9), the free energy for the tail-to-tail Neel wall is integrated in App. A.3 with the result

$$U = M_{\rm s}\mathcal{A}\left(\frac{A_{\rm ex.s}}{\lambda_{\rm w}} + 2B_0 r_{\rm w} + K_1\lambda_{\rm w} + K_2\lambda_{\rm w}\cos^2\phi_{\rm w}\right). \tag{3.11}$$

The generalized forces F_i are now found from Eqs. (3.4) and (3.11), such that

$$F_r = -2M_{\rm s}\mathcal{A}B_0, \tag{3.12}$$

$$F_\phi = M_{\rm s}\mathcal{A}K_2\lambda_{\rm w}\sin 2\phi_{\rm w}, \tag{3.13}$$

$$F_\lambda = M_{\rm s}\mathcal{A}\left(\frac{A_{\rm ex.s}}{\lambda_{\rm w}^2} - K_1 - K_2\cos^2\phi_{\rm w}\right). \tag{3.14}$$

For the damping tensor, Γ_{ij}, in Eq. (3.5) the non-diagonal terms are all zero from Eq. (A.17), while the diagonal terms are

$$\Gamma_{rr} = \mathcal{A}\frac{M_{\rm s}}{\gamma}\frac{2\alpha}{\lambda_{\rm w}}, \tag{3.15}$$

$$\Gamma_{\phi\phi} = \mathcal{A}\frac{M_{\rm s}}{\gamma}2\alpha\lambda_{\rm w}, \tag{3.16}$$

$$\Gamma_{\lambda\lambda} = \mathcal{A}\frac{M_{\rm s}}{\gamma}\frac{\pi^2}{6\lambda_{\rm w}}. \tag{3.17}$$

The gyrotropic tensor, G_{ij}, in Eq. (3.6) is antisymmetric, so all the diagonal terms are zero: $G_{ii} = 0$. Also four of the off-diagonal terms are zero from Eqs. (A.14), (A.15) and (A.16), and thus the only non-zero terms are

$$G_{r\phi} = -G_{\phi r} = \frac{2M_{\rm s}\mathcal{A}}{\gamma}. \tag{3.18}$$

The equations of motion for the tail-to-tail Neel-type domain wall derived from Eq. (3.3) now read

$$2\alpha\lambda_{\mathrm{w}}\dot{\phi}_{\mathrm{w}} + 2\dot{r}_{\mathrm{w}} = \gamma K_2 \lambda_{\mathrm{w}} \sin 2\phi_{\mathrm{w}}, \tag{3.19}$$

$$\dot{\phi}_{\mathrm{w}} - \frac{\alpha}{\lambda_{\mathrm{w}}}\dot{r}_{\mathrm{w}} = \gamma B_0, \tag{3.20}$$

$$\frac{A_{\mathrm{ex.s}}}{\lambda_{\mathrm{w}}^2} - \frac{\pi^2}{6\gamma\lambda_{\mathrm{w}}}\dot{\lambda}_{\mathrm{w}} = K_1 + K_2 \cos^2\phi_{\mathrm{w}}, \tag{3.21}$$

in terms of the collective coordinates $r_{\mathrm{w}}, \phi_{\mathrm{w}}$ and λ_{w}.

3.2.1 Walker Domain

If the magnetization evolves adiabatically and the applied fields are small, the length and shape of the domain wall is assumed to be constant, as discussed in Ref. [30]. The Walker domain is defined when

$$|B_0| < \frac{K_2\alpha}{2}, \tag{3.22}$$

which gives simple and stable solutions for the collective coordinates. In this case $\dot{\phi}_{\mathrm{w}}$ and $\dot{\lambda}_{\mathrm{w}}$ are zero, such that ϕ_{w} and λ_{w} are constants. The whole domain wall then moves with a velocity

$$\dot{r}_{\mathrm{w}} = -\frac{B_0\gamma\lambda_{\mathrm{w}}}{\alpha}, \tag{3.23}$$

where the direction of movement is opposite of the direction of the external field.

Under the Walker threshold the shape of the wall is given by

$$\phi_{\mathrm{w}} = \frac{1}{2}\arcsin\left(\frac{2B_0}{K_2\alpha}\right), \tag{3.24}$$

and

$$\lambda_{\mathrm{w}} = \sqrt{\frac{A_{\mathrm{ex.s}}}{K_1 + K_2\cos^2\phi_{\mathrm{w}}}}, \tag{3.25}$$

such that the anisotropy in the transverse direction pins the angle ϕ_{w} to a constant value.

3.2.2 Vanishing Transverse Anisotropy

For a cylindrical wire without any anisotropy in the transverse direction, i.e. $K_2 = 0$, the equations of motion simplify to

$$\dot{r}_{\mathrm{w}} = -\frac{B_0\alpha\gamma}{1+\alpha^2}\lambda_{\mathrm{w}}, \tag{3.26}$$

$$\dot{\phi}_{\mathrm{w}} = \frac{\gamma}{1+\alpha^2}B_0, \tag{3.27}$$

and

$$\lambda_{\mathrm{w}} = \sqrt{\frac{A_{\mathrm{ex.s}}}{K_1}}. \tag{3.28}$$

In this case the Neel-type domain wall is both rotating around the $\hat{z}$-axis with a constant angular velocity, $\omega_{\mathrm{w}} = \dot{\phi}_{\mathrm{w}}$ from Eq. (3.27), and moving in the $\pm\hat{z}$-direction with a constant velocity, $\dot{r}_{\mathrm{w}}$. This is shown in Fig. 4.

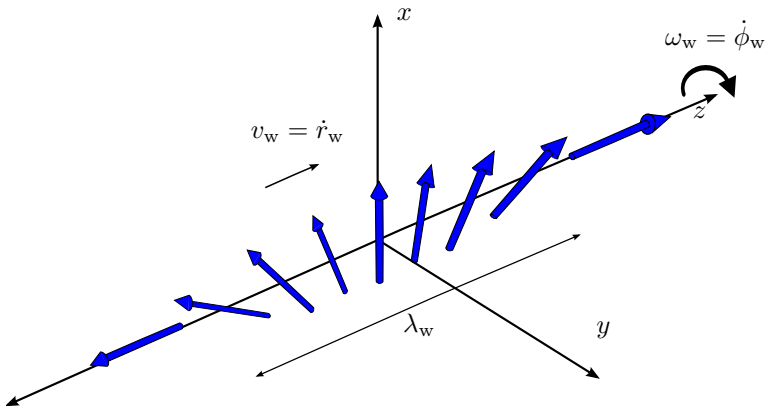

Figure 4: The Neel-type domain wall moves with a velocity $\dot{r}_{\mathrm{w}}$ along the wire, in the opposite direction of the applied external magnetic field. With no transverse anisotropy the domain wall rotates around the $\hat{z}$-axis with a constant angular velocity $\dot{\phi}_{\mathrm{w}} = \gamma B_0$.

This type of domain wall, in a thin wire with no transverse anisotropy, is used in the calculation for electron transport in section 7.

4 Spin-Motive Force

The spin-motive force on conduction electrons in a ferromagnet is found by rederiving the calculations by Tserkovnyak and Mecklenburg in Ref. [27]. In this section the units for the particle charge and the speed of light is set to unity, i.e. $(-e) = 1$ and $c = 1$. The main results are in the end expressed in terms of SI-units.

4.1 SU(2) Gauge Transformation and Effective Fields

The presence of inhomogeneous and time-dependent magnetic fields affects the motion of the conduction electrons in ferromagnets. This phenomenon induces spin-dependent transport of electrons. Electrons with opposite spins experience different spin-motive forces, which can be described through effective electric and magnetic fields.

The motion of conduction electrons in a metal ferromagnet is modeled by the Hamiltonian

$$H(t) = \hat{1}\left(\frac{p^2}{2m_e} + V(\vec{r},t)\right) - \frac{\Delta_{\text{ex}}}{2}\vec{\sigma}\cdot\vec{m}(\vec{r},t), \tag{4.1}$$

where $\vec{p} = -i\hbar\nabla$ is the momentum operator and Δ_{ex} is the strength of the ferromagnetic exchange band splitting [27]. The conduction electron mass is m_e, the matrix $\hat{1}$ is the unit matrix and the vector $\vec{\sigma}$ is given from Eq. (2.8). The unit vector $\vec{m}$ follows the local magnetization, $\vec{M} = M_{\text{s}}\vec{m}$, which is assumed to have constant length M_{s}. The scalar potential $V(\vec{r},t)$ is independent of spin, but depends on the structure of the crystal lattice.

The Hamiltonian in Eq. (4.1) defines the time-dependent Schrödinger equation

$$H(t)\Psi = i\hbar\frac{\partial}{\partial t}\Psi, \tag{4.2}$$

where Ψ is a two dimensional spinor. We now perform an SU(2) gauge transformation on Eq. (4.2), such that $\vec{m}$ points in the $\hat{z}$-direction at all times and at every point in space. This is done by introducing the two-by-two spin-rotation matrix, $\hat{U}$, which satisfies

$$\hat{U}(\vec{\sigma}\cdot\vec{m})\hat{U} = \sigma_z, \tag{4.3}$$

such that the quantization axis is $+\hat{z}$ in the transformed frame.

The SU(2) gauge transformation gives a Schrödinger equation for the transformed eigenspinor $\Phi = \hat{U}\Psi$, i.e. $H_{\text{eff}}\Phi = i\hbar\frac{\partial}{\partial t}\Phi$, with an effective Hamiltonian

$$H_{\text{eff}}(t) = \frac{1}{2m}\left(\vec{p} - \vec{A}\right)^2 + V(\vec{r},t) + \hat{V} - \frac{\Delta_{\text{ex}}}{2}\sigma_z, \tag{4.4}$$

which introduces the effective gauge potentials $\vec{A}$ and $\hat{V}$.

The matrix $\hat{U}$ is later shown to be both hermitian and unitary, i.e. $\hat{U} = \hat{U}^\dagger = \hat{U}^{-1}$,

where † means hermitian conjugation (matrix transpose and complex conjugation). With $\Psi = \hat{U}\Phi$ the gauge transformation follows from

$$H\Psi = i\hbar\frac{\partial}{\partial t}\left(\hat{U}\Phi\right) = i\hbar\frac{\partial\hat{U}}{\partial t}\Phi + i\hbar\hat{U}\frac{\partial}{\partial t}\Phi, \tag{4.5}$$

which by multiplying Eq. (4.5) with $\hat{U}$ from the left and using that $\hat{U}\hat{U} = \hat{1}$ then

$$i\hbar\frac{\partial}{\partial t}\Phi = \left(\hat{U}\frac{p^2}{2m}\hat{U} + V(\vec{r},t) - \frac{\Delta_{\text{ex}}}{2}\hat{U}(\vec{\sigma}\cdot\vec{m})\hat{U} - i\hbar\hat{U}\frac{\partial\hat{U}}{\partial t}\right)\Phi. \tag{4.6}$$

Eq. (4.6) is just the Scrödinger equation for the transformed Hamiltonian, $H_{\text{eff}}(t)$, with its corresponding eigenspinor Φ. The matrix $\hat{U}$ is calculated in App. B.1.

The effective gauge potentials are found by comparing Eqs. (4.4) and (4.6), and using the matrix $\hat{U}$ defined in Eq. (4.3). The calculation is done in App. B.2, and the solutions for the gauge potentials are

$$\hat{V} = -i\hbar\hat{U}\frac{\partial\hat{U}}{\partial t}, \tag{4.7}$$

and for each component $i = 1,2,3 \leftrightarrow x,y,z$, then

$$A_i = i\hbar\hat{U}\frac{\partial\hat{U}}{\partial x_i}. \tag{4.8}$$

The local magnetization is parametrized by the spherical angles $\theta = \theta(\vec{r},t)$ and $\phi = \phi(\vec{r},t)$ such that

$$\vec{m} = \hat{x}\sin\theta\cos\phi + \hat{y}\sin\theta\sin\phi + \hat{z}\cos\theta, \tag{4.9}$$

which is of unit length. It is shown in App. B.1 that $\hat{U}$ can be written in terms of another unit matrix

$$\vec{n} = \frac{\vec{m}+\hat{z}}{|\vec{m}+\hat{z}|} = \hat{x}\sin\frac{\theta}{2}\cos\phi + \hat{y}\sin\frac{\theta}{2}\sin\phi + \hat{z}\cos\frac{\theta}{2}, \tag{4.10}$$

such that $\hat{U} = \vec{\sigma}\cdot\vec{n}$.

In the following we make an approximation by assuming that the exchange field Δ_{ex} is so strong that we only need to consider the projection of the potentials $\vec{A}$ and $\hat{V}$ on the $\hat{z}$-axis. This means that $\vec{\sigma} \to \sigma_z\hat{z}$ in the expressions for the potentials. This projection corresponds to the adiabatic approximation, where it is assumed that the conduction electron moments follow parallel or anti-parallel to the local magnetization at all times, such that, in the transformed frame, the moments always point along the $\hat{z}$-axis.

The projected potentials are now expressed in spherical coordinates as

$$\begin{aligned}\hat{V} = -i\hbar\hat{U}\frac{\partial\hat{U}}{\partial t} &= \hbar\vec{\sigma}\cdot\left(\vec{n}\times\frac{\partial\vec{n}}{\partial t}\right)\\ \to \hbar\sigma_z\hat{z}\cdot\left(\vec{n}\times\frac{\partial\vec{n}}{\partial t}\right) &= \hbar\sigma_z\sin^2\frac{\theta}{2}\left(\frac{\partial\phi}{\partial t}\right),\end{aligned} \tag{4.11}$$

and

$$A_i = i\hbar\hat{U}\frac{\partial \hat{U}}{\partial x_i} = -\hbar\vec{\sigma}\cdot\left(\vec{n}\times\frac{\partial\vec{n}}{\partial x_i}\right)$$
$$\rightarrow -\hbar\sigma_z\hat{z}\cdot\left(\vec{n}\times\frac{\partial\vec{n}}{\partial x_i}\right) = -\hbar\sigma_z\sin^2\frac{\theta}{2}\left(\frac{\partial\phi}{\partial x_i}\right). \tag{4.12}$$

Now the effective electric and magnetic fields are found from

$$\vec{E} = -\frac{\partial}{\partial t}\vec{A} - \nabla\hat{V}, \tag{4.13}$$

and

$$\vec{B} = \nabla\times\vec{A}, \tag{4.14}$$

by using the projected potentials in Eqs. (4.11) and (4.12).

The effective electric field is then written in SI-units as

$$\vec{E} = \frac{\hbar}{2(-e)}\sigma_z\sin\theta\left(\frac{\partial\theta}{\partial t}(\nabla\phi) - (\nabla\theta)\frac{\partial\phi}{\partial t}\right), \tag{4.15}$$

while the magnetic field reads

$$\vec{B} = \frac{\hbar}{2(-e)}\sigma_z\sin\theta(\nabla\phi)\times(\nabla\theta). \tag{4.16}$$

With $\sigma_z|\chi_\pm\rangle = \pm|\chi_\pm\rangle$ for spin up and spin down respectively, the spin-motive force is

$$\vec{F}_s = -e\left(\vec{E}_s + \vec{v}\times\vec{B}_s\right), \tag{4.17}$$

with $\vec{E}_s$ and $\vec{B}_s$ from Eqs. (4.15) and (4.16), where the sign for spin $s = \pm$ corresponds to $\pm$ from σ_z in the expressions for the effective fields.

The effective electric field, $\vec{E}_s$, drives electrons with opposite spins in opposite directions. The effective magnetic field, $\vec{B}_s$, acts perpendicular to the propagation direction of an electron, with opposite directions for opposite spins. This is shown in Fig. 5.

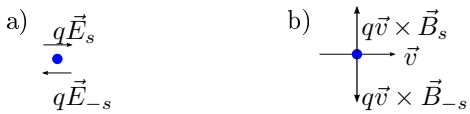

Figure 5: a) The effective electric field, $\vec{E}_s$, exerts a force on a charge, q, which acts in opposite directions for opposite spin-species.
b) The effective magnetic field acts on a charge with velocity, $\vec{v}$, with a force $q\vec{v}\times\vec{B}_s$, and this force bends the path of the charge in opposite directions for opposite spin-directions.

It is further possible to write the effective fields in terms of $\vec{m}$ and its derivatives.

From calculations in App. B.2 the components of the effective electric field in Eq. (4.15) is expressed as

$$E_i = \frac{\hbar}{2(-e)}\sigma_z \vec{m} \cdot \left(\left(\frac{\partial \vec{m}}{\partial t} \right) \times \left(\frac{\partial \vec{m}}{\partial x_i} \right) \right). \tag{4.18}$$

In Ref. [27] Tserkovnyak and Mecklenburg proposes another contribution to the spin-motive force, which from symmetry arguments can be expressed as a term $\sim \beta \vec{m} \times \vec{E} \sim \beta \dot{\vec{m}} \cdot \nabla \vec{m}$, by introducing the phenomenological parameter β. This term is often referred to as non-adiabatic in the literature, but this can be misleading, since both contributions to the spin-motive force are first order in the gradient of the magnetization. In Ref. [27] they argue that the β-correction comes from a small disalignment between electron spins and the local magnetization. However, the β-correction can be non-zero even when spins are aligned with the local magnetization, if there is a strong spin-orbit coupling [15]. Since we assume a strong exchange interaction and no spin-orbit coupling, we neglect the β-correction in the following.

4.1.1 Neel-Type Domain Wall with No Transverse Anisotropy

For the 180° domain wall of Neel-type with tail-to-tail configuration, subject to an external magnetic field, the solution for the magnetization was expressed in spherical coordinates, $\theta(z,t)$ and $\phi(z,t)$. The spin-motive force generated from the dynamics of this magnetization is found by using the angle $\theta(z,t)$ from Eq. (3.9) and the solution for $\dot{\phi} = \gamma B_0$ from Eq. (3.27), when $\alpha \ll 1$.

By using these solutions and Eqs. (4.15) and (4.16) the spin-motive force generated by the moving Neel-type domain wall is

$$\begin{aligned} \vec{F}_s(z,t) &\equiv F_s(z,t)\hat{z} \\ &= \pm \hat{z} \frac{\hbar}{2\lambda_\mathrm{w}} \gamma B_0 \frac{1}{\cosh^2\left(\frac{z - r_\mathrm{w}(t)}{\lambda_\mathrm{w}}\right)}, \end{aligned} \tag{4.19}$$

since $\vec{B}_s$ is zero. The plus sign corresponds to spin up, while minus corresponds to spin down.

The spin-motive force in Eq. (4.19) is the force of interest for the spin-dependent transport in section 7.

5 Geometric Berry Phase

In section 5.1 the theory of the adiabatic approximation in quantum mechanics is reviewed, and this part is based on Ref. [23]. Section 5.2 shows how the spin-motive force generated by a rotating domain wall of the Neel-type is explained in terms of Berry's phase and a modified Faraday's law. These calculations are a rederivation of the work by Barnes and Maekawa in Ref. [33].

5.1 Adiabatic Approximation in Quantum Mechanics

Suppose a quantum system is at time $t = t_0$ prepared in an eigenstate, $|\psi_n(t_0)\rangle$, and is subject to a time dependent Hamilton-operator, $H = H(t)$. The system evolves adiabatically if it gradually evolves from its initial n'th eigenstate to the corresponding n'th eigenstate of the final hamiltonian, $H(t = t_f)$. We now show how this is formulated in the adiabatic approximation.

Consider a general quantum system described by the state vector $|\psi(t)\rangle$ and a hermitian Hamilton-operator H. The evolution of the system is found by solving the Schrödinger equation

$$i\hbar\frac{\partial}{\partial t}|\psi(t)\rangle = H(t)|\psi(t)\rangle, \tag{5.1}$$

where the state $|\psi(t)\rangle$ is expanded in an orthonormal basis of stationary states $\{|\psi_n(t)\rangle\}$, that obey the time-independent Scrödinger equation

$$H(t)|\psi_n(t)\rangle = E_n(t)|\psi_n(t)\rangle. \tag{5.2}$$

A general solution of the state vector in Eq. (5.1) is

$$|\psi(t)\rangle = \sum_n c_n(t)e^{-\frac{i}{\hbar}\int_0^t E_n(t')dt'}|\psi_n(t)\rangle \equiv \sum_n c_n(t)e^{-i\epsilon_n(t)}|\psi_n(t)\rangle, \tag{5.3}$$

where c_n are the probability amplitudes and the dynamical phase factor is defined $\epsilon_n(t) = \frac{1}{\hbar}\int_0^t E_n(t')dt'$. The dynamical phase factor is real, since the eigen-energies, E_n, are real.

The probabilities, $|c_n(t)|^2$, of finding the system in an eigenstate $|\psi_n(t)\rangle$ are time-dependent. The time evolution of the amplitudes, $c_n(t)$, is found by inserting the solution from Eq. (5.3) into Eq. (5.1). The details are shown in App. C.1. With the help of Eq. (5.2) and by projecting everything onto an arbitrary bra-vector $\langle\psi_m(t)|$ from the left, the final result is

$$\frac{\partial}{\partial t}c_m(t) = -\sum_n c_n(t)e^{-i(\epsilon_n(t)-\epsilon_m(t))}\langle\psi_m(t)|\frac{\partial}{\partial t}\psi_n(t)\rangle, \tag{5.4}$$

and the notation is such that the time derivative only acts on the ket-vector.

An expression for $\langle\psi_m(t)|\frac{\partial}{\partial t}\psi_n(t)\rangle \equiv \langle\psi_m|\frac{\partial\psi_n}{\partial t}\rangle$ is found by taking the time-derivative of Eq. (5.2) and then multiplying with a bra vector $\langle\psi_m(t)|$ from the left. Thus, when $n \neq m$,

$$\langle\psi_m(t)|\frac{\partial\psi_n}{\partial t}\rangle \cdot (E_n(t) - E_m(t)) = \langle\psi_m(t)|\frac{\partial H}{\partial t}|\psi_n(t)\rangle. \tag{5.5}$$

The full equation of motion for the probability amplitudes now becomes

$$\begin{aligned}\frac{\partial}{\partial t}c_m(t) = &- c_m(t)\langle\psi_m(t)|\frac{\partial\psi_m}{\partial t}\rangle \\ &- \sum_{n\neq m} c_n(t)\frac{\langle\psi_m(t)|\frac{\partial H}{\partial t}|\psi_n(t)\rangle}{(E_n(t) - E_m(t))}e^{-i(\epsilon_n(t)-\epsilon_m(t))},\end{aligned} \tag{5.6}$$

where it is assumed a discrete energyspectrum, $\{E_n(t)\}$. The energies should also be non-degenerate, such that the second term in Eq. (5.6) does not blow up.

The adiabatic approximation is implemented by assuming that the Hamiltonian changes sufficiently slowly as compared to the difference in energy levels, such that the second term in Eq. (5.6) can be neglected. The time evolution of the probability amplitudes is then in the adiabatic approximation determined by

$$\frac{\partial}{\partial t}c_n(t) = -c_n(t)\langle\psi_n(t)|\frac{\partial\psi_n}{\partial t}\rangle, \tag{5.7}$$

with the solution

$$c_n(t) = c_n(t_0)e^{-\int_{t_0}^{t}\langle\psi_n(t')|\frac{\partial}{\partial t'}\psi_n(t')\rangle dt'} \equiv c_n(t_0)e^{i\gamma_n(t)}. \tag{5.8}$$

In Eq. (5.8), t_0 is the initial time, and $c_n(t_0)$ is a probability amplitude where $|c_n(t_0)|^2$ is the probability of the system being in the initial eigenstate $|\psi_n(t_0)\rangle$.

We now define the geometric phase

$$\gamma_n(t) = i\int_{t_0}^{t}\langle\psi_n(t')|\frac{\partial\psi_n(t')}{\partial t'}\rangle dt', \tag{5.9}$$

which is always a real quantity. This is shown by taking the time derivative of the orthonormality condition, $\langle\psi_n(t)|\psi_n(t)\rangle = 1$ which gives

$$0 = \langle\psi_n(t)|\frac{\partial}{\partial t}\psi_n(t)\rangle + (\langle\psi_n(t)|\frac{\partial}{\partial t}\psi_n(t)\rangle)^{\dagger}. \tag{5.10}$$

Eq. (5.10) shows that there is no real part for the innerproduct, thus i times this makes $\gamma_n(t)$ a real quantity.

Suppose a system is prepared in an initial eigenstate, $|\psi_n(t_0)\rangle$, then an adiabatic time evolution of this state is written on the form

$$|\psi(t)\rangle = e^{i\gamma_n(t)}e^{-i\epsilon_n(t)}|\psi_n(t)\rangle, \tag{5.11}$$

by using Eqs. (5.3) and (5.8), with $c_n(t_0) = 1$, since the system is prepared. From Eq. (5.11) it is clear that the evolving state acquires two phase factors with absolute value of unity, since both $\gamma_n(t)$ and $\epsilon_n(t)$ are real.

5.1.1 Berry's Phase

To obtain the Berry Phase, the adiabatic approximation for a quantum mechanical system is used. The validity of this approximation is discussed further in Ref. [34]. We will simply assume that our system's Hamiltonian, $H = H(\vec{R})$, varies smoothly and slowly, compared to the time scales of the system. Here the Hamiltonian is parametrized through a set of time-dependent parameters, $\{R_i(t)\}$, which is put into a vector, $\vec{R} = (R_1(t), ..., R_n(t))$. These n parameters can be coordinates, angles or other quantities that describe the system.

The time dependence of the Hamiltonian is contained in the parameters, and the geometric phase in Eq. (5.9) is rewritten by the change of variables

$$\gamma_n(t) = i\int_{t_0}^{t} \langle\psi_n(t')|\frac{\partial}{\partial t'}\psi_n(t')\rangle dt' = i\int_{\vec{R}(t_0)}^{\vec{R}(t)} d\vec{R}' \cdot \langle\psi_n(R')|\nabla_{\vec{R}'}\psi_n(R')\rangle. \quad (5.12)$$

From Eq. (5.12) the Berry connection is defined as

$$\vec{\mathcal{A}}_n(\vec{R}) = i\langle\psi_n(R)|\nabla_{\vec{R}}\psi_n(R)\rangle. \quad (5.13)$$

The Berry connection in Eq. (5.13) is in general gauge dependent, since changing $|\psi_n(R)\rangle \to e^{f(R)}|\psi_n(R)\rangle$, where $f(R(t))$ is a function of the parameters, then changes the connection $\vec{\mathcal{A}}_n(\vec{R}) \to \vec{\mathcal{A}}_n(\vec{R}) + i\nabla_{\vec{R}}f(R)$. From this it follows that also the geometric phase depends on the gauge choice. It will be shown that when the line integral in Eq. (5.12) is closed, the geometric phase is gauge independent.

If it is assumed that the parameters at some later time, T, are the same as the initial time, that is $\vec{R}(0) = \vec{R}(t = T)$, the parameters form a closed curve in parameter space. By performing the geometric phase integral in Eq. (5.12) over such a closed curve, the aquired phase is called the Berry phase and is written

$$\gamma_n^{\mathcal{C}}(N) = i\int_{\vec{R}(0)}^{\vec{R}(t=T)} d\vec{R}' \cdot \langle\psi_n(R')|\nabla_{\vec{R}'}\psi_n(R')\rangle \equiv \oint_{\mathcal{C}} d\vec{R} \cdot \vec{\mathcal{A}}_n(\vec{R}), \quad (5.14)$$

where N is the winding number, i.e. an integer numbering how many rounds around itself the curve in parameter space is integrated over. Later it is shown explicitly that the Berry phase for a rotating domain wall in a wire is not dependent on the phase $e^{if(R)}$ of the eigenstates $|\psi_n(R)\rangle$.

5.2 Faraday's Law for the Rotating Domain Wall

We now return to the case of a tail-to-tail Neel-type domain wall in a cylindrical wire with no transverse anisotropy, $K_2 = 0$. A static external magnetic field along the wire, $\vec{B}_0 = B_0\hat{z}$, gives rise to a steady rotation of the domain wall around the z-axis, with an angular velocity $\omega_{\mathrm{w}} = \frac{d}{dt}\phi_{\mathrm{w}} = 2\mu_{\mathrm{B}}B_0/\hbar$, from Eq. (3.27) and by using $(1+\alpha^2)^{-1} \approx 1$ when $\alpha \ll 1$. This situation corresponds to the one in Fig. 4.

The Hamiltonian for conduction electrons in a ferromagnetic Neel-type domain wall with an applied field is similar to the Hamiltonian in Eq. (4.1), by using that $JM_s\hbar = \Delta_{ex}$. The last term in Eq. (5.15) is due to the energy splitting from the B_0-field. Since we follow the calculations done by Barnes and Maekawa in Ref. [33], the sign in front of $JM_s\vec{S}\cdot\vec{m}$ is changed, which is just a redefinition of which directions correspond to spin up and spin down. In the end the resulting force from this approach is compared with the spin-motive force calculated in section 4.

The solution of the Schrödinger equation can be expanded in eigenfunctions ψ_n of H, and the Hamiltonian for the rotating Neel wall reads [33]

$$H = \frac{p^2}{2m} + V(\vec{r}) + JM_s\frac{\hbar}{2}\vec{\sigma}\cdot\vec{m} + \frac{2\mu_B B_0}{\hbar}s_z. \tag{5.15}$$

The physics is easier to capture by choosing a frame where the quantization axis is parallel to the magnetization, $\vec{m}$. In the rotated frame, $\psi' = u_\theta u_\phi \psi$ is first rotated around the z-axis by $u_\phi = e^{is_z\phi/\hbar} = \cos\frac{\phi}{2} + i\sigma_z \sin\frac{\phi}{2}$, such that it follows the angular rotation of the wall. Then a rotation around the y-axis by $u_\theta = e^{is'_y\theta/\hbar} = \cos\frac{\theta}{2} + i\sigma'_y \sin\frac{\theta}{2}$, makes the rotated frame follow the magnetization along the length of the wall.

In App C.2. it is shown how to write

$$i\hbar\frac{\partial}{\partial t}|\psi'\rangle = H'|\psi'\rangle, \tag{5.16}$$

where $|\psi'\rangle = \sum_{n,\pm} c_{n\pm}|\psi'_{n\pm}\rangle$, and $|\psi'_{n\pm}\rangle = |\chi'_\pm(\theta,\phi)\rangle\otimes|n\rangle$. With the quantization axis along z' in the rotated frame, the spinors in the transformed frame are

$$|\chi'_+(\theta,\phi)\rangle = \begin{pmatrix}1\\0\end{pmatrix}, \tag{5.17}$$

$$|\chi'_-(\theta,\phi)\rangle = \begin{pmatrix}0\\1\end{pmatrix}. \tag{5.18}$$

By using that ϕ only varies around the z-axis and inserting $\psi' = u_\theta u_\phi \psi$ into $H\psi = i\hbar\partial\psi/\partial t$, the primed Hamiltonian is calculated in App. C.2.2, such that

$$H' = \frac{(\vec{p} - \frac{\hbar}{2}\vec{A}_t)^2}{2m} + V(\vec{r}) + JM_s s'_z, \tag{5.19}$$

with s'_z acting on a spinor in the rotated frame.

Due to the spatial derivatives there is a transverse field, $\vec{A}_t = (2/\hbar)s'_y\frac{\partial\theta}{\partial z}\hat{z}$, in the rotated frame. In the following we assume that $(\hbar/2m)\vec{p}\cdot\vec{A}_t$ is small compared to $\hbar JM$, and $\vec{A}_t$ is replaced with zero. In Ref. [33] Barnes and Maekawa argued that the transverse field $\vec{A}_t$ gives rise to a small correction to the wall position, and that this correction leads to the spin-motive force, via arguments of energy conservation. This is a false statement, which is further explained by Nakabayashi

and Tatara in Ref. [35], and they conclude that Faraday's law is only a consequence of a U(1) gauge symmetry.

With $\vec{A}_t = 0$ in Eq. (5.19) the stationary solutions to $H'\psi'_{n\pm}$ are

$$E_n^{\pm} = E_n^0 \pm \frac{\hbar}{2} J M_{\rm s}, \tag{5.20}$$

since the eigenvalues for spin up/down is $s'_z = \pm\hbar/2$ (the opposite energies in our convention). This corresponds to an energy difference $\hbar J M_{\rm s} = \Delta_{\rm ex}$ between electrons with different spins.

The idea now is to look at Faraday's law for the electromotive force (emf) for the electrons in the wire, where also a spin-dependent nonconservative force is included. In general, Faraday's law relates the emf, $\mathcal{E}$, to the total magnetic flux, Φ, via

$$\mathcal{E} = -\frac{d\Phi}{dt}, \tag{5.21}$$

with the definition

$$q\mathcal{E} = \oint_{\mathcal{C}} \vec{f} \cdot d\vec{r}. \tag{5.22}$$

Eq. (5.22) is in principle the work when a particle with charge q, subject to a force $\vec{f}$, is carried around the curve $\mathcal{C}$, which could e.g. be an electric circuit. In the case of the rotating domain wall, this curve consists of the domain wall along the z-axis, which is connected at the ends via another wire outside the z-axis where there is no domain wall and zero fields.

To include spin contributions, the emf is generalized as

$$\mathcal{E} = \mathcal{E}_e + \mathcal{E}_{\rm s} = -\frac{\hbar}{-e}\frac{d\gamma_{\rm B}}{dt}, \tag{5.23}$$

where the two emf's come from electric charge and spin contributions respectively, and $\gamma_{\rm B}$ is a general Berry phase averaged over spins. The Berry phase, $\gamma_{\rm B}$, is divided into

$$\gamma_{\rm B} = \gamma_e + \gamma_{\rm s}, \tag{5.24}$$

where γ_e comes from the contributions of electric charges, which from Aharonov-Bohm in Ref. [36] is found to be $\gamma_e = -e\Phi/\hbar$. Here Φ is the total magnetic flux. For an electron carried around a closed curve $\mathcal{C}$ this gives the familiar electric emf $\mathcal{E}_e = -d\Phi/dt$. The term $\gamma_{\rm s}$ is the phase with spin origin, and it will be shown that it is written as

$$\gamma_{\rm s} = P_{\rm C}\gamma_{\rm s}^{+}, \tag{5.25}$$

where $P_{\rm C}$ is the spin polarization in terms of the spin-dependent conductivities and $\gamma_{\rm s}^{+}$ is the Berry phase for spin up electrons.

It is assumed a spin-dependent force, $f_{\rm s}^{\pm}$, expressed in terms of potensials, on the form

$$f_{\rm s}^{\pm} = -\frac{\hbar}{2}\frac{\partial \vec{A}_{\rm s}^{\pm}}{\partial t} - \nabla_{\vec{r}}\phi_{\rm s}^{\pm}, \tag{5.26}$$

and here $\hbar/2$ is the spin analogy to an electric charge $-e$, i.e. $\hbar/2$ is the "spin charge". Only nonconservative forces contribute to the total emf, since conservative forces, e.g. $-\nabla_{\vec{r}}\phi_{\rm s}^{\pm}$, integrate to zero in the contour integral in Eq. (5.22). It is assumed that this nonconservative spin-dependent force can be written

$$\vec{f}_{\rm nc}^{\pm} = -\frac{\hbar}{2}\frac{\partial \vec{A}_{\rm s}^{\pm}}{\partial t}. \tag{5.27}$$

The idea is to write the Berry phase in terms of the real space gauge field, $\vec{A}_{\rm s}^{\pm}$, such that the phase is the sum of contributions of the field in real space, that is

$$\gamma_{\rm s}^{\pm}(z) = \frac{1}{2}\int_{\vec{r}_0}^{\vec{r}} \vec{A}_{\rm s}^{\pm}\cdot d\vec{r'}, \tag{5.28}$$

and $\gamma_{\rm s}^{\pm}$ now depends on z.

The quantity in Eq. (5.28) is gauge-dependent, and the integral also has different values for different integration ranges. It is thus useful to calculate the relevant inner products using a general spinor on the form

$$|\eta_{\pm}(\theta,\phi)\rangle = e^{if(\theta,\phi)}|\chi_{\pm}(\theta,\phi)\rangle, \tag{5.29}$$

where $f(\theta,\phi) = f(\vec{R}(t))$ is a function describing the gauge. The spinor $\chi_{\pm} = u_{\phi}^{-1}u_{\theta}^{-1}\chi'_{\pm}$ is found from the rotations in Eqs. (C.8) and (C.10) combined with the spinors in Eqs. (5.17) and (5.18).

By returning to the definition of the geometric phase in Eq. (5.12), the general form of the phase is

$$\begin{aligned}\gamma_{\rm s}^{\pm}(z) &= i\int_{\vec{R}(t_0)}^{\vec{R}(t)}\langle\psi_{m\pm}|\nabla_{\vec{R}}\psi_{m\pm}\rangle\cdot d\vec{R} = i\int_{\vec{R}(t_0)}^{\vec{R}(t)}(\langle\chi_{\pm}|\nabla_{\vec{R}}\chi_{\pm}\rangle + i\nabla_{\vec{R}}f(\vec{R}))\cdot d\vec{R}\\ &= i\int_{\vec{R}(t_0)}^{\vec{R}(t)}\langle\chi_{\pm}|\nabla_{\vec{R}}\chi_{\pm}\rangle\cdot d\vec{R} - (f(\vec{R}(t)) - f(\vec{R}(t_0))).\end{aligned} \tag{5.30}$$

If the line integral in Eq. (5.30) is closed, then $f(\vec{R}(t)) = f(\vec{R}(t_0))$, and the surface terms for f vanishes. Thus for a closed line integral the geometric phase is independent of the gauge.

The issue of finding $\vec{A}_{\rm s}^{\pm}$ from the integral in Eq. (5.28) can be difficult when $f(\vec{R}) \neq 0$, with $\gamma_{\rm s}^{\pm}$ from Eq. (5.30). Therefore the spin-dependent emf and nonconservative force will be calculated in a spesific gauge ($f = 0$), and the issues of gauge invariance of these physical quantities is discussed afterwards.

For the rotating domain wall, the coordinates are given by $\vec{R}(t) = (\theta(t), \phi(t))$, and the contours for the line integrals are curves on the unit sphere. The relevant operators in this case are

$$\nabla_{\vec{R}} = \hat{\theta}\frac{\partial}{\partial\theta} + \hat{\phi}\frac{1}{\sin\theta}\frac{\partial}{\partial\phi}, \tag{5.31}$$

and

$$d\vec{R} = \hat{\theta} d\theta + \hat{\phi} \sin\theta d\phi. \tag{5.32}$$

In App. C.2.3 the relevant inner products in this spesific gauge are calculated, with the result

$$\langle \chi_\pm | \frac{\partial}{\partial \phi} \chi_\pm \rangle = \mp \frac{i}{2} \cos\theta, \tag{5.33}$$

and

$$\langle \chi_\pm | \frac{\partial}{\partial \theta} \chi_\pm \rangle = 0. \tag{5.34}$$

In this gauge, the integral in Eq. (5.12) is only over $d\phi$, and by choosing the starting point at $\phi(t_0) = 0$ the geometric phase becomes

$$\gamma_{\rm s}^{\pm}(z) = i \int_{\vec{R}(t_0)}^{\vec{R}(t)} \langle \psi_{m\pm} | \frac{\partial}{\partial \phi} \psi_{m\pm} \rangle d\phi = \pm \frac{1}{2} \int_0^{\phi} \cos\theta d\phi = \pm \frac{1}{2} \phi \cos\theta. \tag{5.35}$$

With the spin polarization $P_{\rm C} = (\sigma_+ - \sigma_-)/(\sigma_+ + \sigma_-)$ in terms of spin-dependent conductivities, the spin-averaged phase from Eq. (5.35) is

$$\gamma_{\rm s} = P_{\rm C} \gamma_{\rm s}^{+}. \tag{5.36}$$

By choosing the gauge with $f(\theta, \phi) = 0$, and where the integral in Eq. (5.28) is taken from $\vec{r}_0 = 0$ to $\vec{r}$, a solution for the real field, with $\gamma_{\rm s}^{\pm}$ from Eq. (5.35), is

$$\vec{A}_{\rm s}^{\pm} = 2 \frac{\partial}{\partial z} \gamma_{\rm s}^{\pm} \hat{z} = \pm \phi \frac{\partial}{\partial z} \cos\theta \hat{z}. \tag{5.37}$$

The solution in Eq. (5.37) is checked by doing the integral

$$\begin{aligned} \frac{1}{2} \int_{\vec{r}_0}^{\vec{r}} \vec{A}_{\rm s}^{\pm} \cdot d\vec{r} &= \frac{1}{2} \int_{\vec{r}_0=0}^{\vec{r}} 2 \frac{\partial}{\partial z} \gamma_{\rm s}^{\pm} \hat{z} \cdot d\vec{r} \\ &= \gamma_{\rm s}^{\pm}(z) - \gamma_{\rm s}^{\pm}(z=0) = \gamma_{\rm s}^{\pm}(z), \end{aligned} \tag{5.38}$$

since $\gamma_{\rm s}^{\pm}(0)$ corresponds to $\cos\theta = 0$.

Now the nonconservative force is found from Eq. (5.27), such that

$$\begin{aligned} \vec{f}_{\rm nc}^{\pm} &= -\frac{\hbar}{2} \frac{\partial \vec{A}_{\rm s}^{\pm}}{\partial t} = \mp \frac{\hbar}{2} \dot{\phi} \frac{\partial \cos\theta}{\partial z} \hat{z} \\ &= \pm \frac{\hbar}{2} \dot{\phi} \sin\theta \frac{\partial \theta}{\partial z} \hat{z}. \end{aligned} \tag{5.39}$$

The resulting force in Eq. (5.39) reproduces the second term in Eq. (4.15) of the spin-motive force calculated from the gauge transformations in section 4, but with the opposite sign. This sign difference is due to the different definitions of spin up and spin down in sections 4 and 5.2. Since the term $(\partial\theta/\partial t)(\partial\phi/\partial z)$ from Eq. (4.15) is zero for a rotating Neel wall, and the nonconservative force is only defined up to the definition of spin-charge, we conclude that the spin-motive force for a rotating Neel-type domain wall can be captured both from an SU(2) gauge-transformation and from Berry-phases in a generalized Faraday's law.

The spin-dependent emf is found by integrating $\vec{f}_{\rm s}^{\pm}$ from Eq. (5.39) over the circuit

$$-e\mathcal{E}_{\rm s}^{\pm} = \oint \vec{f}_{\rm s}^{\pm} \cdot d\vec{r}, \tag{5.40}$$

which reduces to an integral over the nonconservative spin force along the z-axis, since Eq. (5.40) is a closed integral and $\vec{A}_{\rm s}^{\pm}$ is zero outside the z-axis. This emf should be independent of gauge, and this is shown by writing the spin emf as

$$\begin{aligned}\mathcal{E}_{\rm s}^{\pm} &= -\frac{\hbar}{-2e}\oint \frac{\partial \vec{A}_{\rm s}^{\pm}}{\partial t}\cdot d\vec{r} = \frac{\hbar}{2e}\int_{-\infty\hat{z}}^{\infty\hat{z}} \frac{\partial \vec{A}_{\rm s}^{\pm}}{\partial t}\cdot d\vec{r} \\ &= \lim_{\Delta t\to 0}\frac{\hbar}{2e}\int_{-\infty\hat{z}}^{\infty\hat{z}} \frac{\vec{A}_{\rm s}^{\pm}(\vec{r},t+\Delta t)-\vec{A}_{\rm s}^{\pm}(\vec{r},t)}{\Delta t}\cdot d\vec{r},\end{aligned} \tag{5.41}$$

and by mapping this to spin space, with $\vec{\mathcal{A}}_{\rm s}^{\pm}$ defined from Eq. (5.14),

$$\begin{aligned}\mathcal{E}_{\rm s}^{\pm} &= \lim_{\Delta t\to 0}\frac{2\hbar}{2e\Delta t}\left(\int_{\mathcal{C}(t+\Delta t)}\vec{\mathcal{A}}_{\rm s}^{\pm}\cdot d\vec{R} - \int_{\mathcal{C}(t)}\vec{\mathcal{A}}_{\rm s}^{\pm}\cdot d\vec{R}\right) = \lim_{\Delta t\to 0}\frac{\hbar}{e\Delta t}\oint_{\Delta\mathcal{C}}\vec{\mathcal{A}}_{\rm s}^{\pm}\cdot d\vec{R} \\ &= \lim_{\Delta t\to 0} -\frac{\hbar}{-e}\frac{\Delta\gamma_{\rm s}^{\pm}}{\Delta t}.\end{aligned} \tag{5.42}$$

The term $\Delta\gamma_s^{\pm}$ is a gauge invariant quantity when $\Delta t \to 0$, since the curve $\mathcal{C}(t+\Delta t) - \mathcal{C}(t)$ corresponds to a closed curve, as the wall rotates from $\phi(t)$ to $\phi(t+\Delta t)$, as discussed in Ref. [33].

In total the emf is

$$\mathcal{E} = \mathcal{E}_e + \mathcal{E}_{\rm s}^{\pm} = -\frac{\hbar}{(-e)}\frac{d}{dt}(\gamma_e + P_{\rm C}\gamma_{\rm s}^{+}), \tag{5.43}$$

which is a generalization of Faraday's law, with the general Berry phase from Eqs. (5.23) and (5.24).

6 Spin-Less Particle Transport and the Boltzmann Transport Equation

In this section we use the Boltzmann transport equation (BTE) to describe spin-less transport in a metal wire. The methods of the BTE is well established in the literature, and this part serves as a starting point for the description of spin-dependent transport in section 7.

It is assumed that the mean distribution of particles is written as a distribution function, $f(\vec{r}, \vec{p}, t)$, and the BTE describes how f changes in phase space due to external forces and/or physical processes like particle scattering. The BTE reads

$$\frac{\partial f}{\partial t} + \vec{v} \cdot \nabla_{\vec{r}} f + \frac{\partial \vec{p}}{\partial t} \cdot \nabla_{\vec{p}} f = f_{\text{scattering}}, \tag{6.1}$$

where $\partial \vec{p}/\partial t$ is an external force [37]. The RHS of Eq. (6.1) is a symbolical way of writing the scattering terms, and the LHS is in principle the total time derivative of f.

6.1 Relaxation Time Approximation

A simple case of spin-less electron transport is a metallic wire subject to a small external electric field. One frequently used approximation for the scattering term in Eq. (6.1) is the relaxation time approximation (RTA), with the BTE on the form

$$\frac{\partial f}{\partial t} + \vec{v} \cdot \nabla_{\vec{r}} f + \frac{\partial \vec{p}}{\partial t} \cdot \nabla_{\vec{p}} f = -\frac{f - f_{\text{FD}}}{\tau_{\text{rta}}}, \tag{6.2}$$

where τ_{rta} is the relaxation time for the system.

The RTA means physically that by turning off the external forces, then

$$\frac{\partial f}{\partial t} = -\frac{f - f_{\text{FD}}}{\tau_{\text{rta}}}, \tag{6.3}$$

such that the system returns to its equilibrium distribution, the Fermi-Dirac distribution, f_{FD}, exponentially as

$$f - f_{\text{FD}} = (f(t = 0) - f_{\text{FD}}) e^{-\frac{t}{\tau_{\text{rta}}}}. \tag{6.4}$$

With no time dependence on the external forces, then $\partial f/\partial t = 0$, which is a steady-state situation. In this case, with a small external electric field, $\vec{E}$, in the RTA, the BTE in Eq. (6.2) reduces to

$$\vec{v} \cdot \frac{\partial f}{\partial \vec{r}} + (-e)\vec{E} \cdot \frac{\partial f}{\partial \vec{k}} = -\frac{f - f_{\text{FD}}}{\tau_{\text{rta}}}. \tag{6.5}$$

With a weak external field, the system is near equilibrium, and the solution is assumed on the form $f = f_{\text{FD}} + g$, with a small deviation, $g \ll f_{\text{FD}}$. Since g is induced from the external field, it should be proportional to $\vec{E}$. For small fields

the second order terms $\propto \vec{E} \cdot g$ are neglected. With a constant external electric field the deviation, g, should also be spatially uniform, i.e. $\partial g/\partial \vec{r} = 0$. With these approximations Eq. (6.5) reads

$$-\frac{g}{\tau_{\text{rta}}} = -e\vec{E} \cdot \vec{v}\frac{\partial f_{\text{FD}}}{\partial \varepsilon_k}. \tag{6.6}$$

Consider the case of a constant electric field along the wire in the $\hat{z}$-direction, $\vec{E} = E_z\hat{z}$. The solution for the distribution function is then

$$f(z, \vec{k}) = f_{\text{FD}}(\varepsilon_k - \mu_0) - ev_z\tau_{\text{rta}}E_z\left(-\frac{\partial f_{\text{FD}}}{\partial \varepsilon_k}\right), \tag{6.7}$$

which is uniform in space. The distribution function in Eq. (6.7) is similar to a shifted equilibrium distribution where the momentum is shifted in the field direction by $k_z \to k_z + (e\tau_{\text{rta}}/\hbar)E_z$.

The electric current is calculated from the mean velocity of the electrons, which includes summing over momentum and both spins. At zero temperature the electric current is

$$\begin{aligned} j_z(z) &= -2e\int \frac{d^3k}{(2\pi)^3}v_z\left(f_{\text{FD}}(\varepsilon_k - \mu_0) - ev_z\tau_{\text{rta}}E_z\left(-\frac{\partial f_{\text{FD}}}{\partial \varepsilon_k}\right)\right) \\ &= 2e\int_0^\infty \frac{k^2dk2\pi}{(2\pi)^3}\int_0^\pi d\theta \sin\theta\cos^2\theta ev^2\tau_{\text{rta}}E_z\delta(\varepsilon_F - \varepsilon_k) \\ &= \frac{e^2\tau_{\text{rta}}n^0}{m}E_z, \end{aligned} \tag{6.8}$$

where the first term integrates to zero, since f_{FD} is independent of the direction of $\vec{k}$, but v_z is odd in the momentum. Eq. (6.8) recovers the Drude model of the electric conductivity, $\sigma = e^2n^0\tau/m$, with τ as some relaxation time [38].

6.2 Elastic Scattering

Elastic scattering is scattering of particles onto particles with the same energy. This type of scattering is modeled by the RHS of Eq. (6.9). For a steady-state with transport along $\hat{z}$, the Boltzmann equation for elastic scattering is

$$v_z\frac{\partial f}{\partial z} + \vec{F} \cdot \frac{\partial f}{\partial \vec{p}} = -\frac{f - \langle f\rangle_{\hat{p}}}{\tau_{\text{el}}}, \tag{6.9}$$

where the brackets in Eq. (6.9) denote an average over the directions of the momentum, $\vec{p} = m\vec{v}$. Here, τ_{el}, is the elastic scattering time, and $\vec{F}$ is an external force.

Elastic scattering is special, since elastic scattering only changes the direction of the momentum, and thus the number of electrons at a given energy is held constant. For a non-equilibrium system with only elastic scattering present, it can never reach an equilibrium if this system has a different number of particles at one

or more electron energies, than the system in equilibrium.

If the direction of the momentum, $\hat{p}$, is written in terms of spherical coordinates, θ and ϕ, the average over momentum directions is defined

$$\langle f(\vec{r},\vec{p})\rangle_{\hat{p}} = \int \frac{d\Omega_{\hat{p}}}{4\pi} f(\vec{r},p,\theta,\phi) = \frac{1}{4\pi}\int_0^{2\pi} d\phi \int_0^{\pi} d\theta \sin\theta f(\vec{r},p,\theta,\phi), \tag{6.10}$$

where $d\Omega_{\hat{p}}$ is the differential solid angle in momentum space.

6.2.1 Constant Electric Field in a Wire

Consider a metal wire of length, L, along the $\hat{z}$-axis, from $z = 0$ to $z = L$, with an applied electric field $\vec{F} = -eE_z\hat{z}$. The two ends of the wire are assumed to be attached to two reservoirs which are always in equilibrium, and the reservoirs have chemical and electric potential μ_L and $-eV_L$ for the left reservoir, $(z < 0)$, and μ_R and $-eV_R$ for the right reservoir $(z > L)$. In the reservoirs the electrons are filled according to the Pauli principle from the bottom of the electric potential energy up to the chemical potential, such that

$$\begin{aligned} \mu_L &= \mu_0 + (-e)V_L, \\ \mu_R &= \mu_0 + (-e)V_R, \end{aligned} \tag{6.11}$$

and the electrons in both reservoirs are thus described by Fermi-Dirac distributions. The potentials are defined such that $-eV_L$ and $-eV_R$ are positive, and the potentials are shown schematically in Fig. 6.

For such a system with elastic scattering in the wire, the BTE given by Eq. (6.9) is for a small external field reduced to

$$-\frac{f - \langle f\rangle_{\hat{p}}}{\tau_{\rm el}} = -eE_z\frac{\partial f_{\rm FD}}{\partial p_z} = -eE_z v_z \frac{\partial f_{\rm FD}}{\partial \varepsilon_p}, \tag{6.12}$$

and since the electric field is only present in the wire, the solution for the distribution function is

$$f(\vec{p}) = f_{\rm FD}(\varepsilon_p - \mu_0) + eE_z v_z \tau_{\rm el}\frac{\partial f_{\rm FD}}{\partial \varepsilon_p}, \tag{6.13}$$

which is also spatially uniform. The electric current is given by integrating in the same manner as in Eq. (6.8), which again gives the current $j_z(z) = \sigma E_z$, with σ given by the Drude conductivity in terms of the elastic scattering time $\tau_{\rm el}$.

Another quantity which is calculated from the distribution function is the distribution of charges. The electron charge density in equilibrium, $\rho_0 = -en^0$, with n^0 as the number of conduction electrons per volume, is calculated by summing the equilibrium distribution function over spin and momentum. The equilibrium charge density is thus

$$\rho_0 = -2e\int \frac{d^3k}{(2\pi)^3} f_{\rm FD}(\varepsilon_p - \mu_0) = -e\frac{1}{\pi^2}\int_0^{k_F} k^2 dk = -en^0, \tag{6.14}$$

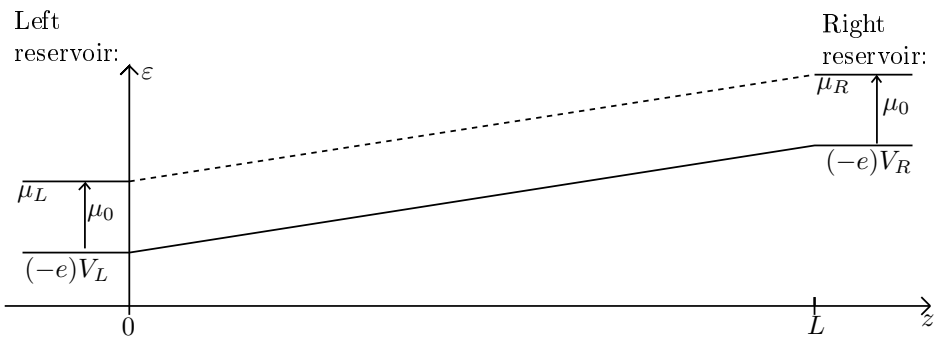

Figure 6: The metal wire is subject to a constant electric field due to a potential difference between the reservoirs, at the ends of the wire. The reservoirs are in equilibrium, and electron states in the left/(right) reservoir are filled, according to the Pauli principle, from the bottom of the electric potential, $-eV_{L/(R)}$, up to a chemical potential, $\mu_{L/(R)}$. In the case of a constant electric field, the electric potential grows linearly from one end of the wire to the other, shown with the solid line. Since the wire is out of equilibrium and the scattering is elastic, the chemical potential is not defined inside the wire, but the difference is visualized with a dotted line.

by evaluating the integral at zero temperature.

When the electric field is applied, the accumulated electron charge density, ρ, is calculated from the distribution function by subtracting the background charges from positive ions, ρ_0, such that

$$\rho = -2e \int \frac{d^3k}{(2\pi)^3}(f - f_{\mathrm{FD}}) = -2e \int \frac{d^3k}{(2\pi)^3} eEv_z\tau_{\mathrm{el}} \frac{\partial f_{\mathrm{FD}}}{\partial \varepsilon_p} = 0, \tag{6.15}$$

since v_z is antisymmetric in the momentum. This agrees with Gauss' Law

$$\frac{\rho}{\epsilon} = \nabla \cdot \vec{E}, \tag{6.16}$$

since the eletric field is constant. Here ϵ is the permittivity of the metal.

The conservation of charge is ensured by

$$\frac{\partial \rho}{\partial t} + \nabla \cdot \vec{j} = 0, \tag{6.17}$$

which is true for a constant electric current.

6.2.2 Diffusive Electron Transport

Another physical picture is the diffusion picture, where it is assumed that the electric current in the wire is driven by diffusion due to a difference in chemical

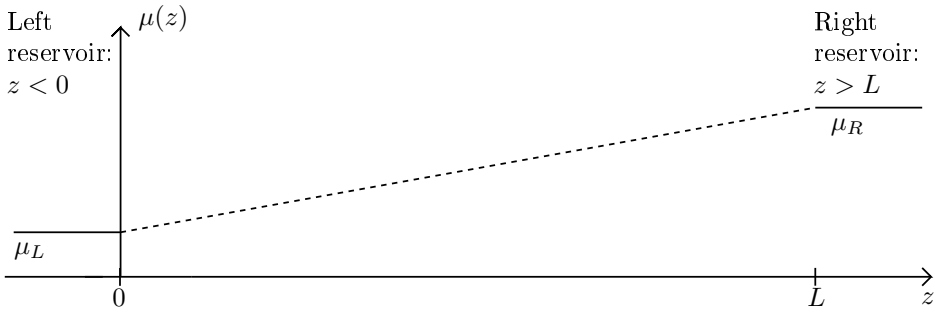

Figure 7: Chemical potentials at the endpoints of a wire of length L, in the diffusion picture. The reservoirs are in equilibrium and fixed at chemical potentials μ_L for $z < 0$ and μ_R for $z > L$. Inside the wire there is a net electric current. Elastic scattering is in general not sufficient for the system to reach neither a local or global equilibrium, and thus the chemical potential is not defined inside the wire.

potentials in the reservoirs, with no electric field present. The chemical potentials for this diffusion picture is shown in Fig. 7. With chemical potentials $\mu_L < \mu_R$ for the left and right reservoirs respectively, the boundary conditions for the distribution function give Fermi-Dirac distributions with different chemical potentials,

$$f(z \leq 0, \vec{p}) = f_{\mathrm{FD}}(\varepsilon_p - \mu_L), \tag{6.18}$$

$$f(z \geq L, \vec{p}) = f_{\mathrm{FD}}(\varepsilon_p - \mu_R). \tag{6.19}$$

It is assumed that the equilibrium distribution consists of a Fermi-Dirac distribution with chemical potential μ_0 throughout the whole wire. The out-of-equilibrium situation has changed both chemical potentials, such that in the left reservoir: $\mu_0 \to \mu_L$ and in the right reservoir: $\mu_0 \to \mu_R$. In the case of a weak current it is also assumed that $\mu_R - \mu_0 \ll \mu_0$.

The solution ansatz for the distribution function is

$$f(z, \vec{p}) = f_{\mathrm{S}}(z, \varepsilon_p) + \hat{p} \cdot \vec{f_{\mathrm{P}}}(z, \varepsilon_p), \tag{6.20}$$

where the labels S and P indicate analogies to s- and p-waves in the hydrogen atom, i.e. a spherically symmetric momentum part and a part with a specific momentum direction.

The BTE for elastic scattering and steady state in Eq. (6.9) is in the diffusion picture reduced to

$$v_z \frac{\partial f}{\partial z} = -\frac{f - \langle f \rangle_{\hat{p}}}{\tau_{\mathrm{el}}} = -\frac{\hat{p} \cdot \vec{f_{\mathrm{P}}}}{\tau_{\mathrm{el}}}, \tag{6.21}$$

by inserting the ansatz from Eq. (6.20).

With f given by Eq. (6.20) and then averaging Eq. (6.21) over momentum directions, as defined in Eq. (6.10),then

$$0 = \frac{\left\langle v_z^2 \right\rangle_{\hat{p}}}{v} \frac{\partial f_{\mathrm{P}z}(z,k)}{\partial z}, \tag{6.22}$$

which states that $f_{\mathrm{P}z}(z,k) = f_{\mathrm{P}z}(k)$ is independent of z.

By multiplying Eq. (6.21) with a component of the velocity, v_i, and then averaging over momentum directions, another relationship is

$$\begin{aligned} -\frac{1}{\tau_{\mathrm{el}}} \left\langle v_i \hat{p} \cdot \vec{f}_{\mathrm{P}} \right\rangle_{\hat{p}} &= -\frac{1}{\tau_{\mathrm{el}} v} \left\langle v_i^2 \right\rangle_{\hat{p}} f_{\mathrm{P}i} \\ &= \left\langle v_i v_z \frac{\partial}{\partial z} f_{\mathrm{S}} \right\rangle = \delta_{iz} \left\langle v_i^2 \right\rangle_{\hat{p}} \frac{\partial f_{\mathrm{S}}}{\partial z}. \end{aligned} \tag{6.23}$$

Now we combine Eqs. (6.22) and (6.23) to write the electron distribution function as

$$f(z,\vec{p}) = f_{\mathrm{S}}(z,\varepsilon_p) - v_z \tau_{\mathrm{el}} \frac{\partial f_{\mathrm{S}}}{\partial z}. \tag{6.24}$$

The spherically symmetric part of the distribution function must satisfy the boundary conditions in Eqs. (6.18) and (6.19), which gives

$$\begin{aligned} f(z,\vec{p}) =& f_{\mathrm{FD}}(\varepsilon_p - \mu_L) + \frac{z}{L} \left(f_{\mathrm{FD}}(\varepsilon_p - \mu_R) - f_{\mathrm{FD}}(\varepsilon_p - \mu_L) \right) \\ &- \frac{v_z \tau_{\mathrm{el}}}{L} \left(f_{\mathrm{FD}}(\varepsilon_p - \mu_R) - f_{\mathrm{FD}}(\varepsilon_p - \mu_L) \right). \end{aligned} \tag{6.25}$$

Since $\mu_R - \mu_0 \ll \mu_0$ it is possible to approximate the following term by a first order Taylor-expansion

$$f_{\mathrm{FD}}(\varepsilon_p - \mu_R) - f_{\mathrm{FD}}(\varepsilon_p - \mu_L) \approx -\frac{\partial f_{\mathrm{FD}}}{\partial \varepsilon_p} \Delta\mu, \tag{6.26}$$

where the difference in chemical potentials is defined as $\Delta\mu \equiv \mu_R - \mu_L$. With the approximation from Eq. (6.26) and the distribution function from Eq. (6.25) the electric current in the diffusion picture is integrated to

$$\begin{aligned} j_z &= -2e \int \frac{d^3k}{(2\pi)^3} v_z f(z,\vec{k}) \\ &= 2e\tau_{\mathrm{el}} \frac{\Delta\mu}{L} \int \frac{d^3k}{(2\pi)^3} v_z^2 \left(-\frac{\partial f_{\mathrm{FD}}}{\partial \varepsilon_p} \right) = -\frac{e\tau_{\mathrm{el}} n}{m} \left(\frac{-\Delta\mu}{L} \right) \\ &= \sigma \frac{\Delta\mu}{eL}, \end{aligned} \tag{6.27}$$

which is similar to the solution with an electric field in Eq. (6.8) with the Drude conductivity, σ, but here $-\Delta\mu/L$ is the analogy to the constant electric force $-eE_z$. If one uses the diffusive current calculated in Eq. (6.27) and compares that with the electric potentials in Eq. (6.11) given in the constant electric field picture, then $\Delta\mu/(eL) \leftrightarrow -(V_R - V_L)/L$, such that the two physical pictures are equivalent.

Diffusive transport means that the net movement of the electrons is due to concentration gradients, such that the accumulation of charges, $\rho(z)$, varies along the wire. The electron charge density in the diffusion picture varies linearly from one reservoir to the other, and it is

$$\begin{aligned}\rho(z) &= -2e \int \frac{d^3k}{(2\pi)^3} \left(f - f_{\mathrm{FD}}(\varepsilon_p - \mu_0)\right) \\ &= -2e \int \frac{d^3k}{(2\pi)^3} \left(- \left(\mu_L - \mu_0\right) \left(\frac{\partial f_{\mathrm{FD}}}{\partial \varepsilon_p}\right) + \frac{z}{L} \left(- \frac{\partial f_{\mathrm{FD}}}{\partial \varepsilon_p} \right) \Delta\mu \right) \\ &= e^2 d(\varepsilon_{\mathrm{F}}) \left(V_L + \frac{z}{L} \left(V_R - V_L\right) \right). \end{aligned} \tag{6.28}$$

The total density of states at the Fermi energy, $d(\varepsilon_{\mathrm{F}})$, is

$$d(\varepsilon_{\mathrm{F}}) = 2 \int \frac{d^3k}{(2\pi)^3} \left(- \frac{\partial f_{\mathrm{FD}}}{\partial \varepsilon_k} \right) = \frac{m}{(\pi\hbar)^2} k_{\mathrm{F}}, \tag{6.29}$$

and the factor of two accounts for both spins in the case of spin-less transport. $d(\varepsilon_{\mathrm{F}})$ has dimensions of inverse energy and volume.

From Eq. (6.28) it is evident that the accumulated charges at the wire ends depend on how much the chemical potentials are raised compared to μ_0, and $\rho(z)$ decreases linearly from $z = L$ to $z = 0$, since $\mu_R > \mu_L$.

7 Spin-Dependent Transport

The main goal for this section is to find out how the spin-motive force and Coulomb interaction affect the motion of conduction electrons in a thin ferromagnetic metal wire with a domain wall of the Neel type, subject to a weak external magnetic field, $\vec{B}_0 = B_0\hat{z}$. The Coulomb interaction is included via an electric potential, which is generated by the accumulation of charges.

The Boltzmann transport equation is extended for spin-dependent transport by introducing two electron distribution functions, $f_s(\vec{r},\vec{p},t)$, labeled by their spin, $s = \pm$. By finding the solutions for both distribution functions it is possible to calculate important transport quantities like spin-dependent currents, the total electric current and the distributions of charges in space.

The general BTE for spin-dependent transport is

$$\frac{\partial f_s}{\partial t} + \vec{v}\cdot\frac{\partial f_s}{\partial \vec{r}} + \vec{F}^s_{\text{tot}}(\vec{r},t)\cdot\frac{\partial f_s}{\partial \vec{p}} = f_{\text{scattering}}, \tag{7.1}$$

where $\vec{F}^s_{\text{tot}}(\vec{r},t)$ is the total spin-dependent force acting on the conduction electrons.

The total spin-dependent force consists in general of the spin-motive force with the effective fields $\vec{E}_s$ and $\vec{B}_s$ in Eq. (4.17), but it is important to also include an electric field, $\vec{E}^{\text{in}}$, which is induced by the accumulation of electric charges. We neglect the Lorentz force, $-e\vec{v}\times B_0\hat{z}$, on the electrons due to the external magnetic field, since B_0 is weak and this force does not influence the electron paths significantly when scattering events happen often. The total force is thus

$$\vec{F}^s_{\text{tot}} = -e\left(\vec{E}_s + \vec{v}\times\vec{B}_s\right) - e\vec{E}^{\text{in}}, \tag{7.2}$$

where the induced electric field is found by solving Poisson's equation.

In the following the main focus will be on $\vec{E}_s$, since in the special case of a tail-to-tail Neel-type domain wall in a metal wire, the term $\vec{B}_s = 0$, which follows from Eq. (4.16) and the solution for θ in Eq. (3.9). For a Neel-type domain wall with direction along the z-axis, the spin-motive force only depends spatially on the z-coordinate, and this spin-dependent force, $\vec{F}_s(z,t)$, is found from Eq. (4.19).

For a Neel-wall the total force is thus

$$\begin{aligned}\vec{F}^s_{\text{tot}}(z,t) &\equiv F^s_{\text{tot}}(z,t)\hat{z}\\ &= \left(F_s(z,t) - eE^{\text{in}}(z,t)\right)\hat{z},\end{aligned} \tag{7.3}$$

with $F_s(z,t)$ given by Eq. (4.19), and it is assumed that the induced electric field is a function of z, since the spin-motive force only acts in the $\pm z$-direction.

The induced electric field can be written in terms of an electric potential, $V(z,t)$, such that

$$E^{\text{in}}(z,t) = -\frac{\partial}{\partial z}V(z,t), \tag{7.4}$$

where it should be possible to find $V(z,t)$ from the charge density and by solving Poisson's equation. With a charge distribution as a function of z, Gauss' law states that,

$$\frac{\partial}{\partial z}E^{\text{in}}(z,t) = \frac{\rho(z,t)}{\epsilon}, \tag{7.5}$$

where ϵ is the permittivity of the wire.

7.1 Spin-Motive Force and Elastic Scattering

The physical situation consists of a ferromagnetic Neel-type domain wall in a wire aligned with the z-axis from $z = -L$ to $z = L$, with a total length of $2L$ and cross-sectional area $\mathcal{A}$. The spin-motive force inside the metal wire is shown in Fig. 8. The wire is connected to reservoirs at $z = -L$ and $z = L$, which have constant chemical potentials, i.e. μ_L for $z \leq -L$ and μ_R for $z \geq L$. The chemical potentials in the reservoirs are expressed in terms of the equilibrium chemical potential and the boundary values for the electric potential, such that $\mu_L = \mu_0 + (-e)V_L$ and $\mu_R = \mu_0 + (-e)V_R$.

A constant weak external magnetic field, $\vec{B}_0 = B_0\hat{z}$, makes the Neel-type domain wall move in terms of the collective coordinates r_{w}, ϕ_{w} and λ_{w}, with solutions from Eqs. (3.26), (3.27) and (3.28). It is assumed a small damping, such that $\alpha^2 \approx 0$, and there is no transverse anisotropy, $K_2 = 0$, such that the Neel wall is free to rotate around the z-axis. It is also assumed that the wire has macroscopic length compared to the domain wall, and that the DW is not near the reservoirs, i.e. $L \pm r_{\text{w}} \gg \lambda_{\text{w}}$.

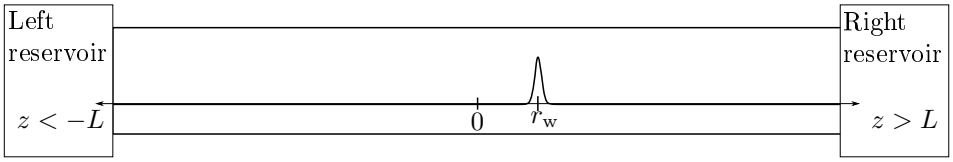

Figure 8: The ferromagnetic metal wire is connected to two reservoirs at $z = -L$ and $z = L$, and it has total length $2L$. The spin-motive force is sharply located around r_{w}, with the max-value $\pm\frac{\hbar}{2\lambda_{\text{w}}}\gamma B_0$ for spin up/down conduction electrons.

The goal is to find transport equations for the conduction electrons inside this wire. The spin-motive force is a consequence of an inhomogeneous magnetization changing with time. In order to get a nice analytical solution for this problem the approach is to look at a steady-state situation, i. e. $\partial f_s/\partial t = 0$, and solve the BTE with the spin-motive force in Eq. (4.19), but assume that r_{w} is a constant. This

is not exact, since the Neel wall is moving with velocity $\dot{r}_{\mathrm{w}} = -\alpha\sqrt{(A_{\mathrm{ex.s}}/K_1)}\gamma B_0$ and rotating around the z-axis with angular velocity $\dot{\phi}_{\mathrm{w}} = \gamma B_0$. The idea is that in the adiabatic approximation the wall moves sufficiently slowly along the wire, that the steady-state solution follows the position of the Neel wall as it moves in the z-direction. The validity of this approach is discussed in section 7.4.

In this approximation it is assumed that the total force is time-independent, such that $F^s_{\mathrm{tot}}(z,t) \to F^s_{\mathrm{tot}}(z)$.

In the case of elastic scattering, a steady-state situation and transport only in the $\hat{z}$-direction, the linearized version of the BTE in Eq. (7.1) reads

$$v_z \frac{\partial f_s}{\partial z} + F^s_{\mathrm{tot}}(z) v_z \frac{\partial f_{\mathrm{FD}}(\varepsilon_{k,s} - \mu_0)}{\partial \varepsilon_{k,s}} = -\frac{f_s - \langle f_s \rangle_{\hat{p}}}{\tau_{\mathrm{el}}}, \tag{7.6}$$

where the elastic scattering time is given by τ_{el}, and $\langle f_s \rangle_{\hat{p}}$ is the average of f_s over momentum directions, defined in Eq. (6.10). In this linear response approximation, the term $\partial f_s / \partial \varepsilon_{k,s} \approx \partial f_{\mathrm{FD}} / \partial \varepsilon_{k,s}$.

An ansatz for the electron distribution function is

$$\begin{aligned} f_s(z, \vec{k}) = {} & f_{\mathrm{FD}}(\varepsilon_{k,s} - \mu_L) + \frac{1}{2}\left(\frac{z}{L} + 1\right)\left(f_{\mathrm{FD}}(\varepsilon_{k,s} - \mu_R) - f_{\mathrm{FD}}(\varepsilon_{k,s} - \mu_L)\right) \\ & + \left(-\frac{\partial f_{\mathrm{FD}}(\varepsilon_{k,s} - \mu_0)}{\partial \varepsilon_{k,s}}\right)\left(g^{(0)}_s(z,k) + \cos\theta\, g^{(1)}_s(z,k)\right), \end{aligned} \tag{7.7}$$

where we introduce the functions $g^{(0)}_s(z,k)$ and $g^{(1)}_s(z,k)$. We use the boundary condition $g^{(0)}_s(z = \pm L, k) = 0$, which guarantees that the part of f_s which is symmetric in the momentum reduces to different Fermi-Dirac distributions at the endpoints of the wire, which are connected to the reservoirs.

It is shown in App. D.1 how to insert the ansatz for f_s from Eq. (7.7) into the linearized BTE in Eq. (7.6) and integrating over different moments of the momentum directions to get differential equations for the functions $g^{(0)}_s(z,k)$ and $g^{(1)}_s(z,k)$. One equation is

$$\frac{\partial g^{(1)}_s(z,k)}{\partial z} = 0, \tag{7.8}$$

which states that $g^{(1)}_s(z,k) = g^{(1)}_s(k)$ is independent of z.

By integrating Eq. (D.3) over the moment $\int \frac{d^3k}{(2\pi)^3} \cos\theta$, another relation is

$$g^{(1)}_s(k) = v_{\mathrm{F}_s} \tau_{\mathrm{el}} \left(F^s_{\mathrm{tot}}(z) - \frac{\partial g^{(0)}_s(z,k)}{\partial z} - \frac{\Delta\mu}{2L} \right). \tag{7.9}$$

The function $g^{(0)}_s(z,k)$ is found by taking the spatial derivative of Eq. (7.9) and using Eq. (7.8), then

$$\frac{\partial^2 g^{(0)}_s(z,k)}{\partial z^2} = \frac{\partial F^s_{\mathrm{tot}}(z)}{\partial z}, \tag{7.10}$$

such that $g_s^{(0)}(z,k) = g_s^{(0)}(z)$ is independent of k.

The solution of Eq. (7.10) is

$$g_s^{(0)}(z) = \frac{1}{2}\left(\left(1-\frac{z}{L}\right)\int_{-L}^{L} F_{\rm tot}^s(z')dz' - 2\int_z^L F_{\rm tot}^s(z')dz'\right), \tag{7.11}$$

which satisfies the boundary conditions $g_s^{(0)}(z=\pm L)=0$.

By using that

$$\Delta\mu = \mu_R - \mu_L = -e\Delta V, \tag{7.12}$$

and Eqs. (7.9) and (7.11) then

$$\begin{aligned} g_s^{(1)}(k_{{\rm F}_s}) &= v_{{\rm F}_s}\tau_{\rm el}\left(\frac{1}{2L}\int_{-L}^{L} dz' F_{\rm tot}^s(z') - \frac{-e\Delta V}{2L}\right) \\ &= v_{{\rm F}_s}\tau_{\rm el}\left(\frac{1}{2L}\int_{-L}^{L} dz' F_s(z') + \frac{1}{2L}\left(\int_{-L}^{L} dz'(-e)\left(-\frac{\partial V}{\partial z'}\right) + e\Delta V\right)\right) \\ &= v_{{\rm F}_s}\tau_{\rm el}\left(F_{\rm av}^s + \frac{e\Delta V}{L}\right). \end{aligned} \tag{7.13}$$

Here we define the average of the spin-motive force along the wire, $F_{\rm av}^s = -eE_{\rm av}^s$ as

$$F_{\rm av}^s = \frac{1}{2L}\int_{-L}^{L} dz F_s(z), \tag{7.14}$$

and since the force is exponentially small at $z > L$ and $z < -L$ the integral can be extended to $\pm\infty$ such that

$$F_{\rm av}^s = \frac{\hbar}{2L}\gamma B_0. \tag{7.15}$$

The current density, $\vec{j}_s = j_s\hat{z}$, for spin s is found from the mean velocity of the electrons, which from Eqs. (7.7) and (7.13) result in

$$\begin{aligned} j_s &= -e\int \frac{d^3k}{(2\pi)^3} v_z f_s = -e\int \frac{d^3k}{(2\pi)^3} v_z \cos\theta\, g_s^{(1)}(k_{{\rm F}_s})\left(-\frac{\partial f_{\rm FD}(\varepsilon_{k,s}-\mu_0)}{\partial\varepsilon_{k,s}}\right) \\ &= \sigma_s\left(E_{\rm av}^s - \frac{\Delta V}{L}\right), \end{aligned} \tag{7.16}$$

where $\sigma_s = \frac{e^2\tau_{\rm el}n_s^0}{m}$.

The spin-dependent charge density is found from the distribution function by subtracting the background ions in equilibrium, $f_s - f_{\rm FD}(\varepsilon_{k,s}-\mu_0)$, and summing over all states. The details is shown in App. D.1.1, and the result is

$$\begin{aligned} \rho_s(z) =& e^2 d_s(\varepsilon_F)\Bigg(V_L + V_R + \frac{z}{L}\Delta V - V(z) \\ &+ E_{\rm av.}^s L\left(\tanh\left(\frac{z-r_{\rm w}}{\lambda_{\rm w}}\right) - \frac{z}{L}\right)\Bigg). \end{aligned} \tag{7.17}$$

The total charge density is the sum of densities from spin up and spin down electrons. The total density of states at the Fermi energy is defined as

$$d(\varepsilon_F) = d_+(\varepsilon_F) + d_-(\varepsilon_F), \tag{7.18}$$

and since the spin-motive force is such that $E^s_{\text{av.}} = -E^{-s}_{\text{av.}}$, then Eq. (7.17) leads to the total accumulated charge, $\rho = \rho_+ + \rho_-$, written as

$$\begin{aligned}\rho(z) =& e^2 d(\varepsilon_F)\Bigg(V_L + V_R + \frac{z}{L}\Delta V - V(z) \\ &+ P_{\text{D}} E^+_{\text{av.}} L\left(\tanh\left(\frac{z - r_{\text{w}}}{\lambda_{\text{w}}}\right) - \frac{z}{L}\right)\Bigg).\end{aligned} \tag{7.19}$$

The quantity P_{D} is the spin polarization in terms of the densities of states at the Fermi energy,

$$P_{\text{D}} \equiv \frac{d+(\varepsilon_F) - d_-(\varepsilon_F)}{d_+(\varepsilon_F) + d_-(\varepsilon_F)}. \tag{7.20}$$

With the charge density from Eq. (7.19) combined with Eqs. (7.4) and (7.5) the differential equation for the electric potential is

$$V(z) - l^2_{\text{TF}}\frac{\partial^2 V}{\partial z^2} = V_L + V_R + \frac{z}{L}\Delta V + P_{\text{D}} E^+_{\text{av.}} L\left(\tanh\left(\frac{z - r_{\text{w}}}{\lambda_{\text{w}}}\right) - \frac{z}{L}\right), \tag{7.21}$$

where the values for V_L and V_R are to be determined by the appropriate boundary conditions. The quantity l_{TF} is the Thomas-Fermi screening length, defined as

$$l_{\text{TF}} \equiv \sqrt{\epsilon/(e^2 d(\varepsilon_F))}, \tag{7.22}$$

which is usually in the order of nanometers [39] in metals.

The boundary conditions for the system is determined by the ideal reservoirs located at $z \leq -L$ and $z \geq L$. The ideal reservoirs are assumed to be infinitely big compared to the wire, such that any charge accumulated inside the wire near the boundaries are immediately screened by the vast sea of particles in the reservoirs. This leads to the boundary conditions $\rho(z = -L) = 0$ and $\rho(z = L) = 0$. By using these boundary conditions on Eq. (7.19) the result is

$$V_L = V_R = 0, \tag{7.23}$$

such that the two reservoirs have a chemical potential equal to the equilibrium chemical potential, μ_0.

The total current density, $\vec{j} = j_z\hat{z}$, is the sum of both spin-dependent currents, which from Eq. (7.16) is

$$\begin{aligned} j_z &= P_{\text{C}}\sigma E^+_{\text{av}} - \sigma\frac{\Delta V}{L} \\ &= P_{\text{C}}\sigma E^+_{\text{av}}, \end{aligned} \tag{7.24}$$

since $\Delta V = 0$ and P_{C} is the spin polarization in terms of conductivities, $P_{\mathrm{C}} \equiv (\sigma_+ - \sigma_-)/\sigma$. The spin-motive force generates a spin-polarized electric current.

With the boundary conditions in Eq. (7.23) the differential equation in Eq. (7.21) is reduced to

$$V(z) - l_{\mathrm{TF}}^2 \frac{\partial^2 V}{\partial z^2} = P_{\mathrm{D}} E_{\mathrm{av.}}^{+} L \left(\tanh\left(\frac{z - r_{\mathrm{w}}}{\lambda_{\mathrm{w}}} \right) - \frac{z}{L} \right). \tag{7.25}$$

It will be necessary to make some approximations in order to solve Eq. (7.25) analytically. Two types of regimes for the solution of $V(z)$ will be investigated. The first regime is when $L \gg \lambda_{\mathrm{w}} \gg l_{\mathrm{TF}}$, and the other regime is when $L \gg l_{\mathrm{TF}} \gg \lambda_{\mathrm{w}} \to 0$. The full solution for $V(z)$ in the limit $\lambda_{\mathrm{w}} \to 0$ is calculated in App. D.2 with non-zero constants V_L and V_R, which is the general case. In the following only the solutions with $V_L = V_R = 0$ are discussed.

7.1.1 Long Domain Wall

The differential equation for $V(z)$ in Eq. (7.25) does not have a nice analytical solution, due to the term $\tanh\left(\frac{z-r_{\mathrm{w}}}{\lambda_{\mathrm{w}}}\right)$. When $\lambda_{\mathrm{w}} \gg l_{\mathrm{TF}}$ it is possible to approximate the solution of Eq.(7.25) by

$$V(z) \simeq P_{\mathrm{D}} E_{\mathrm{av.}}^{+} L \left(\tanh\left(\frac{z - r}{\lambda} \right) - \frac{z}{L} \right), \tag{7.26}$$

since the term

$$\begin{aligned} l_{\mathrm{TF}}^2 \frac{\partial^2 V}{\partial z^2} &= -2 \left(\frac{l_{\mathrm{TF}}}{\lambda_{\mathrm{w}}} \right)^2 \tanh\left(\frac{z - r_{\mathrm{w}}}{\lambda_{\mathrm{w}}} \right) \cosh^{-2}\left(\frac{z - r_{\mathrm{w}}}{\lambda_{\mathrm{w}}} \right) \\ &\ll 0, \end{aligned} \tag{7.27}$$

inside the wire, when $\lambda_{\mathrm{w}} \gg l_{\mathrm{TF}}$.

In this limit the accumulated charge along the wire is zero for all z. This makes physical sense, since the screening length is on a much smaller scale than the other physical parameters, such that any accumulated charge is instantly screened by nearby charges.

The generated spin-polarized electric current remains as $j_z = P_{\mathrm{C}} \sigma E_{\mathrm{av}}^{+}$.

7.1.2 Abrupt Domain Wall

In this section it is assumed that the Thomas Fermi screening length is much larger than the domain wall length, which will be taken to zero: $\lambda_{\mathrm{w}} \to 0$. With this assumption one can approximate the term

$$\tanh\left(\frac{z - r_{\mathrm{w}}}{\lambda_{\mathrm{w}}} \right) \simeq 2\Theta(z - r_{\mathrm{w}}) - 1 = 1 - 2\Theta(r_{\mathrm{w}} - z), \tag{7.28}$$

where $\Theta(x)$ is the Heavi-side step function. By using the approximation from Eq. (7.28) in Eq. (7.25) the differential equation for $V(z)$ is

$$V(z) - l_{\mathrm{tf}}^2 \frac{\partial^2 V}{\partial z^2} = P_{\mathrm{D}} E_{\mathrm{av}}^{+} L\Big(2\theta(z - r_{\mathrm{w}}) - \Big(\frac{z}{L} + 1\Big)\Big), \tag{7.29}$$

which can be solved analytically. The full solution is in Eq. (D.7) in App. D.2 .

Since the system has macroscopic length and the Thomas Fermi screening length is so small, the quantity L/l_{TF} is a really big number. By using this it is possible to approximate terms like $\sinh(L/l_{\mathrm{TF}}) \approx \cosh(L/l_{\mathrm{TF}}) \approx (1/2)\exp(L/l_{\mathrm{TF}})$, and it is shown in App. D.2.1 how to use this approximation on the solution for $V(z)$ given in Eq. (D.7).

The approximate solution of the induced potential is then

$$V(z) \simeq -P_{\mathrm{D}} E_{\mathrm{av}}^{+} L\left(4\theta(z - r_{\mathrm{w}}) \sinh^2\left(\frac{r_{\mathrm{w}} - z}{2l_{\mathrm{TF}}}\right) + \frac{z}{L} + 1 - e^{\frac{z - r_{\mathrm{w}}}{l_{\mathrm{TF}}}}\right), \tag{7.30}$$

which satisfies the solution of Eq. (7.29) and the boundary conditions $V(z = -L) = 0$ and $V(z = L) = 0$, under the condition that $L/l_{\mathrm{TF}} \gg 1$. This is checked in App. D.2.1.

With the solution for the electric potential given in Eq. (7.30), the total current density is, from Eq. (7.24),

$$j_z(z) = P_{\mathrm{C}} \sigma E_{\mathrm{av}}^{+}, \tag{7.31}$$

which is a spin-polarized current in terms of the average of the spin-motive force.

The distribution of charges is given by

$$\rho(z) = e^2 d(\varepsilon_F) P_{\mathrm{D}} E_{\mathrm{av}}^{+} L\left(2\theta(z - r_{\mathrm{w}}) \cosh\left(\frac{r_{\mathrm{w}} - z}{l_{\mathrm{TF}}}\right) - e^{\frac{z - r_{\mathrm{w}}}{l_{\mathrm{TF}}}}\right), \tag{7.32}$$

which physically corresponds to a tiny electric dipole at the position of the domain wall. The charge distribution is shown in Fig. 9.

In this limit it is possible with a non-zero charge, $\rho(z)$, since the Thomas-Fermi screening length is much larger than the size of the domain wall. The screening of charges is thus not effective on the much smaller scale of λ_{w}.

However, there is a problem with the limit of the abrupt wall, when $\lambda_{\mathrm{w}} \to 0$, since an abrupt wall is not energetically favored and thus unrealistic in materials. Earlier, it was assumed that the spin of the conduction electrons continuously aligns itself with the local magnetization direction of the domain wall, due to a strong exchange interaction, but this requires that the DW-length, λ_{w}, has a finite length. Also, the Boltzmann transport equation can not explain processes on

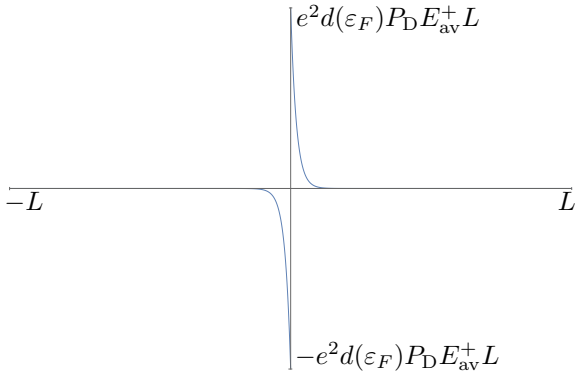

Figure 9: Plot of the accumulated charge distribution, $\rho(z)$, from Eq. (7.32), in the limit of zero DW-length. In this plot the domain wall mid-position is at $z = 0$. To emphasize the functional form of $\rho(z)$ the quantity L/l_{TF} is set to 0.02 which is far too large compared to a realistic scenario. The width of the dipole is of the order of l_{TF}, which is much smaller than the dipole in the figure.

length scales smaller than the Fermi wavelength. The limit of $l_{\mathrm{TF}} \gg \lambda_{\mathrm{w}} \to 0$ is therefore not correct from a physical point of view.

The screening length can be much larger than a non-zero DW-length in a semi-conductor, but the adiabatic approximation does not hold in a semi-conductor. Our calculations are based on a ferromagnetic metal, which differs from the modeling of a semi-conductor where it is required to take care of phenomena such as finite temperatures and the transport of holes.

7.2 Inelastic Scattering

This section combines elastic and inelastic scattering for the transport of conduction electrons subject to the spin-motive force in Eq. (4.19), generated by the moving Neel-type domain wall. The physical system is the same as described for elastic scattering in section 7.1 and Fig. 8.

It is assumed that the rate of inelastic scattering events is much faster than the rate for elastic scattering. In this case the electron distribution is in a local equilibrium on length scales much smaller than the mean length for elastic scattering, $l_{\mathrm{el}} \sim v_{\mathrm{F}} \tau_{\mathrm{el}}$. The local equilibrium is assumed to be described by a Fermi-Dirac distribution, $f_{\mathrm{FD}}(\varepsilon_{k,s} - \mu_s(z))$, where $\mu_s(z)$ is a spin-dependent chemical potential varying in space. The electron current and charge distribution is calculated by finding the chemical potential $\mu_s(z)$.

The solution ansatz for inelastic scattering is

$$f_s(z, \vec{k}) = f_{\mathrm{FD}}\left(\varepsilon_{k,s} - \mu_s(z)\right) + \left(-\frac{\partial f_{\mathrm{FD}}(\varepsilon_{k,s} - \mu_0)}{\partial \varepsilon_{k,s}}\right) \cos\theta g_s^{(1)}(z, k), \qquad (7.33)$$

where $\cos\theta g_s^{(1)}(z,k)$ is the anisotropic part.

The linearized BTE in a steady-state is

$$v_z \frac{\partial f_s}{\partial z} + \vec{F}^s_{\text{tot}} \cdot \frac{\partial f_{\text{FD}}(\varepsilon_{k,s} - \mu_0)}{\partial \vec{p}} = -\frac{f_s - \langle f_s \rangle_{\hat{p}}}{\tau_{\text{el}}}, \tag{7.34}$$

with external force from Eqs. (4.19) and (7.3). The BTE has the same form as in the case for elastic scattering in Eq. (7.6), but the difference in this case is that inelastic scattering is included via the solution ansatz in Eq. (7.33).

The insertion of f_s from Eq. (7.33) in the BTE in Eq. (7.34) is shown in App. D.3, and by integrating over moments of the momentum direction the equations for $\mu_s(z)$ and $g_s^{(1)}(z,k)$ are

$$\frac{\partial g_s^{(1)}(z,k)}{\partial z} = 0, \tag{7.35}$$

and

$$g_s^{(1)}(k_{\text{F}_s}) = v_{\text{F}_s}\tau_{\text{el}} \left(F^s_{\text{tot}}(z) - \frac{\partial \mu_s(z)}{\partial z} \right), \tag{7.36}$$

for the anisotropic part. The chemical potential is found by using Eqs. (7.35) and (7.36) such that

$$\frac{\partial^2 \mu_s(z)}{\partial z^2} = \frac{\partial F^s_{\text{tot}}}{\partial z}, \tag{7.37}$$

where the boundary values for $\mu_s(z)$, i.e. μ_L and μ_R, are determined by the charge density at the ends of the wire.

The boundary conditions are that $\rho(z)$ is zero at the two reservoirs. The result from the calculation in App. D.3 is $\mu_s(z = -L) = \mu_s(z = L) = \mu_0$ and $V_L = V_R = 0$. The solution to Eq. (7.37) is

$$\mu_s(z) = \mu_0 + \frac{1}{2}\left(\left(1 - \frac{z}{L}\right) \int_{-L}^{L} F^s_{\text{tot}}(z')dz' - 2\int_z^L F^s_{\text{tot}}(z')dz' \right). \tag{7.38}$$

The solution in Eq. (7.38) is used in Eq. (7.36) such that

$$\begin{aligned} g_s^{(1)}(k_{\text{F}_s}) &= \frac{v_{\text{F}_s}\tau_{\text{el}}}{2L} \int_{-L}^{L} F^s_{\text{tot}}(z')dz' \\ &= v_{\text{F}_s}\tau_{\text{el}} F^s_{\text{av}}, \end{aligned} \tag{7.39}$$

since $\Delta V = 0$.

From Eqs. (7.33) and (7.39) the current density for spin s is

$$\begin{aligned} j_s &= -e \int \frac{d^3k}{(2\pi)^3} v_z \cos\theta \left(-\frac{\partial f_{\text{FD}}(\varepsilon_{k,s} - \mu_0)}{\partial \varepsilon_{k,s}} \right) g_s^{(1)}(k_{\text{F}_s}) \\ &= \sigma_s E^s_{\text{av}}, \end{aligned} \tag{7.40}$$

such that the electric current density is

$$j_z = P_{\mathrm{C}} \sigma E_{\mathrm{av}}^{+}, \tag{7.41}$$

which is the same result as for elastic scattering.

It is shown in App. D.3 that inelastic scattering leads to the same charge density $\rho(z)$ and differential equation for $V(z)$ as in the case of only elastic scattering. The results for inelastic scattering are the same as for only elastic scattering.

7.3 Spin-Flip Scattering

In the previous sections it was not accounted for scattering-processes which flip the spin. Spin-flipping mechanisms include scattering on magnetic impurities and the spin-orbit interaction. The spin-orbit interaction is a relativistic effect which couples the electrons orbital motion with its spin. In ferromagnets a spin-flip can also occur for scattering on magnons, i.e. spin-waves.

Spin-flip scattering is important in multilayers of ferromagnets and normal metals, where it is often treated phenomenologically by introducing the spin-flip diffusion length, λ_{sfd}. This new length-scale is a measure for how far a spin-polarized current penetrates a non-magnetic normal metal, before electron spins are randomized and the current loses its spin polarization [14].

It is shown in App. D.4.2 that by including spin-flip scattering in the BTE, the spin chemical potentials approximately satisfy the differential equation

$$\frac{\partial^2 \left(\mu_s(z) - \mu_{-s}(z)\right)}{\partial z^2} + \frac{1}{\lambda_{\mathrm{sf}}^2} \left(\mu_s(z) - \mu_{-s}(z)\right) = \frac{\partial F_s(z)}{\partial z}, \tag{7.42}$$

with the constant $1/\lambda_{\mathrm{sf}}^2$ defined as

$$\frac{1}{\lambda_{\mathrm{sf}}^2} = \frac{3}{\tau_{\mathrm{el}}} \left(\frac{1}{\tau_s^{\mathrm{sf}} v_{\mathrm{F}_s}^2} + \frac{1}{\tau_{-s}^{\mathrm{sf}} v_{\mathrm{F}_{-s}}^2} \right). \tag{7.43}$$

Here we introduced τ_s^{sf} as the typical time between scattering events which flips the spin from s to $-s$. A central assumption for the derivation of Eq. (7.42) is that the relaxation time for spin-flip is much longer than other relaxation times, i.e. $\frac{1}{\tau_{\mathrm{el}}} \gg \frac{1}{\tau_s^{\mathrm{sf}}}$. It seems that the inclusion of spin-flipping mechanisms couples the spin chemical potentials, and also we predict that j_s is spatially dependent, since $\partial g_s^{(1)}/\partial z \neq 0$. However, for a steady-state in a metal ferromagnet the total electric dc-current is expected to be constant, due to current-conservation [40].

The effects of spin-flip scattering and spin-orbit interactions remain open for further investigations.

7.4 Time and Length-Scales

In order for a steady-state solution to follow the position of the moving domain wall, it is required that the time it takes for electrons to diffuse a small distance ΔL is much shorter than the time the domain wall uses to travel the same distance. In this regime the diffusion of electrons happens much faster compared to the movement of the domain wall, such that the system is always in a steady-state within the time-scale for the movement of the domain wall.

Diffusion times are proportional to the square of the diffusion length, and we define the time to diffuse a distance ΔL as

$$t_{\mathrm{D}} = \frac{(\Delta L)^2}{D}, \tag{7.44}$$

with diffusion constant D. The diffusion constant depends on the square of the Fermi velocity and some mean time between all kinds of scattering events, τ, such that

$$D = \frac{v_{\mathrm{F}}^2 \tau}{3}. \tag{7.45}$$

The time it takes for the domain wall to travel a distance ΔL is defined as

$$t_{\mathrm{w}} = \frac{\Delta L}{v_{\mathrm{w}}}, \tag{7.46}$$

with the domain wall velocity v_{w}.

For diffusion to propagate much faster than the domain wall, we require that $t_{\mathrm{D}} \ll t_{\mathrm{w}}$, which is satisfied when $v_{\mathrm{w}} \ll D/(\Delta L)$. We now use typical experimental values to make an order of magnitude comparison between the domain wall velocity and diffusive movement.

The domain wall velocity is usually in the range $v_{\mathrm{w}} \sim 10 - 100$ m/s. We estimate a typical length $\Delta L \sim 10^{-6}$ m, the Fermi velocity, $v_{\mathrm{F}} \sim 10^5$ m/s and a scattering time $\tau \sim 10^{-13}$ s [41]. With these values the term

$$\frac{D}{\Delta L} \sim 10^3 \mathrm{m/s}, \tag{7.47}$$

which is larger than $v_{\mathrm{w}} = 100$ m/s, but not much larger.

For the Neel-type domain wall, v_{w} depends linearly on the applied external field, such that a weak external magnetic field is necessary in that case.

We conclude that our steady-state approximation is appropriate, at least for slowly moving domain walls.

8 Conclusions

The magnetization dynamics of a ferromagnetic domain wall subject to a weak external magnetic field were calculated from an effective magnetic field and by assuming a small magnetic damping. For an external magnetic field below the Walker threshold, a Neel-type domain wall in a metal wire keeps its initial shape and moves with constant velocity along the wire. The transverse anisotropy of the wire pins the azimuthal angle of the domain wall. If there is no transverse anisotropy, the Neel-type domain wall both moves with a constant velocity and rotates with a constant angular velocity.

The spin-motive force is a consequence of an inhomogeneous magnetization changing in time. This force is expressed in terms of effective electric and magnetic gauge fields, which push on and bend the path of conduction electrons of opposite spins in opposite directions. An adiabatic approximation was used in our derivation, which corresponds to a strong ferromagnetic exchange energy, where conduction electron spins continuously align parallel or anti-parallel to the local magnetization in the ferromagnet.

In the case of a rotating Neel-type domain wall the spin-motive force was also derived from a geometric Berry-phase and a modified Faraday's law. This method did not capture the aspects of other types of domain walls, since this was a special case. It is however shown in the literature that all terms related to the spin-motive force can be derived from Berry-curvatures in a model of semi-classical wave-packets, which is done by Sundaram and Niu in Ref. [42].

By introducing the methods of the Boltzmann transport equation, we have shown that spin-less electron transport in a metal wire with a constant electric field can be viewed equivalently as diffusion of particles due to unequal chemical potentials in the reservoirs.

The transport of conduction electrons in an isotropic ferromagnetic metal wire subject to the spin-motive force was investigated. We focused on the spin-motive force generated by a Neel-type domain wall both moving along the wire and rotating. The Coulomb interaction between conduction electrons was included via an electric potential generated by the spin-motive induced accumulated charges. The results were the same in the case of only elastic scattering as when inelastic scattering was included. The moving domain wall generates a spin-polarized electric current, which only depends on the average of the spin-motive force. Since our approach to the problem was by looking at a steady-state with no time-dependence on the force, a constant electric current agrees with the continuity equation.

The electric potential induced by the Coulomb interaction between electrons cancels out the accumulated charge density in the whole wire, in the physical limit when the length of the domain wall is much larger than the Thomas-Fermi screening length. This makes physical sense, since the screening length is definitively the smallest length-scale in this limit, and screening is very effective in metals with

high electron density.

The limit of an abrupt domain wall results in the same spin-polarized current, but a non-zero charge density, in the form of a dipole following the position of the domain wall. A vanishing domain wall length is not realistic experimentally, and in this limit the adiabatic approximation breaks down. Another complication is that the Boltzmann equation does not describe processes which happen on length scales smaller than the Fermi wavelength.

We briefly discussed the effects of spin-flipping mechanisms. It seems that these processes couple the spin chemical potentials, but for a steady-state the total electric current is expected to be constant due to current conservation. This topic remains open for further investigations.

By comparing experimental domain wall velocities with typical parameters for diffusion, we conclude that our steady-state approach is a suitable approximation, at least for slowly moving domain walls.

References

[1] M. Johnson and R. H. Silsbee. Interfacial charge-spin coupling: Injection and detection of spin magnetization in metals. *Phys. Rev. Lett.*, 55:1790–1793, Oct 1985.

[2] M. N. Baibich, J. M. Broto, A. Fert, F. Nguyen Van Dau, F. Petroff, P. Etienne, G. Creuzet, A. Friederich, and J. Chazelas. Giant magnetoresistance of (001)fe/(001)cr magnetic superlattices. *Phys. Rev. Lett.*, 61:2472–2475, Nov 1988.

[3] G. Binasch, P. Grünberg, F. Saurenbach, and W. Zinn. Enhanced magnetoresistance in layered magnetic structures with antiferromagnetic interlayer exchange. *Phys. Rev. B*, 39:4828–4830, Mar 1989.

[4] A. Fert. Nobel lecture: Origin, development, and future of spintronics*. *Rev. Mod. Phys.*, 80:1517–1530, Dec 2008.

[5] J. C. Slonczewski. Current-driven excitation of magnetic multilayers. *Journal of Magnetism and Magnetic Materials*, 159(1):L1–L7, 1996.

[6] L. Berger. Emission of spin waves by a magnetic multilayer traversed by a current. *Phys. Rev. B*, 54:9353–9358, Oct 1996.

[7] M. Tsoi, A. G. M. Jansen, J. Bass, W.-C. Chiang, M. Seck, V. Tsoi, and P. Wyder. Excitation of a magnetic multilayer by an electric current. *Phys. Rev. Lett.*, 80:4281–4284, May 1998.

[8] A. Brataas, A. D. Kent, and H. Ohno. Current-induced torques in magnetic materials. *Nature Materials*, 11(5):372–381, April 2012.

[9] J. Xiao, A. Zangwill, and M. D. Stiles. Spin-transfer torque for continuously variable magnetization. *Phys. Rev. B*, 73:054428, Feb 2006.

[10] D. C. Ralph and M. D. Stiles. Spin transfer torques. *Journal of Magnetism and Magnetic Materials*, 320(7):1190 – 1216, 2008.

[11] E. B. Myers, D. C. Ralph, J. A. Katine, R. N. Louie, and R. A. Buhrman. Current-induced switching of domains in magnetic multilayer devices. *Science*, 285(5429):867–870, 1999.

[12] J. A. Katine and E. E. Fullerton. Device implications of spin-transfer torques. *Journal of Magnetism and Magnetic Materials*, 320(7):1217 – 1226, 2008.

[13] Y. Tserkovnyak, A. Brataas, and G. E. W. Bauer. Enhanced gilbert damping in thin ferromagnetic films. *Physical Review Letters*, 88(11):117601, 2002.

[14] Y. Tserkovnyak, A. Brataas, G. E. W. Bauer, and B. I. Halperin. Nonlocal magnetization dynamics in ferromagnetic heterostructures. *Rev. Mod. Phys.*, 77:1375–1421, Dec 2005.

[15] A. Brataas, Y. Tserkovnyak, G. E. W. Bauer, and P. J. Kelly. Spin pumping and spin transfer. In S. Maekawa, S. O. Valenzuela, E. Saitoh, and T. Kimura, editors, *Spin Current*, pages 87 – 135. Oxford University Press, Oxford, 2012.

[16] Y. Kajiwara, K. Harii, S. Takahashi, J. Ohe, K. Uchida, M. Mizuguchi, H. Umezawa, H. Kawai, K. Ando, K. Takanashi, et al. Transmission of electrical signals by spin-wave interconversion in a magnetic insulator. *Nature*, 464(7286):262–266, 2010.

[17] J. E. Hirsch. Spin hall effect. *Phys. Rev. Lett.*, 83:1834–1837, Aug 1999.

[18] G. E. Volovik. Linear momentum in ferromagnets. *Journal of Physics C: Solid State Physics*, 20(7):L83, 1987.

[19] S. A. Yang, G. S. D. Beach, C. Knutson, D. Xiao, Z. Zhang, M. Tsoi, Q. Niu, A. H. MacDonald, and J. L. Erskine. Topological electromotive force from domain-wall dynamics in a ferromagnet. *Phys. Rev. B*, 82:054410, Aug 2010.

[20] D. J. Griffiths. *Introduction to Electrodynamics* . Benjamin Cummings, 3rd edition, 1998.

[21] B. D. Cullity and C. D. Graham. *Introduction to Magnetic Materials*. Wiley-IEEE Press, 2nd edition, 2008.

[22] P. C. Hemmer. *Kvantemekanikk*. Tapir Akademiske Forlag, 5th edition, 2005.

[23] B. H. Bransden and C. J. Joachain. *Quantum Mechanics*. New York: Prentice-Hall, 2nd edition, 2000.

[24] P. J. Mohr, B. N. Taylor, and D. B. Newell. Codata recommended values of the fundamental physical constants: 2010*. *Rev. Mod. Phys.*, 84:1527–1605, Nov 2012.

[25] A. Brataas, G. E. W. Bauer, and P. J. Kelly. *Non-collinear Magnetoelectronics*. Physics reports. Elsevier, 2006.

[26] C. L. Dennis, R. P. Borges, L. D. Buda, U. Ebels, J. F. Gregg, M. Hehn, E. Jouguelet, K. Ounadjela, I. Petej, I. L. Prejbeanu, and M. J. Thornton. The defining length scales of mesomagnetism: a review. *Journal of Physics: Condensed Matter*, 14(49):R1175, 2002.

[27] Y. Tserkovnyak and M. Mecklenburg. Electron transport driven by nonequilibrium magnetic textures. *Physical Review B*, 77(13):134407, 2008.

[28] P. C. Hemmer. *Faste Stoffers Fysikk*. Tapir Akademiske Forlag, 1st edition, 1987.

[29] B. M. Smirnov. *Fermi–Dirac Distribution*, pages 57–73. Wiley-VCH Verlag GmbH and Co. KGaA, 2007.

[30] A. Brataas, Y. Tserkovnyak, and G. E. W. Bauer. Magnetization dissipation in ferromagnets from scattering theory. *Phys. Rev. B*, 84:054416, Aug 2011.

[31] T. L. Gilbert. A phenomenological theory of damping in ferromagnetic materials. *Magnetics, IEEE Transactions on*, 40(6):3443–3449, Nov 2004.

[32] D. J. Clarke, O. A. Tretiakov, G. W. Chern, Y. B. Bazaliy, and O. Tchernyshyov. Dynamics of a vortex domain wall in a magnetic nanostrip: Application of the collective-coordinate approach. *Physical Review B*, 78(13):134412, 2008.

[33] S. E. Barnes and S. Maekawa. Generalization of faraday's law to include nonconservative spin forces. *Phys. Rev. Lett.*, 98:246601, Jun 2007.

[34] B. R. Holstein. The adiabatic theorem and berry's phase. *Am. J. Phys*, 57(12):1079–1084, 1989.

[35] N. Nakabayashi and G. Tatara. Rashba-induced spin electromagnetic fields in the strong sd coupling regime. *New Journal of Physics*, 16(1):015016, January 2014.

[36] Y. Aharonov and D. Bohm. Significance of electromagnetic potentials in the quantum theory. *Phys. Rev.*, 115:485–491, Aug 1959.

[37] J. Singh. *Appendix B: Boltzmann Transport Theory*, pages 353–363. Wiley-VCH Verlag GmbH, 2007.

[38] C. Kittel. *Introduction to Solid State Physics*. J. Wiley, New York, 8th edition, 2005.

[39] F. Haas. Introduction. In *Quantum Plasmas*, volume 65 of *Springer Series on Atomic, Optical, and Plasma Physics*, pages 1–14. Springer New York, 2011.

[40] V. Zayets. Spin and charge transport in materials with spin-dependent conductivity. *Phys. Rev. B*, 86:174415, Nov 2012.

[41] M. Giroud, H. Courtois, K. Hasselbach, D. Mailly, and B. Pannetier. Superconducting proximity effect in a mesoscopic ferromagnetic wire. *Phys. Rev. B*, 58:R11872–R11875, Nov 1998.

[42] G. Sundaram and Q. Niu. Wave-packet dynamics in slowly perturbed crystals: Gradient corrections and berry-phase effects. *Phys. Rev. B*, 59:14915–14925, Jun 1999.

[43] H. Goldstein, C. P. Poole, and J. L. Safko. *Classical Mechanics* . Addison-Wesley, 3rd edition, June 2001.

A Appendix: Magnetization Dynamics

A.1 General Equations of Motion

To find the equations of motion in Eq. (3.3) we start with the LLG equation (3.1) and take the cross product with $\vec{m}$ on both sides, dot with $\dot{\vec{m}}$ and integrate over the sample volume. From this it follows

$$\begin{aligned}\vec{m}\times\dot{\vec{m}} &= -\gamma\mu_0\vec{m}\times\left(\vec{m}\times\vec{H}_{\text{eff}}\right)+\alpha\vec{m}\times\left(\vec{m}\times\dot{\vec{m}}\right)\\ &= -\gamma\mu_0\left(\vec{m}\left(\vec{m}\cdot\vec{H}_{\text{eff}}\right)-\vec{H}_{\text{eff}}\right)-\alpha\dot{\vec{m}},\end{aligned}\tag{A.1}$$

since $\vec{m}\cdot\dot{\vec{m}}=0$ for a unit vector. Then $\frac{d\vec{m}}{dt}=\frac{\partial\vec{m}}{\partial\xi_i}\xi_i$ is inserted into Eq. (A.1) such that

$$\vec{m}\times\frac{\partial\vec{m}}{\partial\xi_i}\dot{\xi}_i+\gamma\mu_0\left(\vec{m}\left(\vec{m}\cdot\vec{H}_{\text{eff}}\right)-\vec{H}_{\text{eff}}\right)+\alpha\frac{\partial\vec{m}}{\partial\xi_i}\dot{\xi}_i=0.\tag{A.2}$$

By multiplying Eq. (A.2) with $\frac{M_{\text{s}}}{\gamma}\frac{\partial\vec{m}}{\partial\xi_j}$, integrating over the volume and using that $\mu_0\vec{H}_{\text{eff}}=-\delta U/\delta\vec{M}_{\text{s}}(\vec{r})=-(1/M_{\text{s}})\delta U/\delta\vec{m}(\vec{r})$ then

$$\begin{aligned}0=&\frac{M_{\text{s}}}{\gamma}\int dV\left(\frac{\partial m}{\partial\xi_j}\right)\cdot\left(\vec{m}\times\frac{\partial\vec{m}}{\partial\xi_i}\right)\dot{\xi}_i-\int dV\frac{\partial\vec{m}}{\partial\xi_j}\cdot\left(-\frac{\delta U}{\delta\vec{m}}\right)\\ &+\alpha\frac{M_{\text{s}}}{\gamma}\int dV\left(\frac{\partial\vec{m}}{\partial\xi_j}\right)\cdot\left(\frac{\partial\vec{m}}{\partial\xi_i}\right)\dot{\xi}_i.\end{aligned}\tag{A.3}$$

If we now change the indices i,j in Eq. (A.3) and use the cyclic property of $\vec{a}\cdot(\vec{b}\times\vec{c})$, the result is

$$\begin{aligned}&-\int dV\frac{\delta U}{\delta\vec{m}}\cdot\frac{\partial\vec{m}}{\partial\xi_i}-\alpha\frac{M_{\text{s}}}{\gamma}\int dV\frac{\partial\vec{m}}{\partial\xi_i}\cdot\frac{\partial\vec{m}}{\partial\xi_j}\dot{\xi}_j+\frac{M_{\text{s}}}{\gamma}\int dV\vec{m}\cdot\left(\frac{\partial\vec{m}}{\partial\xi_i}\times\frac{\partial\vec{m}}{\partial\xi_j}\right)\dot{\xi}_j\\ &=0,\end{aligned}\tag{A.4}$$

and Eq. (A.4) is now on the form of Eq. (3.3), with quantities defined from Eqs. (3.4), (3.5) and (3.6).

A.2 Energy Minimization for the Tail-to-Tail Neel-Type Domain Wall

To minimize the free energy, U, in Eq. (3.7) one can use the Euler-Lagrange equation, since U is an integral of a functional $\varphi[\theta,\theta']$, where $\theta'\equiv\frac{\partial\theta}{\partial z}$ [43]. The Euler-Lagrange equation then reads

$$\frac{d}{dz}\left(\frac{\partial\varphi}{\partial\theta'}\right)=\frac{\partial\varphi}{\partial\theta}.\tag{A.5}$$

If we now write out φ from Eq. (3.8) in terms of the spherical coordinates it reads

$$\begin{aligned}\varphi =& \frac{A_{\mathrm{ex.s}}}{2}\left|\left(\frac{\partial\theta_{\mathrm{w}}}{\partial z}\right)^2(\cos\theta_{\mathrm{w}}\cos\phi_{\mathrm{w}},\cos\theta_{\mathrm{w}}\sin\phi_{\mathrm{w}},-\sin\theta_{\mathrm{w}})\right|^2 \\ & - B_0\cos\theta_{\mathrm{w}} + \frac{K_1}{2}(1-\cos^2\theta_{\mathrm{w}}) + \frac{K_2}{2}\sin^2\theta_{\mathrm{w}}\cos^2\phi_{\mathrm{w}} \\ =& \frac{A_{\mathrm{ex.s}}}{2}\left(\frac{\partial\theta_{\mathrm{w}}}{\partial z}\right)^2 - B_0\cos\theta_{\mathrm{w}} + \frac{1}{2}(K_1+K_2\cos^2\phi_{\mathrm{w}})\sin^2\theta_{\mathrm{w}}. \end{aligned} \tag{A.6}$$

The external magnetic field is ignored in the following, i.e. $B_0 = 0$. By putting the rest of φ from Eq. (A.6) in Eq. (A.5) then

$$\frac{d}{dz}(A_{\mathrm{ex.s}}\theta_{\mathrm{w}}') = (K_1 + K_2\cos^2\phi_{\mathrm{w}})\sin\theta_{\mathrm{w}}\cos\theta_{\mathrm{w}}. \tag{A.7}$$

It is assumed that the wall is prepared with some constant angle ϕ_{w}, such that $\cos^2\phi_{\mathrm{w}}$ is constant. The Eq. (A.7) is now equivalent to solving

$$\frac{\partial^2\theta_{\mathrm{w}}}{\partial z^2} = C^2\sin\theta_{\mathrm{w}}\cos\theta_{\mathrm{w}}, \tag{A.8}$$

where C is some constant. A solution Ansatz is $\theta_{\mathrm{w}}' = C\sin\theta_{\mathrm{w}}$, which solves Eq. (A.8), since

$$\theta_{\mathrm{w}}'' = \frac{\partial}{\partial z}C\sin\theta_{\mathrm{w}} = C\cos\theta_{\mathrm{w}}\frac{\partial\theta_{\mathrm{w}}}{\partial z} = C^2\cos\theta_{\mathrm{w}}\sin\theta_{\mathrm{w}}. \tag{A.9}$$

The solution in Eq. (3.9) solves Eq. (A.8), which follows from

$$\begin{aligned}\frac{\partial^2\theta_{\mathrm{w}}}{\partial z^2} &= \frac{\partial^2}{\partial z^2}\arccos\left(\tanh\left(\frac{z-r_{\mathrm{w}}}{\lambda_{\mathrm{w}}}\right)\right) \\ &= \frac{\partial}{\partial z}\frac{-1}{\lambda_{\mathrm{w}}\sqrt{1-\tanh^2(\frac{z-r_{\mathrm{w}}}{\lambda_{\mathrm{w}}})}}\frac{1}{\cosh^2(\frac{z-r_{\mathrm{w}}}{\lambda_{\mathrm{w}}})} \\ &= \frac{-1}{\lambda_{\mathrm{w}}}\frac{\partial}{\partial z}\frac{1}{\cosh(\frac{z-r_{\mathrm{w}}}{\lambda_{\mathrm{w}}})} \\ &= \frac{1}{\lambda_{\mathrm{w}}^2}\tanh\left(\frac{z-r_{\mathrm{w}}}{\lambda_{\mathrm{w}}}\right)\frac{1}{\cosh(\frac{z-r_{\mathrm{w}}}{\lambda_{\mathrm{w}}})} \\ &= C^2\cos\theta_{\mathrm{w}}\sin\theta_{\mathrm{w}}, \end{aligned} \tag{A.10}$$

with $C = -1/\lambda_{\mathrm{w}}$.

A.3 Magnetic Free Energy Integrals

The integral for the free energy in Eq. (3.7) can be done by taking the expression for φ from Eq. (A.6), using the expressions for $\partial\theta_{\mathrm{w}}/\partial z$ and θ_{w} from Eq. (A.10)

and integrate over z

$$\begin{aligned}\frac{U}{M_{\rm s}\mathcal{A}} =& \int_{-\infty}^{\infty} dz \Bigg(\frac{A_{\rm ex.s}}{2} \left(\frac{-1}{\lambda_{\rm w} \cosh(\frac{z-r_{\rm w}}{\lambda_{\rm w}})} \right)^2 - B_0 \tanh \frac{z-r_{\rm w}}{\lambda_{\rm w}} \\ &+ \frac{1}{2} \left(K_1 + K_2 \cos^2 \phi_{\rm w} \right) \frac{1}{\cosh^2(\frac{z-r_{\rm w}}{\lambda_{\rm w}})} \Bigg) \\ =& \frac{1}{2} \left(\frac{A_{\rm ex.s}}{\lambda_{\rm w}^2} + K_1 + K_2 \cos^2 \phi_{\rm w} \right) \int_{-\infty}^{\infty} dz \frac{1}{\cosh^2(\frac{z-r_{\rm w}}{\lambda_{\rm w}})} \\ &- B_0 \int_{-\infty}^{\infty} dz \tanh \frac{z-r_{\rm w}}{\lambda_{\rm w}}, \end{aligned} \tag{A.11}$$

which by changing variables in Eq. (A.11) to $x = (z - r_{\rm w})/\lambda_{\rm w}$ then it follows

$$\begin{aligned}\frac{U}{M_{\rm s}\mathcal{A}} =& \frac{1}{2} \left(\frac{A_{\rm ex.s}}{\lambda_{\rm w}^2} + K_1 + K_2 \cos^2 \phi_{\rm w} \right) \lambda_{\rm w} \int_{-\infty}^{\infty} dx \frac{1}{\cosh^2 x} - B_0 \lambda_{\rm w} \int_{-\infty}^{\infty} dx \tanh x \\ =& \frac{1}{2} \left(\frac{A_{\rm ex.s}}{\lambda_{\rm w}^2} + K_1 + K_2 \cos^2 \phi_{\rm w} \right) \lambda_{\rm w} \left[\tanh x \right]_{-\infty}^{\infty} - B_0 \lambda_{\rm w} \left[\ln(\cosh x) \right]_{-\infty}^{\infty} \\ =& \frac{1}{2} \left(\frac{A_{\rm ex.s}}{\lambda_{\rm w}^2} + K_1 + K_2 \cos^2 \phi_{\rm w} \right) \lambda_{\rm w} 2 \\ &- B_0 \lambda_{\rm w} \lim_{Z \to \infty} \ln \left[\frac{\cosh\left(\frac{Z-r_{\rm w}}{\lambda_{\rm w}}\right)}{\cosh\left(\frac{-Z-r_{\rm w}}{\lambda_{\rm w}}\right)} \right]. \end{aligned} \tag{A.12}$$

The last term in Eq. (A.12) is found by rewriting the limit such that

$$\begin{aligned} -B_0 \lambda_{\rm w} \lim_{Z \to \infty} \ln \left[\frac{\cosh\left(\frac{Z-r_{\rm w}}{\lambda_{\rm w}}\right)}{\cosh\left(\frac{-Z-r_{\rm w}}{\lambda_{\rm w}}\right)} \right] &= -B_0 \lambda_{\rm w} \lim_{Z \to \infty} \ln \left[\frac{e^{\frac{Z-r_{\rm w}}{\lambda_{\rm w}}} + e^{-\frac{Z-r_{\rm w}}{\lambda_{\rm w}}}}{e^{\frac{-Z-r_{\rm w}}{\lambda_{\rm w}}} + e^{-\frac{-Z-r_{\rm w}}{\lambda_{\rm w}}}} \right] \\ &= -B_0 \lambda_{\rm w} \lim_{Z \to \infty} \ln \left[\frac{e^{\frac{Z-r_{\rm w}}{\lambda_{\rm w}}}}{e^{-\frac{-Z-r_{\rm w}}{\lambda_{\rm w}}}} \right] \\ &= -B_0 \lambda_{\rm w} \lim_{Z \to \infty} \left(\frac{Z-r_{\rm w}}{\lambda_{\rm w}} + \frac{-Z-r_{\rm w}}{\lambda_{\rm w}} \right) \\ &= 2B_0 r_{\rm w}, \end{aligned} \tag{A.13}$$

and now Eqs. (A.12) and (A.13) give the result for U in Eq. (3.11).

To calculate Γ_{ij} in Eq. (3.5) one needs the derivatives of $\vec{m}$ with respect to the collective coordinates, and by recalling the expression for $\theta_{\rm w}$ from Eq. (3.9) it

follows

$$\begin{aligned}\frac{\partial \vec{m}}{\partial r} &= \frac{\partial \theta_{\rm w}}{\partial r}\frac{\partial}{\partial \theta_{\rm w}}\vec{m} = \frac{\partial}{\partial r}\left[\arccos\left(\tanh\left(\frac{z-r_{\rm w}}{\lambda_{\rm w}}\right)\right)\right]\frac{\partial}{\partial \theta_{\rm w}}\vec{m} \\ &= \frac{1}{\lambda_{\rm w}}\frac{1}{\cosh(\frac{z-r_{\rm w}}{\lambda_{\rm w}})}(\cos\theta_{\rm w}\cos\phi_{\rm w}, \cos\theta_{\rm w}\sin\phi_{\rm w}, -\sin\theta_{\rm w}) \\ &= \frac{1}{\lambda_{\rm w}}(\sin\theta_{\rm w}\cos\theta_{\rm w}\cos\phi_{\rm w}, \sin\theta_{\rm w}\cos\theta_{\rm w}\sin\phi_{\rm w}, -\sin^2\theta_{\rm w}). \end{aligned} \tag{A.14}$$

Similarily we have

$$\begin{aligned}\frac{\partial \vec{m}}{\partial \lambda_{\rm w}} &= \frac{\partial \theta_{\rm w}}{\partial \lambda_{\rm w}}\frac{\partial}{\partial \theta_{\rm w}}\vec{m} \\ &= \frac{z-r_{\rm w}}{\lambda_{\rm w}^2}\frac{1}{\cosh(\frac{z-r_{\rm w}}{\lambda_{\rm w}})}(\cos\theta_{\rm w}\cos\phi_{\rm w}, \cos\theta_{\rm w}\sin\phi_{\rm w}, -\sin\theta_{\rm w}) \\ &= \frac{z-r_{\rm w}}{\lambda_{\rm w}^2}(\sin\theta_{\rm w}\cos\theta_{\rm w}\cos\phi_{\rm w}, \sin\theta_{\rm w}\cos\theta_{\rm w}\sin\phi_{\rm w}, -\sin^2\theta_{\rm w}), \end{aligned} \tag{A.15}$$

and

$$\frac{\partial}{\partial \phi_{\rm w}}\vec{m} = (-\sin\theta_{\rm w}\sin\phi_{\rm w}, \sin\theta_{\rm w}\cos\phi_{\rm w}, 0). \tag{A.16}$$

From Eqs. (A.14), (A.15) and (A.16) it is clear that

$$\frac{\partial \vec{m}}{\partial \phi_{\rm w}}\cdot\frac{\partial \vec{m}}{\partial r_{\rm w}} = 0 = \frac{\partial \vec{m}}{\partial \phi_{\rm w}}\cdot\frac{\partial \vec{m}}{\partial \lambda_{\rm w}}. \tag{A.17}$$

The diagonal terms in Eq. (3.5) can now be found. First

$$\begin{aligned}\Gamma_{rr} &= \frac{\mathcal{A}M_{\rm s}}{\gamma}\int_{-\infty}^{\infty} dz \frac{\partial \vec{m}}{\partial r_{\rm w}}\cdot\frac{\partial \vec{m}}{\partial r_{\rm w}} \\ &= \frac{\mathcal{A}M_{\rm s}}{\gamma}\int_{-\infty}^{\infty} dz \frac{1}{\lambda_{\rm w}^2}\sin^2\theta_{\rm w} \\ &= \frac{\mathcal{A}M_{\rm s}}{\gamma\lambda_{\rm w}^2}\int_{-\infty}^{\infty} dz \frac{1}{\cosh^2\left(\frac{z-r_{\rm w}}{\lambda_{\rm w}}\right)} \\ &= \frac{2\mathcal{A}M_{\rm s}}{\gamma\lambda_{\rm w}}, \end{aligned} \tag{A.18}$$

by using the integral from Eq. (A.12). The next term is

$$\begin{aligned}\Gamma_{\phi\phi} &= \frac{\mathcal{A}M_{\rm s}}{\gamma}\int_{-\infty}^{\infty} dz \frac{\partial \vec{m}}{\partial \phi_{\rm w}}\cdot\frac{\partial \vec{m}}{\partial \phi_{\rm w}} \\ &= \frac{\mathcal{A}M_{\rm s}}{\gamma}\int_{-\infty}^{\infty} dz \sin^2\theta_{\rm w} \\ &= \frac{2\mathcal{A}M_{\rm s}\lambda_{\rm w}}{\gamma}. \end{aligned} \tag{A.19}$$

The last term is

$$\begin{aligned}
\Gamma_{\lambda\lambda} &= \frac{\mathcal{A}M_\mathrm{s}}{\gamma}\int_{-\infty}^{\infty} dz \frac{\partial\vec{m}}{\partial\lambda_\mathrm{w}}\cdot\frac{\partial\vec{m}}{\partial\lambda_\mathrm{w}} \\
&= \frac{\mathcal{A}M_\mathrm{s}}{\gamma}\int_{-\infty}^{\infty} dz \frac{(z-r_\mathrm{w})^2}{\lambda_\mathrm{w}^4}\sin^2\theta_\mathrm{w} \\
&= \frac{\mathcal{A}M_\mathrm{s}}{\gamma\lambda_\mathrm{w}^2}\int_{-\infty}^{\infty} dz \frac{(z-r_\mathrm{w})^2}{\lambda_\mathrm{w}^2}\frac{1}{\cosh^2(\frac{z-r_\mathrm{w}}{\lambda_\mathrm{w}})} \\
&= \frac{\mathcal{A}M_\mathrm{s}}{\gamma\lambda_\mathrm{w}}\int_{-\infty}^{\infty} dx \frac{x^2}{\cosh^2 x} \\
&= \frac{\mathcal{A}M_\mathrm{s}}{\gamma\lambda_\mathrm{w}}\frac{\pi^2}{6},
\end{aligned} \tag{A.20}$$

where the last integral in Eq. (A.20) was done with Wolfram Mathematica 10.

To find the components of G_{ij} in Eq. (3.6) we use Eqs. (A.14) and (A.16) to calculate

$$\begin{aligned}
G_{r\phi} &= \frac{M_\mathrm{s}\mathcal{A}}{\gamma}\int dz\vec{m}\cdot\frac{\partial\vec{m}}{\partial r_\mathrm{w}}\times\frac{\partial\vec{m}}{\partial\phi_\mathrm{w}} \\
&= \frac{M_\mathrm{s}\mathcal{A}}{\gamma\lambda_\mathrm{w}}\int dz\sin^2\theta\vec{m}\cdot(\sin\theta_\mathrm{w}\cos\phi_\mathrm{w},\sin\theta_\mathrm{w}\sin\phi_\mathrm{w},\cos\theta_\mathrm{w}) \\
&= \frac{M_\mathrm{s}\mathcal{A}}{\gamma\lambda_\mathrm{w}}\int_{-\infty}^{\infty} dz\sin^2\theta_\mathrm{w} \\
&= \frac{M_\mathrm{s}\mathcal{A}}{\gamma}2,
\end{aligned} \tag{A.21}$$

where the last integral in Eq. (A.21) is solved in a similar way as in Eq. (A.12).

B Appendix: Spin-Motive Force

Some useful trigonometric relations are

$$1 + \cos\theta = 2\cos^2\frac{\theta}{2}, \tag{B.1}$$

$$1 - \cos\theta = 2\sin^2\frac{\theta}{2}, \tag{B.2}$$

$$\sin\theta = 2\sin\frac{\theta}{2}\cos\frac{\theta}{2}, \tag{B.3}$$

and they will be used in the following.

B.1 Diagonalization in the Gauge Transformation

From the Pauli-matrices in Eq. (2.8) and the parametrization of $\vec{m}$ in Eq. (4.9) then

$$\vec{\sigma}\cdot\vec{m} = \begin{pmatrix} \cos\theta & \sin\theta e^{-i\phi} \\ \sin\theta e^{i\phi} & -\cos\theta \end{pmatrix}, \tag{B.4}$$

by using the Euler identity for $e^{\pm i\phi} = \cos\phi \pm i\sin\phi$.

The rotation-matrix $\hat{U}$ is determined by Eq. (4.3), and by using that $\hat{U}^{-1} = \hat{U}$. The condition is

$$\vec{\sigma}\cdot\vec{m} = \hat{U}\sigma_z\hat{U} = \hat{U}^{-1}\sigma_z\hat{U}. \tag{B.5}$$

Eq. (B.5) is equivalent to the diagonalization of the matrix $\vec{\sigma}\cdot\vec{m}$, with σ_z on diagonal form with eigenvalues λ_1, λ_2 equal to +1 and -1 respectively. The matrix $\hat{U}$ can then be found by finding the corresponding eigenvectors, $\vec{x}$, to the eigenvalues, i.e. solving the systems $(\vec{\sigma}\cdot\vec{m} - I\lambda_i)\vec{x} = 0$ for $i = 1, 2$. These eigenvectors correspond to the columns in the $\hat{U}$-matrix, up to a normalization constant.

For the first eigenvalue, $\lambda_1 = +1$, the linear system is

$$\begin{pmatrix} \cos\theta - 1 & \sin\theta e^{-i\phi} \\ \sin\theta e^{i\phi} & -\cos\theta - 1 \end{pmatrix}\begin{pmatrix} x_1 \\ x_2 \end{pmatrix} = 0, \tag{B.6}$$

which via Eqs. (B.1), (B.2) and (B.3) reduces to

$$-\sin\frac{\theta}{2}x_1 + \cos\frac{\theta}{2}e^{-i\phi}x_2 = 0. \tag{B.7}$$

One solution to Eq. (B.7) is $x_1 = \cos\frac{\theta}{2}$, $x_2 = \sin\frac{\theta}{2}e^{i\phi}$. The factors of $e^{\pm i\phi}$ is chosen such that $\hat{U}$ becomes Hermitian.

For the other eigenvalue, $\lambda_2 = -1$, the system is

$$\begin{pmatrix} \cos\theta + 1 & \sin\theta e^{-i\phi} \\ \sin\theta e^{i\phi} & 1 - \cos\theta \end{pmatrix}\begin{pmatrix} x_3 \\ x_4 \end{pmatrix} = 0, \tag{B.8}$$

which similarly is reduced to

$$\cos\frac{\theta}{2}e^{i\phi}x_3 + \sin\frac{\theta}{2}x_4 = 0. \tag{B.9}$$

A solution to Eq. (B.9) is $x_3 = \sin\frac{\theta}{2}e^{-i\phi}$ and $x_4 = -\cos\frac{\theta}{2}$.

The matrix $\hat{U}$ consists of the two eigenvectors, found from the systems in Eqs. (B.6) and (B.8), as its column vectors. The transformation matrix is then

$$\hat{U} = \begin{pmatrix} \cos\frac{\theta}{2} & \sin\frac{\theta}{2}e^{-i\phi} \\ \sin\frac{\theta}{2}e^{i\phi} & -\cos\frac{\theta}{2} \end{pmatrix}. \tag{B.10}$$

From Eq. (B.10) then $\hat{U}$ is hermitian, i. e. $\hat{U} = \hat{U}^\dagger$, and $\hat{U}$ satisfies $\hat{U}\hat{U} = \hat{1}$.

It is helpful to write the matrix $\hat{U}$ as the dot product between the Pauli matrix vector, σ, and a vector $\vec{n}$, such that

$$\hat{U} = (\vec{\sigma}\cdot\vec{n}) = \sigma_x n_x + \sigma_y n_y + \sigma_z n_z. \tag{B.11}$$

The unit vector $\vec{n}$ is found by inspecting $\hat{U}$ from Eq. (B.10) and using the sigma-matrices in Eq. (2.8), resulting in

$$\vec{n} = \vec{n}(\theta,\phi) = \hat{x}\sin\frac{\theta}{2}\cos\phi + \hat{y}\sin\frac{\theta}{2}\sin\phi + \hat{z}\cos\frac{\theta}{2}. \tag{B.12}$$

It is shown that $\vec{n} \propto \vec{m} + \hat{z}$ by calculating

$$\begin{aligned}
\frac{\vec{m}+\hat{z}}{|\vec{m}+\hat{z}|} &= \frac{\hat{x}\sin\theta\cos\phi + \hat{y}\sin\theta\sin\phi + \hat{z}(\cos\theta+1)}{\sqrt{\sin^2\theta\cos^2\phi + \sin^2\theta\sin^2\phi + (1+\cos\theta)^2}} \\
&= \frac{\hat{x}2\sin\frac{\theta}{2}\cos\frac{\theta}{2}\cos\phi + \hat{y}2\sin\frac{\theta}{2}\cos\frac{\theta}{2}\sin\phi + \hat{z}2\cos^2\frac{\theta}{2}}{\sqrt{\sin^2\theta + 1 + 2\cos\theta + \cos^2\theta}} \\
&= \frac{2\cos\frac{\theta}{2}}{\sqrt{4\cos^2\frac{\theta}{2}}}\left(\hat{x}\sin\frac{\theta}{2}\cos\phi + \hat{y}\sin\frac{\theta}{2}\sin\phi + \hat{z}\cos\frac{\theta}{2}\right) \\
&= \vec{n},
\end{aligned} \tag{B.13}$$

which agrees with Eq. (B.12).

B.2 Gauge Fields

The effective vector potential, $\vec{A}$, in Eq. (4.8) is found by comparing Eqs. (4.4) and (4.6). This leads to the condition

$$\hat{U}\frac{p^2}{2m}\hat{U} = \frac{1}{2m}\left(\vec{p} - \vec{A}\right)^2, \tag{B.14}$$

which is expanded as

$$-\hbar^2\hat{U}\frac{\partial}{\partial x_i}\frac{\partial}{\partial x_i}\hat{U} = -\hbar^2\frac{\partial}{\partial x_i}\frac{\partial}{\partial x_i} + i\hbar\frac{\partial}{\partial x_i}A_i + i\hbar A_i\frac{\partial}{\partial x_i} + A^2. \tag{B.15}$$

It is reasonable from Eq. (B.15) to guess that A_i is proportional to $i\hbar$, i.e. $A_i = i\hbar X_i$ for some $\vec{X}$. This relates the operators by

$$\hat{U}\frac{\partial}{\partial x_i}\frac{\partial}{\partial x_i}\hat{U} = \frac{\partial}{\partial x_i}\frac{\partial}{\partial x_i} + \frac{\partial}{\partial x_i}X_i + X_i\frac{\partial}{\partial x_i} + X^2. \tag{B.16}$$

One solution for $\vec{X}$ is $X_i = \hat{U}\frac{\partial \hat{U}}{\partial x_i}$.

To show that this is right, one must remember that the operators in Eq. (B.16) are acting on something (e.g a spinor). Therefore one must distinguish between the notation $\frac{\partial}{\partial x_i}\hat{U}$ and $\frac{\partial \hat{U}}{\partial x_i}$, which are not the same. We start by expanding the left-hand side of equation (B.16),

$$\begin{aligned}\hat{U}\frac{\partial}{\partial x_i}\frac{\partial}{\partial x_i}\hat{U} &= \hat{U}\frac{\partial}{\partial x_i}\left(\frac{\partial \hat{U}}{\partial x_i} + \hat{U}\frac{\partial}{\partial x_i}\right) = \hat{U}\left(\frac{\partial^2 \hat{U}}{\partial x_i^2} + \frac{\partial \hat{U}}{\partial x_i}\frac{\partial}{\partial x_i} + \frac{\partial \hat{U}}{\partial x_i}\frac{\partial}{\partial x_i} + \hat{U}\frac{\partial^2}{\partial x_i^2}\right) \\ &= \hat{U}\frac{\partial^2 \hat{U}}{\partial x_i^2} + 2\hat{U}\frac{\partial \hat{U}}{\partial x_i}\frac{\partial}{\partial x_i} + \frac{\partial^2}{\partial x_i^2}.\end{aligned} \tag{B.17}$$

One trick that is useful in the next is that

$$0 = \frac{\partial}{\partial x_i}\hat{1} = \frac{\partial}{\partial x_i}\hat{U}\hat{U} = \frac{\partial \hat{U}}{\partial x_i}\hat{U} + \hat{U}\frac{\partial \hat{U}}{\partial x_i}, \tag{B.18}$$

so $\frac{\partial \hat{U}}{\partial x_i}\hat{U} = -\hat{U}\frac{\partial \hat{U}}{\partial x_i}$. Now if we insert $X_i = \hat{U}\frac{\partial \hat{U}}{\partial x_i}$ in the right-hand side of equation (B.16) it follows

$$\begin{aligned}&\frac{\partial^2}{\partial x_i^2} + \frac{\partial}{\partial x_i}\hat{U}\frac{\partial \hat{U}}{\partial x_i} + \hat{U}\frac{\partial \hat{U}}{\partial x_i}\frac{\partial}{\partial x_i} + \hat{U}\frac{\partial \hat{U}}{\partial x_i}\hat{U}\frac{\partial \hat{U}}{\partial x_i} \\ &\qquad = \frac{\partial^2}{\partial x_i^2} + \frac{\partial \hat{U}}{\partial x_i}\frac{\partial \hat{U}}{\partial x_i} + \hat{U}\frac{\partial^2 \hat{U}}{\partial x_i^2} + \hat{U}\frac{\partial \hat{U}}{\partial x_i}\frac{\partial}{\partial x_i} + \hat{U}\frac{\partial \hat{U}}{\partial x_i}\frac{\partial}{\partial x_i} - \frac{\partial \hat{U}}{\partial x_i}\hat{U}\hat{U}\frac{\partial \hat{U}}{\partial x_i} \\ &\qquad = \frac{\partial^2}{\partial x_i^2} + \hat{U}\frac{\partial^2 \hat{U}}{\partial x_i^2} + 2\hat{U}\frac{\partial \hat{U}}{\partial x_i}\frac{\partial}{\partial x_i} + \frac{\partial \hat{U}}{\partial x_i}\frac{\partial \hat{U}}{\partial x_i} - \frac{\partial \hat{U}}{\partial x_i}\frac{\partial \hat{U}}{\partial x_i} \\ &\qquad = \frac{\partial^2}{\partial x_i^2} + \hat{U}\frac{\partial^2 \hat{U}}{\partial x_i^2} + 2\hat{U}\frac{\partial \hat{U}}{\partial x_i}\frac{\partial}{\partial x_i},\end{aligned} \tag{B.19}$$

which is the same as in equation (B.17).

Further, it is possible to show that the vector potential can be written as

$$\vec{A}_i = i\hbar\hat{U}\frac{\partial \hat{U}}{\partial x_i} = -\hbar\vec{\sigma}\cdot\left(\vec{n}\times\frac{\partial \vec{n}}{\partial x_i}\right), \tag{B.20}$$

for the i'th component of $\vec{A}$. To show this, we use the relationship between the multiplication of the Pauli spin matrices

$$\sigma_i\sigma_j = \delta_{ij} + i\epsilon_{ijk}\sigma_k, \tag{B.21}$$

where ϵ_{ijk} is the Levi-Cevita tensor and δ_{ij} is the Kronecker delta (with a 2x2 identity matrix implied) [23]. Eq. (B.20) is checked by using Eq. (B.21) and also that $\vec{n}\cdot(\partial_i\vec{n})=0$, since the change of a unit vector is always perpendicular to the vector itself. The effective vector potential is thus

$$\begin{aligned}\vec{A}_i &= i\hbar\hat{U}[\partial_i\hat{U}] = i\hbar\vec{\sigma}\cdot\vec{n}(\partial_i\vec{\sigma}\cdot\vec{n}) = i\hbar\sigma_j n_j\sigma_k\partial_i n_k \\ &= i\hbar(\delta_{jk}+i\epsilon_{jkl}\sigma_l)n_j(\partial_i n_k) = i\hbar n_j(\partial_i n_j) - \hbar\epsilon_{jkl}\sigma_l n_j(\partial_i n_k) \\ &= i\hbar\vec{n}\cdot(\partial_i\vec{n}) - \hbar\epsilon_{ljk}n_j(\partial_i n_k)\sigma_l = 0 - \hbar[\vec{n}\times(\partial_i\vec{n})]_l\sigma_l \\ &= -\hbar\vec{\sigma}\cdot(\vec{n}\times\partial_i\vec{n}). \end{aligned} \tag{B.22}$$

In a similar way the potential $\hat{V}$ is written as

$$\begin{aligned}\hat{V} &= -i\hbar\hat{U}(\partial_t\hat{U}) = -i\hbar\sigma_i n_i(\partial_t\sigma_j n_j) = -i\hbar(n_i(\partial_t n_i) + i\epsilon_{ijk}\sigma_k n_i(\partial_t n_j)) \\ &= 0 + \hbar\epsilon_{kij}\sigma_k n_i(\partial_t n_j) = \hbar\sigma_k[\vec{n}\times(\partial_t\vec{n})]_k \\ &= \hbar\vec{\sigma}\cdot(\vec{n}\times(\partial_t\vec{n})). \end{aligned} \tag{B.23}$$

By using this we can simplify the equations further, but first it is useful to calculate the derivatives of $\vec{n}$,

$$\begin{aligned}\frac{\partial}{\partial x_i}\vec{n} =& \frac{\partial}{\partial x_i}\left(\hat{x}\sin\frac{\theta}{2}\cos\phi + \hat{y}\sin\frac{\theta}{2}\sin\phi + \hat{z}\cos\frac{\theta}{2}\right) \\ =& \frac{\hat{x}}{2}\cos\frac{\theta}{2}\cos\phi\left(\frac{\partial\theta}{\partial x_i}\right) - \hat{x}\sin\frac{\theta}{2}\sin\phi\left(\frac{\partial\phi}{\partial x_i}\right) + \frac{\hat{y}}{2}\cos\frac{\theta}{2}\sin\phi\left(\frac{\partial\theta}{\partial x_i}\right) \\ &+ \hat{y}\sin\frac{\theta}{2}\cos\phi\left(\frac{\partial\phi}{\partial x_i}\right) - \frac{\hat{z}}{2}\sin\frac{\theta}{2}\left(\frac{\partial\theta}{\partial x_i}\right), \end{aligned} \tag{B.24}$$

and similarily for the time derivative

$$\begin{aligned}\frac{\partial}{\partial t}\vec{n} =& \frac{\hat{x}}{2}\cos\frac{\theta}{2}\cos\phi\left(\frac{\partial\theta}{\partial t}\right) - \hat{x}\sin\frac{\theta}{2}\sin\phi\left(\frac{\partial\phi}{\partial t}\right) + \frac{\hat{y}}{2}\cos\frac{\theta}{2}\sin\phi\left(\frac{\partial\theta}{\partial t}\right) \\ &+ \hat{y}\sin\frac{\theta}{2}\cos\phi\left(\frac{\partial\phi}{\partial t}\right) - \frac{\hat{z}}{2}\sin\frac{\theta}{2}\left(\frac{\partial\theta}{\partial t}\right). \end{aligned} \tag{B.25}$$

Now the projected potentials are

$$\begin{aligned}\hat{V} =& \hbar\vec{\sigma}\cdot\left(\vec{n}\times\frac{\partial\vec{n}}{\partial t}\right) \to \hbar\sigma_z\hat{z}\cdot\left(\vec{n}\times\frac{\partial\vec{n}}{\partial t}\right) \\ =& \hbar\sigma_z\left(\epsilon_{312}n_1\left(\frac{\partial\vec{n}}{\partial t}\right)_2 + \epsilon_{321}n_2\left(\frac{\partial\vec{n}}{\partial t}\right)_1\right) \\ =& \hbar\sigma_z\Bigg(\sin\frac{\theta}{2}\cos\phi\left(\frac{1}{2}\cos\frac{\theta}{2}\sin\phi\left(\frac{\partial\theta}{\partial t}\right) + \sin\frac{\theta}{2}\cos\phi\left(\frac{\partial\phi}{\partial t}\right)\right) \\ &- \sin\frac{\theta}{2}\sin\phi\left(\frac{1}{2}\cos\frac{\theta}{2}\cos\phi\left(\frac{\partial\theta}{\partial t}\right) - \sin\frac{\theta}{2}\sin\phi\left(\frac{\partial\phi}{\partial t}\right)\right)\Bigg) \\ =& \hbar\sigma_z\frac{\partial\phi}{\partial t}\left(\sin^2\frac{\theta}{2}\cos^2\phi + \sin^2\frac{\theta}{2}\sin^2\phi\right) \\ =& \hbar\sigma_z\sin^2\frac{\theta}{2}\left(\frac{\partial\phi}{\partial t}\right), \end{aligned} \tag{B.26}$$

and smiliarily for the vector potential (by the symmetry of the derivatives of $\vec{n}$, $\partial_i \leftrightarrow \partial_t$) one gets

$$\begin{aligned}\vec{A}_i &= -\hbar\vec{\sigma}\cdot\left(\vec{n}\times\frac{\partial\vec{n}}{\partial x_i}\right) \to -\hbar\sigma_z\hat{z}\cdot\left(\vec{n}\times\frac{\partial\vec{n}}{\partial x_i}\right)\\ &= -\hbar\sigma_z\sin^2\frac{\theta}{2}\left(\frac{\partial\phi}{\partial x_i}\right).\end{aligned} \tag{B.27}$$

From Eqs. (B.26) and (B.27) the components of the effective electric field is

$$\begin{aligned}E_i &= -\frac{\partial}{\partial t}A_i - \frac{\partial}{\partial x_i}\hat{V} = -\frac{\partial}{\partial t}\left(-\hbar\sigma_z\sin^2\frac{\theta}{2}\left(\frac{\partial\phi}{\partial x_i}\right)\right) - \frac{\partial}{\partial x_i}\hbar\sigma_z\sin^2\frac{\theta}{2}\left(\frac{\partial\phi}{\partial t}\right)\\ &= \hbar\sigma_z\left(\sin^2\frac{\theta}{2}\frac{\partial^2\phi}{\partial t\partial x_i} + \sin\frac{\theta}{2}\cos\frac{\theta}{2}\frac{\partial\theta}{\partial t}\frac{\partial\phi}{\partial x_i} - \sin\frac{\theta}{2}\cos\frac{\theta}{2}\frac{\partial\theta}{\partial x_i}\frac{\partial\phi}{\partial t} - \sin^2\frac{\theta}{2}\frac{\partial^2\phi}{\partial x_i\partial t}\right)\\ &= \frac{\hbar}{2}\sigma_z\sin\theta\left(\frac{\partial\theta}{\partial t}\frac{\partial\phi}{\partial x_i} - \frac{\partial\theta}{\partial x_i}\frac{\partial\phi}{\partial t}\right),\end{aligned} \tag{B.28}$$

where we have used that $\frac{\partial}{\partial x_i}$ and $\frac{\partial}{\partial t}$ commutes and also the trigonometric relation in (B.3). The components of the magnetic field then are

$$\begin{aligned}B_i &= [\nabla\times\vec{A}]_i = \epsilon_{ijk}\frac{\partial}{\partial x_j}A_k\\ &= -\hbar\sigma_z\epsilon_{ijk}\left(\left(\frac{\partial\sin^2\frac{\theta}{2}}{\partial x_j}\right)\left(\frac{\partial\phi}{\partial x_k}\right) + \sin^2\frac{\theta}{2}\frac{\partial^2\phi}{\partial x_j\partial x_k}\right)\\ &= -\hbar\sigma_z\epsilon_{ijk}\sin\frac{\theta}{2}\cos\frac{\theta}{2}\frac{\partial\theta}{\partial x_j}\frac{\partial\phi}{\partial x_k}\\ &= \frac{\hbar}{2}\sigma_z\sin\theta[\nabla\phi\times\nabla\theta]_i,\end{aligned} \tag{B.29}$$

where we have used that $\epsilon_{ijk}\partial_j\partial_k = 0$, since one can just interchange the labels j,k and get the negative of what one started with, i.e. it has to be zero.

We now show the equivalence between Eqs. (4.15) and (4.18). The derivatives of $\vec{m}$ is

$$\begin{aligned}\partial_t\vec{m} &= \partial_t(\sin\theta\cos\phi,\sin\theta\sin\phi,\cos\theta)\\ &= ((\partial_t\theta)\cos\theta\cos\phi - (\partial_t\phi)\sin\theta\sin\phi, (\partial_t\theta)\cos\theta\sin\phi + (\partial_t\phi)\sin\theta\cos\phi, -(\partial_t\theta)\sin\theta)\\ &= (\partial_t\theta)(\cos\theta\cos\phi,\cos\theta\sin\phi,-\sin\theta) + (\partial_t\phi)(-\sin\theta\sin\phi,\sin\theta\cos\phi,0)\\ &\equiv (\partial_t\theta)\vec{a} + (\partial_t\phi)\vec{b},\end{aligned} \tag{B.30}$$

where we have just defined two vectors $\vec{a}$ and $\vec{b}$ to make the calculations easier. In the same way one finds that the spatial derivatives are

$$\partial_i\vec{m} = (\partial_i\theta)\vec{a} + (\partial_i\phi)\vec{b}. \tag{B.31}$$

From Eqs. (B.30) and (B.31) the crossproduct between the derivatives is

$$\begin{aligned}(\partial_t\vec{m})\times(\partial_i\vec{m}) &= [(\partial_t\theta)\vec{a}+(\partial_t\phi)\vec{b}]\times[(\partial_i\theta)\vec{a}+(\partial_i\phi)\vec{b}]\\ &= (\partial_t\theta)(\partial_i\theta)\vec{a}\times\vec{a}+(\partial_t\theta)(\partial_i\phi)\vec{a}\times\vec{b}+(\partial_i\phi)(\partial_t\theta)\vec{b}\times\vec{a}+(\partial_t\phi)(\partial_i\phi)\vec{b}\times\vec{b}\\ &= [(\partial_t\theta)(\partial_i\phi)-(\partial_i\phi)(\partial_t\theta)]\vec{a}\times\vec{b}, \qquad \text{(B.32)}\end{aligned}$$

where we have used that the crossproduct between a vector and itself is zero and also that $\vec{a}\times\vec{b}=-\vec{b}\times\vec{a}$. We can now calculate the dot product between $\vec{m}$ and the crossproduct-term in Eq. (B.32).

$$\begin{aligned}\vec{m}\cdot(\vec{a}\times\vec{b}) =& m_i\epsilon_{ijk}a_jb_k\\ =& m_1(a_2b_3-a_3b_2)+m_2(a_3b_1-a_1b_3)+m_3(a_1b_2-a_2b_1)\\ =& \sin\theta\cos\phi(0-(-)\sin\theta\sin\theta\cos\phi)+\sin\theta\sin\phi((-\sin\theta)(-)\sin\theta\sin\phi-0)\\ &+\cos\theta(\cos\theta\cos\phi\sin\theta\cos\phi-\cos\theta\sin\phi(-\sin\theta)\sin\phi)\\ =& \sin\theta(\sin^2\theta\cos^2\phi+\sin^2\phi\sin^2\theta+\cos^2\theta\cos^2\phi+\cos^2\theta\sin^2\phi)\\ =& \sin\theta. \qquad \text{(B.33)}\end{aligned}$$

From Eqs. (B.32) and (B.33) we now have that

$$\begin{aligned}\frac{\hbar}{2}\sigma_z\vec{m}\cdot[(\partial_t\vec{m})\times(\partial_i\vec{m})] &= \frac{\hbar}{2}\sigma_z[(\partial_t\theta)(\partial_i\phi)-(\partial_i\theta)(\partial_t\phi)]\vec{m}\cdot(\vec{a}\times\vec{b})\\ &= \frac{\hbar}{2}\sigma_z[(\partial_t\theta)(\partial_i\phi)-(\partial_i\theta)(\partial_t\phi)]\sin\theta, \qquad \text{(B.34)}\end{aligned}$$

and thus Eqs. (4.15) and (4.18) are equivalent.

C Appendix: Berry's Phase

C.1 Adiabatic Approximation

By inserting Eq. (5.3) in Eq. (5.1) it follows

$$\begin{aligned} i\hbar\frac{\partial}{\partial t}|\psi(t)\rangle =& i\hbar\frac{\partial}{\partial t}\sum_n c_n(t)e^{-\frac{i}{\hbar}\int_0^t E_n(t')dt'}|\psi_n(t)\rangle \\ =& i\hbar\sum_n \frac{\partial c_n(t)}{\partial t}e^{-i\epsilon_n(t)}|\psi_n(t)\rangle + \sum_n c_n(t)E_n(t)e^{-i\epsilon_n(t)}|\psi_n(t)\rangle \\ &+\sum_n c_n(t)e^{-i\epsilon_n(t)}(i\hbar\frac{\partial}{\partial t}|\psi_n(t)\rangle) \qquad \text{(C.1)} \\ =& H(t)|\psi(t)\rangle = \sum_n c_n(t)e^{-i\epsilon_n(t)}H(t)|\psi_n(t)\rangle, \qquad \text{(C.2)} \end{aligned}$$

since $H|\psi_n\rangle = E_n|\psi_n\rangle$, and the term in Eq. (C.2) cancels the second term in Eq. (C.1). What remains is then

$$\sum_n \frac{\partial c_n(t)}{\partial t}e^{-i\epsilon_n(t)}|\psi_n(t)\rangle = -\sum_n c_n(t)e^{-i\epsilon_n(t)}\frac{\partial}{\partial t}|\psi_n(t)\rangle. \qquad \text{(C.3)}$$

By projecting Eq, (C.3) onto an arbitrary $\langle\psi_m(t)|$ and using that $\langle\psi_m|\psi_n\rangle = \delta_{mn}$, then

$$\frac{\partial c_m(t)}{\partial t}e^{-i\epsilon_m(t)} = -\sum_n c_n(t)e^{-i\epsilon_n(t)}\langle\psi_m(t)|\frac{\partial}{\partial t}|\psi_n(t)\rangle, \qquad \text{(C.4)}$$

which is the same as Eq. (5.4).

The off-diagonal elements of $\langle\psi_m(t)|\frac{\partial}{\partial t}|\psi_n(t)\rangle$ in Eq. (C.4) are found by taking the time derivative of the time independent Schrodinger equation

$$\begin{aligned} \frac{\partial}{\partial t}H(t)|\psi_n(t)\rangle &= \frac{\partial H}{\partial t}|\psi_n(t)\rangle + H\left(\frac{\partial}{\partial t}|\psi_n(t)\rangle\right) \\ &= \frac{\partial}{\partial t}E_n(t)|\psi_n(t)\rangle = \dot{E_n}|\psi_n(t)\rangle + E_n(t)\frac{\partial}{\partial t}|\psi_n(t)\rangle. \qquad \text{(C.5)} \end{aligned}$$

By projecting everything in Eq. (C.5) onto $\langle\psi_m|$ the result is

$$\langle\psi_m(t)|\frac{\partial H}{\partial t}|\psi_n(t)\rangle = E_n(t)\langle\psi_m|\frac{\partial}{\partial t}|\psi_n\rangle - \langle\psi_m|H\frac{\partial}{\partial t}|\psi_n\rangle + \dot{E_n}\delta_{mn}, \qquad \text{(C.6)}$$

and since H is hermitian it can act to the left onto $\langle\psi_m(t)|$ and give $E_m(t)$. For the diagonal elements $n \neq m$ the Eq. (C.6) is reduced to

$$\langle\psi_m(t)|\frac{\partial H}{\partial t}|\psi_n(t)\rangle = (E_n(t) - E_m(t))\langle\psi_m|\frac{\partial}{\partial t}|\psi_n\rangle. \qquad \text{(C.7)}$$

By assuming that there are no degeneracies one can divide Eq. (C.7) by $E_n - E_m$, and then Eq. (5.6) follows.

C.2 Rotating Domain Wall of the Neel-Type

These calculations are related to section 5.2.

C.2.1 Spin-Rotation Matrices

The rotation matrices are given by

$$\begin{aligned} u_\phi =& e^{is_z\phi/\hbar} = 1 + i\sigma_z\frac{\phi}{2} - \frac{1}{2}(\frac{\phi}{2})^2 - i\sigma_z\frac{1}{3!}(\frac{\phi}{2})^3 + \cdots = \cos\frac{\phi}{2} + i\sigma_z\sin\frac{\phi}{2} \\ =& \begin{pmatrix} \cos\frac{\phi}{2} + i\sin\frac{\phi}{2} & 0 \\ 0 & \cos\frac{\phi}{2} - i\sin\frac{\phi}{2} \end{pmatrix} = \begin{pmatrix} e^{i\frac{\phi}{2}} & 0 \\ 0 & e^{-i\frac{\phi}{2}} \end{pmatrix}, \end{aligned} \tag{C.8}$$

and the inverse rotation is

$$u_\phi^{-1} = \cos\frac{\phi}{2} - i\sigma_z\sin\frac{\phi}{2}. \tag{C.9}$$

A rotation followed by the inverse rotation gives unity, since $u_\phi^{-1}u_\phi = u_\phi u_\phi^{-1} = \cos^2\frac{\phi}{2} + \sin^2\frac{\phi}{2} = 1$. In the same way the matrices of rotation around the y-axis, $u_\theta = e^{is_y\theta/\hbar}$, is

$$u_\theta = \cos\frac{\theta}{2} + i\sigma_y\sin\frac{\theta}{2} = \begin{pmatrix} \cos\frac{\theta}{2} & \sin\frac{\theta}{2} \\ -\sin\frac{\theta}{2} & \cos\frac{\theta}{2} \end{pmatrix}, \tag{C.10}$$

with the inverse $u_\theta^{-1} = \cos\frac{\theta}{2} - i\sigma_y\sin\frac{\theta}{2}$.

C.2.2 Gauge Transformation

By using that $\psi' = u_\theta u_\phi\psi$ the gauge rotation in section 5.2 is

$$\begin{aligned} i\hbar\frac{\partial\psi'}{\partial t} &= i\hbar\frac{\partial}{\partial t}u_\theta u_\phi\psi = u_\theta u_\phi i\hbar\frac{\partial\psi}{\partial t} + i\hbar u_\theta\frac{\partial u_\phi}{\partial t}\psi = u_\theta u_\phi H\psi + i\hbar u_\theta u_\phi\frac{i}{\hbar}s_z\dot{\phi}\psi \\ &= u_\theta u_\phi\left(\frac{p^2}{2m} + V(\vec{r}) + JM_\mathrm{s}\frac{\hbar}{2}\vec{\sigma}\cdot\vec{m} + \frac{2\mu_\mathrm{B}B_0}{\hbar}s_z - \frac{2\mu_\mathrm{B}B_0}{\hbar}s_z\right)\psi \\ &= u_\theta u_\phi\left(\frac{p^2}{2m} + V(\vec{r}) + JM_\mathrm{s}\frac{\hbar}{2}\vec{\sigma}\cdot\vec{m}\right)u_\phi^{-1}u_\theta^{-1}\psi' \\ &= u_\theta u_\phi\frac{p^2}{2m}u_\phi^{-1}u_\theta^{-1}\psi' + V(\vec{r})\psi' + JM_\mathrm{s}\frac{\hbar}{2}u_\theta u_\phi\vec{\sigma}\cdot\vec{m}u_\phi^{-1}u_\theta^{-1}\psi'. \end{aligned} \tag{C.11}$$

Since ϕ in this case is independent of the spacial derivatives, u_ϕ and its inverse commutes with the $\vec{p}$-operator. Thus

$$\begin{aligned} u_\theta u_\phi p^2 u_\phi^{-1}u_\theta^{-1} &= u_\theta u_\phi u_\phi^{-1}p^2u_\theta^{-1} = u_\theta p^2 e^{is_y'\frac{\theta}{\hbar}} \\ &= u_\theta\left(\frac{\hbar}{i}\frac{\partial}{\partial z}\right)\left(u_\theta^{-1}\frac{\hbar}{i}\frac{\partial}{\partial z} - s_y'\left(\frac{\partial\theta}{\partial z}\right)u_\theta^{-1}\right) \\ &= u_\theta\left(u_\theta^{-1}p^2 - 2s_y'u_\theta^{-1}\left(\frac{\partial\theta}{\partial z}\right)\left(\frac{\hbar}{i}\frac{\partial}{\partial z}\right) - u_\theta^{-1}s_y'\frac{\hbar}{i}\frac{\partial^2\theta}{\partial z^2} + s_y'^2\left(\frac{\partial\theta}{\partial z}\right)^2u_\theta^{-1}\right) \\ &= p^2 - 2s_y'\left(\frac{\partial\theta}{\partial z}\right)p_z - s_y'\frac{\hbar}{i}\frac{\partial^2\theta}{\partial z^2} + s_y'^2\left(\frac{\partial\theta}{\partial z}\right)^2, \end{aligned} \tag{C.12}$$

and if we compare this with $(\vec{p}-(\hbar/2)\vec{A}_t)^2$, inserting $\vec{A}_t = (2/\hbar)s'_y\frac{\partial\theta}{\partial z}\hat{z}$, then

$$\begin{aligned}\left(\vec{p}-\frac{\hbar}{2}\vec{A}_t\right)^2 &= p^2 - \frac{\hbar}{2}\left(\vec{p}\cdot\vec{A}_t + \vec{A}_t\cdot\vec{p}\right) + \left(s'_y\frac{\partial\theta}{\partial z}\right)^2 \\ &= p^2 - \frac{\hbar}{2}\left(\frac{\hbar}{i}\frac{\partial}{\partial z}\frac{2}{\hbar}s'_y\left(\frac{\partial\theta}{\partial z}\right) + \frac{2}{\hbar}s'_y\left(\frac{\partial\theta}{\partial z}\right)\frac{\hbar}{i}\frac{\partial}{\partial z}\right) + s'^2_y\left(\frac{\partial\theta}{\partial z}\right)^2 \\ &= p^2 - 2s'_y\left(\frac{\partial\theta}{\partial z}\right)p_z - s'_y\frac{\hbar}{i}\frac{\partial^2\theta}{\partial z^2} + s'^2_y\left(\frac{\partial\theta}{\partial z}\right)^2, \end{aligned} \tag{C.13}$$

and now Eqs. (C.12) and (C.13) are the same. The last term in Eq. (C.11) is calculated by inserting $\vec{m}$ in terms of the spherical coordinates, then

$$\begin{aligned} u_\theta u_\phi\vec{\sigma}\cdot\vec{m}u_\phi^{-1}u_\theta^{-1} &= \begin{pmatrix}\cos\frac{\theta}{2} & \sin\frac{\theta}{2}\\ -\sin\frac{\theta}{2} & \cos\frac{\theta}{2}\end{pmatrix}\begin{pmatrix}e^{i\frac{\phi}{2}} & 0\\ 0 & e^{-i\frac{\phi}{2}}\end{pmatrix}\begin{pmatrix}\cos\theta & \sin\theta e^{-i\phi}\\ \sin\theta e^{i\phi} & -\cos\theta\end{pmatrix} \\ &\quad \begin{pmatrix}e^{-i\frac{\phi}{2}} & 0\\ 0 & e^{i\frac{\phi}{2}}\end{pmatrix}\begin{pmatrix}\cos\frac{\theta}{2} & -\sin\frac{\theta}{2}\\ \sin\frac{\theta}{2} & \cos\frac{\theta}{2}\end{pmatrix} \\ &= \begin{pmatrix}\cos\frac{\theta}{2}e^{\frac{i\phi}{2}} & \sin\frac{\theta}{2}e^{-i\frac{\phi}{2}}\\ -\sin\frac{\theta}{2}e^{i\frac{\phi}{2}} & \cos\frac{\theta}{2}e^{-\frac{i\phi}{2}}\end{pmatrix}\begin{pmatrix}\cos\theta & \sin\theta e^{-i\phi}\\ \sin\theta e^{i\phi} & -\cos\theta\end{pmatrix}\begin{pmatrix}\cos\frac{\theta}{2}e^{-i\frac{\phi}{2}} & -\sin\frac{\theta}{2}e^{-i\frac{\phi}{2}}\\ \sin\frac{\theta}{2}e^{i\frac{\phi}{2}} & \cos\frac{\theta}{2}e^{i\frac{\phi}{2}}\end{pmatrix} \\ &= \begin{pmatrix}\cos\frac{\theta}{2}e^{\frac{i\phi}{2}} & \sin\frac{\theta}{2}e^{-i\frac{\phi}{2}}\\ -\sin\frac{\theta}{2}e^{i\frac{\phi}{2}} & \cos\frac{\theta}{2}e^{-\frac{i\phi}{2}}\end{pmatrix} \\ &\quad \begin{pmatrix}(\cos\theta\cos\frac{\theta}{2}+\sin\theta\sin\frac{\theta}{2})e^{-\frac{i\phi}{2}} & (-\cos\theta\sin\frac{\theta}{2}+\sin\theta\cos\frac{\theta}{2})e^{-\frac{i\phi}{2}}\\ (\sin\theta\cos\frac{\theta}{2}-\cos\theta\sin\frac{\theta}{2})e^{\frac{i\phi}{2}} & (-\sin\theta\sin\frac{\theta}{2}-\cos\theta\cos\frac{\theta}{2})e^{\frac{i\phi}{2}}\end{pmatrix} \\ &= \begin{pmatrix}\cos\theta(\cos^2\frac{\theta}{2}-\sin^2\frac{\theta}{2})+2\sin\theta\sin\frac{\theta}{2}\cos\frac{\theta}{2} & 0\\ 0 & -\cos\theta(\cos^2\frac{\theta}{2}-\sin^2\frac{\theta}{2})-2\sin\theta\sin\frac{\theta}{2}\cos\frac{\theta}{2}\end{pmatrix} \\ &= \begin{pmatrix}1 & 0\\ 0 & -1\end{pmatrix} = \sigma'_z, \end{aligned} \tag{C.14}$$

such that Eqs. (C.11) and (5.19) correspond to the same Hamiltonian H'.

C.2.3 Expectation Values and the Berry Phase

The expectation value in Eq. (5.13) combined with the rotation matrices in Eqs. (C.8) and (C.10) and spherical coordinates leads to

$$\begin{aligned}
\langle\psi_{m+}|\frac{\partial}{\partial\phi}\psi_{m+}\rangle &= \langle\psi_{m+}|\frac{\partial}{\partial\phi}u_\phi^{-1}u_\theta^{-1}|\psi'_{m+}\rangle \\
&= \langle\chi_+|\frac{\partial}{\partial\phi}\begin{pmatrix} e^{-i\frac{\phi}{2}} & 0 \\ 0 & e^{i\frac{\phi}{2}}\end{pmatrix}\begin{pmatrix}\cos\frac{\theta}{2} & -\sin\frac{\theta}{2} \\ \sin\frac{\theta}{2} & \cos\frac{\theta}{2}\end{pmatrix}\begin{pmatrix}1\\0\end{pmatrix} \\
&= \langle\chi_+|\frac{\partial}{\partial\phi}\begin{pmatrix}\cos(\frac{\theta}{2})e^{-i\frac{\phi}{2}} \\ -\sin(\frac{\theta}{2})e^{i\frac{\phi}{2}}\end{pmatrix} \\
&= -\frac{i}{2}\begin{pmatrix}\cos(\frac{\theta}{2})e^{i\frac{\phi}{2}} & -\sin(\frac{\theta}{2})e^{-i\frac{\phi}{2}}\end{pmatrix}\begin{pmatrix}\cos(\frac{\theta}{2})e^{-i\frac{\phi}{2}} \\ \sin(\frac{\theta}{2})e^{i\frac{\phi}{2}}\end{pmatrix} \\
&= -\frac{i}{2}\left(\cos^2\frac{\theta}{2} - \sin^2\frac{\theta}{2}\right) \\
&= -\frac{i}{2}\cos\theta, \qquad \text{(C.15)}
\end{aligned}$$

and similarly we find

$$\begin{aligned}
\langle\psi_{m-}|\frac{\partial}{\partial\phi}\psi_{m-}\rangle &= \langle\chi_-|\frac{\partial}{\partial\phi}\begin{pmatrix} e^{-i\frac{\phi}{2}} & 0 \\ 0 & e^{i\frac{\phi}{2}}\end{pmatrix}\begin{pmatrix}\cos\frac{\theta}{2} & -\sin\frac{\theta}{2} \\ \sin\frac{\theta}{2} & \cos\frac{\theta}{2}\end{pmatrix}\begin{pmatrix}0\\1\end{pmatrix} \\
&= \langle\chi_-|\frac{\partial}{\partial\phi}\begin{pmatrix}-\sin(\frac{\theta}{2})e^{-i\frac{\phi}{2}} \\ \cos(\frac{\theta}{2})e^{i\frac{\phi}{2}}\end{pmatrix} \\
&= \frac{i}{2}\begin{pmatrix}-\sin(\frac{\theta}{2})e^{i\frac{\phi}{2}} & \cos(\frac{\theta}{2})e^{-i\frac{\phi}{2}}\end{pmatrix}\begin{pmatrix}\sin(\frac{\theta}{2})e^{-i\frac{\phi}{2}} \\ \cos(\frac{\theta}{2})e^{i\frac{\phi}{2}}\end{pmatrix} \\
&= \frac{i}{2}\cos\theta. \qquad \text{(C.16)}
\end{aligned}$$

For the other angle then

$$\begin{aligned}
\langle\psi_{m+}|\frac{\partial}{\partial\theta}\psi_{m+}\rangle &= \langle\chi_+|\frac{\partial}{\partial\theta}\begin{pmatrix}\cos(\frac{\theta}{2})e^{-i\frac{\phi}{2}} \\ -\sin(\frac{\theta}{2})e^{i\frac{\phi}{2}}\end{pmatrix} \\
&= \frac{1}{2}\begin{pmatrix}\cos(\frac{\theta}{2})e^{i\frac{\phi}{2}} & -\sin(\frac{\theta}{2})e^{-i\frac{\phi}{2}}\end{pmatrix}\begin{pmatrix}-\sin(\frac{\theta}{2})e^{-i\frac{\phi}{2}} \\ -\cos(\frac{\theta}{2})e^{i\frac{\phi}{2}}\end{pmatrix} = 0, \qquad \text{(C.17)}
\end{aligned}$$

and

$$\begin{aligned}
\langle\psi_{m-}|\frac{\partial}{\partial\theta}\psi_{m-}\rangle &= \langle\chi_-|\frac{\partial}{\partial\theta}\begin{pmatrix}-\sin(\frac{\theta}{2})e^{-i\frac{\phi}{2}} \\ \cos(\frac{\theta}{2})e^{i\frac{\phi}{2}}\end{pmatrix} \\
&= \frac{1}{2}\begin{pmatrix}-\sin(\frac{\theta}{2})e^{i\frac{\phi}{2}} & \cos(\frac{\theta}{2})e^{-i\frac{\phi}{2}}\end{pmatrix}\begin{pmatrix}-\cos(\frac{\theta}{2})e^{-i\frac{\phi}{2}} \\ -\sin(\frac{\theta}{2})e^{i\frac{\phi}{2}}\end{pmatrix} = 0, \qquad \text{(C.18)}
\end{aligned}$$

and these expectation values satisfies that the Berry phase is real.

D Appendix: Spin-Transport

D.1 Distribution Function for Elastic Scattering

By inserting the ansatz for f_s from Eq. (7.7) into Eq. (7.6) then

$$\left(\frac{\partial f_{\mathrm{FD}}}{\partial \varepsilon_{k,s}}\right)\frac{\cos\theta g_s^{(1)}}{v\tau_{\mathrm{el}}} = \frac{\cos\theta}{2L}\left(f_{\mathrm{FD}}(\varepsilon_{k,s}-\mu_R) - f_{\mathrm{FD}}(\varepsilon_{k,s}-\mu_L)\right) + \left(-\frac{\partial f_{\mathrm{FD}}}{\partial \varepsilon_{k,s}}\right)\left(\cos\theta\frac{\partial g_s^{(0)}}{\partial z} + \cos^2\theta\frac{\partial g_s^{(1)}}{\partial z} - F_{\mathrm{tot}}^s(z)\cos\theta\right). \tag{D.1}$$

It is assumed that $\mu_R - \mu_0 \ll \mu_0$, and then it is possible to approximate the term

$$\begin{aligned} f_{\mathrm{FD}}(\varepsilon_{k,s}-\mu_R) - f_{\mathrm{FD}}(\varepsilon_{k,s}-\mu_L) \approx &-(\mu_R-\mu_0)\frac{\partial f_{\mathrm{FD}}(\varepsilon_{k,s}-\mu_0)}{\partial \varepsilon_{k,s}} \\ &+(\mu_L-\mu_0)\frac{\partial f_{\mathrm{FD}}(\varepsilon_{k,s}-\mu_0)}{\partial \varepsilon_{k,s}} \\ =&\Delta\mu\left(-\frac{\partial f_{\mathrm{FD}}(\varepsilon_{k,s}-\mu_0)}{\partial \varepsilon_{k,s}}\right), \end{aligned} \tag{D.2}$$

such that all terms in Eq. (D.1) are proportional to $\partial f_{\mathrm{FD}}/\partial\varepsilon_{k,s}$.

With the approximation from Eq. (D.2), an integration over k in Eq. (D.1) will give all terms a common factor, and v is replaced with v_{F_s}. This gives

$$-\frac{\cos\theta g_s^{(1)}}{v_{\mathrm{F}_s}\tau_{\mathrm{el}}} = \cos\theta\left(\frac{\Delta\mu}{2L} - F_{\mathrm{tot}}^s(z) + \frac{\partial g_s^{(0)}(z,k)}{\partial z} + \cos\theta\frac{\partial g_s^{(1)}(z,k)}{\partial z}\right). \tag{D.3}$$

By integrating Eq. (D.3) over momentum directions, only the term proportional to $\cos^2\theta$ will be non-zero, since $\int_0^\pi \sin\theta\cos\theta = 0$. This leads to Eq. (7.8).

By multiplying Eq. (D.3) with $\cos\theta$ and then integrating over momentum directions, then Eq. (7.9) follows.

D.1.1 Charge Density for Elastic Scattering

In order to find the charge density, $\rho(z)$, it will be necessary to integrate the spin-motive force in its explicit form given in Eq. (4.19). From the solution for $g_s^{(0)}(z)$

in Eq. (7.11) it follows

$$\begin{aligned}
g_s^{(0)}(z) =& \frac{1}{2}\left(\left(1-\frac{z}{L}\right)\int_{-L}^{L} F_{\mathrm{tot}}^s(z')dz' - 2\int_z^L F_{\mathrm{tot}}^s(z')dz'\right),\\
=& \frac{1}{2}\left(1-\frac{z}{L}\right)\left(\int_{-L}^{L} F_s(z')dz' - e\int_{-L}^{L}\left(-\frac{\partial V}{\partial z'}\right)dz'\right)\\
&- \frac{L}{\lambda_{\mathrm{w}}}F_{\mathrm{av.}}^s\int_z^L \frac{dz'}{\cosh^2\left(\frac{z'-r_{\mathrm{w}}}{\lambda_{\mathrm{w}}}\right)} + e\int_z^L\left(-\frac{\partial V}{\partial z'}\right)dz'\\
=& \frac{1}{2}\left(1-\frac{z}{L}\right)\left(2LF_{\mathrm{av.}}^s + e\Delta V\right) + e\big(V(z)-V(z=L)\big)\\
&+ LF_{\mathrm{av.}}^s\left(\tanh\left(\frac{z-r_{\mathrm{w}}}{\lambda_{\mathrm{w}}}\right) - \tanh\left(\frac{L-r_{\mathrm{w}}}{\lambda_{\mathrm{w}}}\right)\right)\\
=& -e\left(V_R - \frac{1}{2}\left(1-\frac{z}{L}\right)\Delta V - V(z) + E_{\mathrm{av.}}^s L\left(\tanh\left(\frac{z-r_{\mathrm{w}}}{\lambda_{\mathrm{w}}}\right) - \frac{z}{L}\right)\right),
\end{aligned} \tag{D.4}$$

where the term $\tanh(\frac{L-r_{\mathrm{w}}}{\lambda_{\mathrm{w}}}) \approx 1$, since it is assumed that $|L-r_{\mathrm{w}}| \gg \lambda_{\mathrm{w}}$.

The spin-dependent charge density is found by subtracting the positive ions and integrating over all states. By using Eqs. (7.7), (7.13) and (D.4) then

$$\begin{aligned}
\rho_s(z) =& -e\int\frac{d^3k}{(2\pi)^3}(f_s(z,\vec{k}) - f_{\mathrm{FD}}(\varepsilon_{k,s}-\mu_0))\\
=& -e\int\frac{d^3k}{(2\pi)^3}\Bigg(f_{\mathrm{FD}}(\varepsilon_{k,s}-\mu_L) - f_{\mathrm{FD}}(\varepsilon_{k,s}-\mu_0)\\
&+ \frac{1}{2}\left(\frac{z}{L}+1\right)\left(f_{\mathrm{FD}}(\varepsilon_{k,s}-\mu_R) - f_{\mathrm{FD}}(\varepsilon_{k,s}-\mu_L)\right) + g_s^{(0)}(z)\left(-\frac{\partial f_{\mathrm{FD}}(\varepsilon_{k,s}-\mu_0)}{\partial\varepsilon_{k,s}}\right)\Bigg)\\
=& -e\int\frac{d^3k}{(2\pi)^3}\left(-\frac{\partial f_{\mathrm{FD}}(\varepsilon_{k,s}-\mu_0)}{\partial\varepsilon_{k,s}}\right)\left(\mu_L-\mu_0+\frac{1}{2}\left(\frac{z}{L}+1\right)\Delta\mu + g_s^0(z)\right)\\
=& e^2 d_s(\varepsilon_F)\Bigg(V_L + \frac{1}{2}\left(\frac{z}{L}+1\right)\Delta V + V_R - \frac{1}{2}\left(1-\frac{z}{L}\right)\Delta V - V(z)\\
&+ E_{\mathrm{av.}}^s L\left(\tanh\left(\frac{z-r}{\lambda}\right) - \frac{z}{L}\right)\Bigg)\\
=& e^2 d_s(\varepsilon_F)\left(V_L + V_R + \frac{z}{L}\Delta V - V(z) + E_{\mathrm{av.}}^s L\left(\tanh\left(\frac{z-r}{\lambda}\right) - \frac{z}{L}\right)\right),
\end{aligned} \tag{D.5}$$

which is Eq. (7.17).

D.2 Electric Potential in Elastic Scattering

The differential equation for $V(z)$ in Eq. (7.21) is difficult to solve analytically as it stands, but it is possible to solve it in the limit when $l_{\mathrm{TF}} \gg \lambda_{\mathrm{w}} \to 0$. This is done by using the approximation in Eq. (7.28), such that Eq. (7.21) is reduced to

$$V(z) - l_{\mathrm{TF}}^2 \frac{\partial^2 V}{\partial z^2} = V_L + V_R + \Delta V \frac{z}{L} + P_{\mathrm{D}} E_{\mathrm{av}}^+ L\Big(2\theta(z - r_{\mathrm{w}}) - \Big(\frac{z}{L} + 1\Big)\Big). \quad \text{(D.6)}$$

The solution to Eq. (D.6) is

$$\begin{aligned} V(z) =& V_L + V_R + \Delta V \frac{z}{L} - P_{\mathrm{D}} E_{\mathrm{av}}^+ L \left(4\theta(z - r_{\mathrm{w}}) \sinh^2\left(\frac{r_{\mathrm{w}} - z}{2l_{\mathrm{TF}}}\right) + \left(\frac{z}{L} + 1\right)\right) \\ & - \frac{1}{\sinh(\frac{2L}{l_{\mathrm{TF}}})} \Bigg((V_L + V_R - 2P_{\mathrm{D}} E_{\mathrm{av}}^+ L) \cosh\left(\frac{z}{l_{\mathrm{TF}}}\right) \sinh\left(\frac{L}{l_{\mathrm{TF}}}\right) \\ & + (\Delta V - 2P_{\mathrm{D}} E_{\mathrm{av}}^+ L) \cosh\left(\frac{L}{l_{\mathrm{TF}}}\right) \sinh\left(\frac{z}{l_{\mathrm{TF}}}\right) \\ & - 4P_{\mathrm{D}} E_{\mathrm{av}}^+ L \sinh^2\left(\frac{L - r_{\mathrm{w}}}{2l_{\mathrm{TF}}}\right) \sinh\left(\frac{L + z}{l_{\mathrm{TF}}}\right) \Bigg), \end{aligned} \quad \text{(D.7)}$$

which is checked by calculating the derivatives of $V(z)$. The first derivative of Eq. (D.7) is

$$\begin{aligned} l_{\mathrm{TF}} \frac{\partial V}{\partial z} =& \Delta V \frac{l_{\mathrm{TF}}}{L} + P_{\mathrm{D}} E_{\mathrm{av}}^+ L \left(4\theta(z - r_{\mathrm{w}}) \sinh\left(\frac{r_{\mathrm{w}} - z}{2l_{\mathrm{TF}}}\right) \cosh\left(\frac{r_{\mathrm{w}} - z}{2l_{\mathrm{TF}}}\right) - \left(\frac{l_{\mathrm{TF}}}{L}\right)\right) \\ & - \frac{1}{\sinh(\frac{2L}{l_{\mathrm{TF}}})} \Bigg((V_L + V_R - 2P_{\mathrm{D}} E_{\mathrm{av}}^+ L) \sinh\left(\frac{z}{l_{\mathrm{TF}}}\right) \sinh\left(\frac{L}{l_{\mathrm{TF}}}\right) \\ & + (\Delta V - 2P_{\mathrm{D}} E_{\mathrm{av}}^+ L) \cosh\left(\frac{L}{l_{\mathrm{TF}}}\right) \cosh\left(\frac{z}{l_{\mathrm{TF}}}\right) \\ & - 4P_{\mathrm{D}} E_{\mathrm{av}}^+ L \sinh^2\left(\frac{L - r_{\mathrm{w}}}{2l_{\mathrm{TF}}}\right) \cosh\left(\frac{L + z}{l_{\mathrm{TF}}}\right) \Bigg), \end{aligned} \quad \text{(D.8)}$$

and the second derivative is

$$\begin{aligned} l_{\mathrm{TF}}^2 \frac{\partial^2 V}{\partial z^2} =& 4P_{\mathrm{D}} E_{\mathrm{av}}^+ L\theta(z - r_{\mathrm{w}}) \frac{1}{2} \left(-\sinh^2\left(\frac{r_{\mathrm{w}} - z}{2l_{\mathrm{TF}}}\right) - \cosh^2\left(\frac{r_{\mathrm{w}} - z}{2l_{\mathrm{TF}}}\right)\right) \\ & - \frac{1}{\sinh(\frac{2L}{l_{\mathrm{TF}}})} \Bigg((V_L + V_R - 2P_{\mathrm{D}} E_{\mathrm{av}}^+ L) \cosh\left(\frac{z}{l_{\mathrm{TF}}}\right) \sinh\left(\frac{L}{l_{\mathrm{TF}}}\right) \\ & + (\Delta V - 2P_{\mathrm{D}} E_{\mathrm{av}}^+ L) \cosh\left(\frac{L}{l_{\mathrm{TF}}}\right) \sinh\left(\frac{z}{l_{\mathrm{TF}}}\right) \\ & - 4P_{\mathrm{D}} E_{\mathrm{av}}^+ L \sinh^2\left(\frac{L - r_{\mathrm{w}}}{2l_{\mathrm{TF}}}\right) \sinh\left(\frac{L + z}{l_{\mathrm{TF}}}\right) \Bigg). \end{aligned} \quad \text{(D.9)}$$

The solution in Eq. (D.7) is now checked by combining Eqs. (D.7) and (D.9) such that

$$\begin{aligned}
V(z) - l_{\mathrm{TF}}^2 \frac{\partial^2 V}{\partial z^2} =& V_L + V_R + \Delta V \frac{z}{L} \\
& - P_{\mathrm{D}} E_{\mathrm{av}}^{+} L \left(4\theta(z - r_{\mathrm{w}}) \sinh^2 \left(\frac{r_{\mathrm{w}} - z}{2 l_{\mathrm{TF}}} \right) + \left(\frac{z}{L} + 1 \right) \right) \\
& + 2 P_{\mathrm{D}} E_{\mathrm{av}}^{+} L \theta(z - r_{\mathrm{w}}) \left(\sinh^2 \left(\frac{r_{\mathrm{w}} - z}{2 l_{\mathrm{TF}}} \right) + \cosh^2 \left(\frac{r_{\mathrm{w}} - z}{2 l_{\mathrm{TF}}} \right) \right) \\
=& V_L + V_R + \Delta V \frac{z}{L} + P_{\mathrm{D}} E_{\mathrm{av}}^{+} L \Bigg(2\theta(z - r_{\mathrm{w}}) \Bigg(\cosh^2 \left(\frac{r_{\mathrm{w}} - z}{2 l_{\mathrm{TF}}} \right) \\
& - \sinh^2 \left(\frac{r_{\mathrm{w}} - z}{2 l_{\mathrm{TF}}} \right) \Bigg) - \left(\frac{z}{L} + 1 \right) \Bigg) \\
=& V_L + V_R + \Delta V \frac{z}{L} + P_{\mathrm{D}} E_{\mathrm{av}}^{+} L \Big(2\theta(z - r_{\mathrm{w}}) - \left(\frac{z}{L} + 1 \right) \Big), \qquad \text{(D.10)}
\end{aligned}$$

which satisfies the differential Eq. (D.6).

The boundaries for $V(z)$ in Eq. (D.7) is checked by

$$\begin{aligned}
V(z = -L) =& V_L + V_R + \Delta V(-1) \\
& - \frac{1}{\sinh(\frac{2L}{l_{\mathrm{TF}}})} \Bigg((V_L + V_R - 2 P_{\mathrm{D}} E_{\mathrm{av}}^{+} L) \cosh \left(\frac{L}{l_{\mathrm{TF}}} \right) \sinh \left(\frac{L}{l_{\mathrm{TF}}} \right) \\
& + (\Delta V - 2 P_{\mathrm{D}} E_{\mathrm{av}}^{+} L) \cosh \left(\frac{L}{l_{\mathrm{TF}}} \right) \sinh \left(\frac{-L}{l_{\mathrm{TF}}} \right) \\
& - 4 P_{\mathrm{D}} E_{\mathrm{av}}^{+} L \sinh^2 \left(\frac{L - r_{\mathrm{w}}}{2 l_{\mathrm{TF}}} \right) \sinh \left(\frac{L - L}{l_{\mathrm{TF}}} \right) \Bigg) \\
=& 2V_L - \frac{\cosh \left(\frac{L}{l_{\mathrm{TF}}} \right) \sinh \left(\frac{L}{l_{\mathrm{TF}}} \right)}{\sinh(\frac{2L}{l_{\mathrm{TF}}})} (V_L + V_R - \Delta V) \\
=& 2V_L - \frac{1}{2} \cdot 2V_L = V_L, \qquad \text{(D.11)}
\end{aligned}$$

and for the other boundary, $z = L$, then

$$\begin{aligned}
V(z=L) =& V_L + V_R + \Delta V - P_\mathrm{D} E^+_\mathrm{av} L \left(4 \sinh^2 \left(\frac{r_\mathrm{w} - L}{2 l_\mathrm{TF}} \right) + 2 \right) \\
& - \frac{1}{\sinh(\frac{2L}{l_\mathrm{TF}})} \Bigg((V_L + V_R - 2P_\mathrm{D} E^+_\mathrm{av} L) \cosh \left(\frac{L}{l_\mathrm{TF}} \right) \sinh \left(\frac{L}{l_\mathrm{TF}} \right) \\
& + (\Delta V - 2P_\mathrm{D} E^+_\mathrm{av} L) \cosh \left(\frac{L}{l_\mathrm{TF}} \right) \sinh \left(\frac{L}{l_\mathrm{TF}} \right) \\
& - 4P_\mathrm{D} E^+_\mathrm{av} L \sinh^2 \left(\frac{L - r_\mathrm{w}}{2 l_\mathrm{TF}} \right) \sinh \left(\frac{L + L}{l_\mathrm{TF}} \right) \Bigg) \\
=& 2V_R - 2P_\mathrm{D} E^+_\mathrm{av} L - \frac{\cosh \left(\frac{L}{l_\mathrm{TF}} \right) \sinh \left(\frac{L}{l_\mathrm{TF}} \right)}{\sinh(\frac{2L}{l_\mathrm{TF}})} (V_L + V_R + \Delta V - 4P_\mathrm{D} E^+_\mathrm{av} L) \\
=& 2V_R - \frac{1}{2} \cdot 2V_R = V_R,
\end{aligned} \tag{D.12}$$

as required.

D.2.1 Approximate Solution

With the approximations $\sinh(L/l_\mathrm{TF}) \approx \cosh(L/l_\mathrm{TF}) \approx (1/2)\exp(L/l_\mathrm{TF})$ it is possible to write the following term from Eq. (D.7) as

$$\begin{aligned}
& \frac{1}{\sinh(\frac{2L}{l_\mathrm{TF}})} \Bigg((V_L + V_R - 2P_\mathrm{D} E^+_\mathrm{av} L) \cosh \left(\frac{z}{l_\mathrm{TF}} \right) \sinh \left(\frac{L}{l_\mathrm{TF}} \right) \\
& + (\Delta V - 2P_\mathrm{D} E^+_\mathrm{av} L) \cosh \left(\frac{L}{l_\mathrm{TF}} \right) \sinh \left(\frac{z}{l_\mathrm{TF}} \right) \\
& - 4P_\mathrm{D} E^+_\mathrm{av} L \sinh^2 \left(\frac{L - r_\mathrm{w}}{2 l_\mathrm{TF}} \right) \sinh \left(\frac{L + z}{l_\mathrm{TF}} \right) \Bigg) \\
\simeq & 2e^{-\frac{2L}{l_\mathrm{TF}}} \Bigg((V_L + V_R - 2P_\mathrm{D} E^+_\mathrm{av} L) \cosh \left(\frac{z}{l_\mathrm{TF}} \right) \frac{1}{2} e^{\frac{L}{l_\mathrm{TF}}} \\
& + (\Delta V - 2P_\mathrm{D} E^+_\mathrm{av} L) \frac{1}{2} e^{\frac{L}{l_\mathrm{TF}}} \sinh \left(\frac{z}{l_\mathrm{TF}} \right) \\
& - 4P_\mathrm{D} E^+_\mathrm{av} L \sinh^2 \left(\frac{L - r_\mathrm{w}}{2 l_\mathrm{TF}} \right) \frac{1}{2} e^{\frac{L}{l_\mathrm{TF}}} \left(\cosh \left(\frac{z}{l_\mathrm{TF}} \right) + \sinh \left(\frac{z}{l_\mathrm{TF}} \right) \right) \Bigg) \\
= & V_L e^{-\frac{L}{l_\mathrm{TF}}} \left(\cosh \left(\frac{z}{l_\mathrm{TF}} \right) - \sinh \left(\frac{z}{l_\mathrm{TF}} \right) \right) + V_R e^{-\frac{L}{l_\mathrm{TF}}} \left(\cosh \left(\frac{z}{l_\mathrm{TF}} \right) + \sinh \left(\frac{z}{l_\mathrm{TF}} \right) \right) \\
& - 2P_\mathrm{D} E^+_\mathrm{av} L e^{-\frac{L}{l_\mathrm{TF}}} \left(\cosh \left(\frac{z}{l_\mathrm{TF}} \right) + \sinh \left(\frac{z}{l_\mathrm{TF}} \right) + \left(\cosh \left(\frac{L - r_\mathrm{w}}{l_\mathrm{TF}} \right) - 1 \right) e^{\frac{z}{l_\mathrm{TF}}} \right) \\
= & V_L e^{-\frac{L+z}{l_\mathrm{TF}}} + V_R e^{-\frac{L-z}{l_\mathrm{TF}}} - P_\mathrm{D} E^+_\mathrm{av} L e^{\frac{z - r_\mathrm{w}}{l_\mathrm{TF}}}.
\end{aligned} \tag{D.13}$$

By combining the approximations in Eq. (D.13) with Eq. (D.7) the approximate solution for the electric potential, in the limit $l_{\mathrm{TF}} \gg \lambda_{\mathrm{w}} \to 0$, is

$$\begin{aligned} V(z) \simeq & V_L \left(1 - \frac{z}{L} - e^{-\frac{L+z}{l_{\mathrm{TF}}}}\right) + V_R \left(1 + \frac{z}{L} - e^{-\frac{L-z}{l_{\mathrm{TF}}}}\right) \\ & - P_{\mathrm{D}} E_{\mathrm{av}}^{+} L \left(4\theta(z - r_{\mathrm{w}}) \sinh^2 \left(\frac{r_{\mathrm{w}} - z}{2 l_{\mathrm{TF}}}\right) + \frac{z}{L} + 1 - e^{\frac{z - r_{\mathrm{w}}}{l_{\mathrm{TF}}}} \right), \end{aligned} \tag{D.14}$$

which satisfies the solution of Eq. (D.6) and the boundary conditions $V(z = -L) = V_L$ and $V(z = L) = V_R$, under the condition that $L/l_{\mathrm{TF}} \gg 1$. The solution in Eq. (D.14) is checked by calculating the derivatives.

The first derivative of Eq. (D.14) is

$$\begin{aligned} l_{\mathrm{TF}} \frac{\partial V(z)}{\partial z} = & - V_L \left(\frac{l_{\mathrm{TF}}}{L} - e^{-\frac{L+z}{l_{\mathrm{TF}}}}\right) + V_R \left(\frac{l_{\mathrm{TF}}}{L} - e^{-\frac{L+z}{l_{\mathrm{TF}}}}\right) \\ & - P_{\mathrm{D}} E_{\mathrm{av}}^{+} L \left(- 4\theta(z - r_{\mathrm{w}}) \sinh \left(\frac{r_{\mathrm{w}} - z}{2 l_{\mathrm{TF}}}\right) \cosh \left(\frac{r_{\mathrm{w}} - z}{2 l_{\mathrm{TF}}}\right) + \frac{l_{\mathrm{TF}}}{L} - e^{\frac{z - r_{\mathrm{w}}}{l_{\mathrm{TF}}}} \right), \end{aligned} \tag{D.15}$$

and the second derivative of Eq. (D.14) is

$$\begin{aligned} l_{\mathrm{TF}}^2 \frac{\partial^2 V(z)}{\partial z^2} = & - V_L e^{-\frac{L+z}{l_{\mathrm{TF}}}} - V_R e^{-\frac{L-z}{l_{\mathrm{TF}}}} \\ & - P_{\mathrm{D}} E_{\mathrm{av}}^{+} L \left(2\theta(z - r_{\mathrm{w}}) \left(\sinh^2 \left(\frac{r_{\mathrm{w}} - z}{2 l_{\mathrm{TF}}}\right) + \cosh^2 \left(\frac{r_{\mathrm{w}} - z}{2 l_{\mathrm{TF}}}\right) \right) - e^{\frac{z - r_{\mathrm{w}}}{l_{\mathrm{TF}}}} \right). \end{aligned} \tag{D.16}$$

Then Eqs. (D.14) and (D.16) are combined such that

$$\begin{aligned} V(z) - l_{\mathrm{TF}}^2 \frac{\partial^2 V(z)}{\partial z^2} = & V_L + V_R + \Delta V \frac{z}{L} - P_{\mathrm{D}} E_{\mathrm{av}}^{+} L \left(\left(\frac{z}{L} + 1\right) \right. \\ & \left. + 2\theta(z - r_{\mathrm{w}}) \left(\sinh^2 \left(\frac{r_{\mathrm{w}} - z}{2 l_{\mathrm{TF}}}\right) - \cosh^2 \left(\frac{r_{\mathrm{w}} - z}{2 l_{\mathrm{TF}}}\right) \right) \right) \\ = & V_L + V_R + \Delta V \frac{z}{L} + P_{\mathrm{D}} E_{\mathrm{av}}^{+} L \left(2\theta(z - r_{\mathrm{w}}) - \left(\frac{z}{L} + 1\right) \right), \end{aligned} \tag{D.17}$$

which is the same as Eq. (D.6).

The boundaries for $V(z)$ from Eq. (D.14) is checked by inserting $z = -L$, then

$$\begin{aligned} V(z = -L) &= V_L \left(2 - e^{-\frac{L-L}{l_{\mathrm{TF}}}}\right) - V_R e^{-\frac{2L}{l_{\mathrm{TF}}}} + P_{\mathrm{D}} E_{\mathrm{av}}^{+} L e^{-\frac{L + r_{\mathrm{w}}}{l_{\mathrm{TF}}}} \\ &\approx V_L, \end{aligned} \tag{D.18}$$

since $L \pm r_\mathrm{w} \gg l_\mathrm{TF}$. The other boundary at $z = L$ is

$$\begin{aligned} V(z=L) &= -V_L e^{-\frac{2L}{l_\mathrm{TF}}} + V_R - P_\mathrm{D} E^+_\mathrm{av} L \left(4 \sinh^2 \left(\frac{L - r_\mathrm{w}}{2 l_\mathrm{TF}} \right) + 2 - e^{\frac{L-r_\mathrm{w}}{l_\mathrm{TF}}} \right) \\ &\approx V_R - P_\mathrm{D} E^+_\mathrm{av} L \left(\left(e^{\frac{L-r_\mathrm{w}}{2 l_\mathrm{TF}}} - e^{-\frac{L-r_\mathrm{w}}{2 l_\mathrm{TF}}} \right)^2 + 2 - e^{\frac{L-r_\mathrm{w}}{l_\mathrm{TF}}} \right) \\ &= V_R - P_\mathrm{D} E^+_\mathrm{av} L e^{-\frac{L-r_\mathrm{w}}{l_\mathrm{TF}}} \\ &\approx V_R. \end{aligned} \tag{D.19}$$

With the solution for the electric potential given in Eq. (7.30), the total current density is, from Eq. (7.24),

$$j_z(z) = P_\mathrm{C} \sigma E^+_\mathrm{av} - \sigma \frac{V_R - V_L}{L}, \tag{D.20}$$

and the distribution of charges is

$$\begin{aligned} \rho(z) =& e^2 d(\varepsilon_F) \Bigg(V_L e^{-\frac{L+z}{l_\mathrm{tf}}} + V_R e^{-\frac{L-z}{l_\mathrm{tf}}} \\ &+ P_\mathrm{D} E^+_\mathrm{av} L \left(2\theta(z-r) \cosh \left(\frac{r-z}{l_\mathrm{tf}} \right) - e^{\frac{z-r}{l_\mathrm{tf}}} \right) \Bigg). \end{aligned} \tag{D.21}$$

The boundary values for the charge density is thus from Eq. (D.21)

$$\begin{aligned} \rho(z=-L) &= e^2 d(\varepsilon_F) \left(V_L + V_R - \Delta V - V_L + P_\mathrm{D} E^+_\mathrm{av.} L \left(\tanh \left(\frac{-L - r_\mathrm{w}}{\lambda_\mathrm{w}} \right) + 1 \right) \right) \\ &\simeq e^2 d(\varepsilon_F) \Big(V_L + P_\mathrm{D} E^+_\mathrm{av.} L(-1+1) \Big) = e^2 d(\varepsilon_F) V_L, \end{aligned} \tag{D.22}$$

and

$$\begin{aligned} \rho(z=L) &= e^2 d(\varepsilon_F) \left(V_L + V_R + \Delta V - V_R + P_\mathrm{D} E^+_\mathrm{av.} L \left(\tanh \left(\frac{L - r}{\lambda} \right) - 1 \right) \right) \\ &\simeq e^2 d(\varepsilon_F) \Big(V_R + P_\mathrm{D} E^+_\mathrm{av.} L(1-1) \Big) = e^2 d(\varepsilon_F) V_R, \end{aligned} \tag{D.23}$$

and with the boundary conditions that $\rho(z = \pm L) = 0$ the values for the electric potential at the boundaries are $V_L = V_R = 0$.

D.3 Inelastic Scattering

The electron distribution function for inelastic scattering is found by inserting the ansatz for $f_s(z, \vec{k})$ in Eq. (7.33) into the BTE in Eq. (7.34). By using that

$$\frac{\partial f_\mathrm{FD}(\varepsilon_{k,s} - \mu_s(z, \vec{p}))}{\partial z} = \frac{\partial f_\mathrm{FD}}{\partial \varepsilon_{k,s}} \left(-\frac{\partial \mu_s(z)}{\partial z} \right), \tag{D.24}$$

the result for the ansatz is

$$v\cos\theta\left(\frac{\partial f_{\mathrm{FD}}}{\partial\varepsilon_{k,s}}\right)\left(F^s_{\mathrm{tot}}(z)-\frac{\partial\mu_s}{\partial z}+\cos\theta\frac{\partial g^{(1)}_s}{\partial z}\right)=\left(\frac{\partial f_{\mathrm{FD}}}{\partial\varepsilon_{k,s}}\right)\frac{\cos\theta g^{(1)}_s}{\tau_{\mathrm{el}}}. \tag{D.25}$$

Since all terms in Eq. (D.25) are proportional to $\partial f_{\mathrm{FD}}/\partial\varepsilon_{k,s}$, an integration over energy replaces $v\to v_{\mathrm{F}_s}$. By integrating Eq. (D.25) over momentum directions, then $\partial g^{(1)}_s(z,k)/\partial z=0$, which is Eq. (7.35).

A multiplication of Eq. (D.25) by $\cos\theta$ followed by an integration over momentum directions leads to Eq. (7.36).

The general solution for the differential equation for $\mu_s(z)$ in Eq. (7.37) is

$$\begin{aligned}\mu_s(z)=&\mu_L+\frac{1}{2}\left(1+\frac{z}{L}\right)(\mu_R-\mu_L)\\&+\frac{1}{2}\left(\left(1-\frac{z}{L}\right)\int_{-L}^{L}F^s_{\mathrm{tot}}(z')dz'-2\int_z^L F^s_{\mathrm{tot}}(z')dz'\right),\end{aligned} \tag{D.26}$$

which satisfies $\mu_s(z=-L)=\mu_L$ and $\mu_s(z=L)=\mu_R$. The values for $\mu_L=\mu_0-eV_L$ and $\mu_R=\mu_0-eV_R$ are determined by the boundary values for the charge density, $\rho(z)$.

The charge density for spin s is found by using the general solution for $\mu_s(z)$ from Eq. (D.26) and the ansatz for f_s in Eq. (7.33). A first order Taylor expansion of $f_{\mathrm{FD}}(\varepsilon_{k,s}-\mu_s(z))$ is used, since it is assumed that $\mu_s(z)-\mu_0\ll\mu_0$. The charge density is thus

$$\begin{aligned}\rho_s(z)=&-e\int\frac{d^3k}{(2\pi)^3}\left(f_s(z,\vec{p})-f_{\mathrm{FD}}(\varepsilon_{k,s}-\mu_0)\right)\\=&-e\int\frac{d^3k}{(2\pi)^3}\left(-\frac{\partial f_{\mathrm{FD}}}{\partial\varepsilon_{k,s}}\right)(\mu_s(z)-\mu_0)\\=&-ed_s(\varepsilon_F)\Bigg(-eV_L+\frac{1}{2}\left(1+\frac{z}{L}\right)(-e\Delta V)\\&+\frac{1}{2}\left(\left(1-\frac{z}{L}\right)\int_{-L}^{L}F^s_{\mathrm{tot}}(z')dz'-2\int_z^L F^s_{\mathrm{tot}}(z')dz'\right)\Bigg)\\=&e^2d_s(\varepsilon_{\mathrm{F}})\Bigg(V_L+V_R+\frac{z}{L}\Delta V-V(z)\\&+E^s_{\mathrm{av}}(L-z)-\frac{1}{-e}\int_z^L F_s(z')dz'\Bigg),\end{aligned} \tag{D.27}$$

in terms of the electric potential, since $\Delta\mu=-e\Delta V$.

The total charge density consists of contributions from both spins, i.e.

$$\rho(z) = e^2 d(\varepsilon_{\mathrm{F}}) \Bigg(V_L + V_R + \frac{z}{L}\Delta V - V(z) + P_{\mathrm{D}} \Big(E^+_{\mathrm{av}}(L-z) - \frac{1}{-e}\int_z^L F_+(z')dz' \Big) \Bigg), \tag{D.28}$$

with the polarization P_{D} from Eq. (7.20).

The values for V_L and V_R are determined from $\rho(z=-L)=0$ and $\rho(z=L)=0$, by using Eq. (D.28). For the left reservoir

$$\rho(z=-L) = e^2 d(\varepsilon_{\mathrm{F}}) V_L, \tag{D.29}$$

such that $V_L = 0$. For the right reservoir

$$\rho(z=L) = e^2 d(\varepsilon_{\mathrm{F}}) V_R, \tag{D.30}$$

and $V_R = 0$.

The result from Eqs. (D.29) and (D.30) is equivalent with $\mu_L = \mu_R = \mu_0$, such that the reservoirs are at the equilibrium chemical potential. This reduces the general solution for $\mu_s(z)$ in Eq. (D.26) to the solution used in Eq. (7.38).

The electric potential is found from the charge density in Eq. (D.28) with $V_L = V_R = 0$, and by using that $\rho(z)/\epsilon = -\partial^2 V/\partial z^2$. This gives the differential equation

$$\begin{aligned} V(z) - l_{\mathrm{TF}}\frac{\partial^2 V}{\partial z^2} &= P_{\mathrm{D}} E^+_{\mathrm{av}} L \left(1 - \frac{z}{L} + \frac{1}{\lambda_{\mathrm{w}}}\int_L^z \frac{dz'}{\cosh^2\left(\frac{z'-r_{\mathrm{w}}}{\lambda_{\mathrm{w}}}\right)} \right) \\ &= P_{\mathrm{D}} E^+_{\mathrm{av}} L \left(\tanh\left(\frac{z-r_{\mathrm{w}}}{\lambda_{\mathrm{w}}}\right) - \frac{z}{L} \right), \end{aligned} \tag{D.31}$$

by using that $L - r_{\mathrm{w}} \gg \lambda_{\mathrm{w}}$.

The differential equation for the electric potential in Eq. (D.31) is the same differential equation as in the case of elastic scattering in Eq. (7.25). This leads to the same electric potential for inelastic scattering as for the case of elastic scattering.

D.4 Spin-Flip

D.4.1 Useful Integrals

Some useful integrals used in the following are

$$\begin{aligned} \int \frac{d^3k}{(2\pi)^3}\cos^2\theta \left(-\frac{f_{\mathrm{FD}}(\varepsilon_{k,s}-\mu_0)}{\partial \varepsilon_{k,s}} \right) &= d_s(\varepsilon_{\mathrm{F}}) \frac{\int_0^\pi d\theta \sin\theta \cos^2\theta}{\int_0^\pi d\theta \sin\theta} \\ &= \frac{1}{3} d_s(\varepsilon_{\mathrm{F}}), \end{aligned} \tag{D.32}$$

$$\int \frac{d^3k}{(2\pi)^3} v \cos^2\theta \left(-\frac{f_{\mathrm{FD}}(\varepsilon_{k,s}-\mu_0)}{\partial\varepsilon_{k,s}}\right)$$
$$= \frac{1}{(2\pi)^2}\int_0^\pi d\theta \sin\theta\cos^2\theta \int_0^\infty \frac{\hbar k^3}{m} dk\delta\left(\varepsilon_F - \varepsilon_s^0 - \frac{\hbar^2k^2}{2m}\right)$$
$$= \frac{1}{(2\pi)^2}\cdot\frac{2}{3}\int_0^\infty dk \frac{\hbar k^3}{m}\frac{m}{\hbar^2 k}\delta(k-k_{\mathrm{F}_s})$$
$$= \frac{1}{6\pi^2\hbar}k_{\mathrm{F}_s}^2, \tag{D.33}$$

and

$$\int \frac{d^3k}{(2\pi)^3} v^2 \cos^2\theta \left(-\frac{f_{\mathrm{FD}}(\varepsilon_{k,s}-\mu_0)}{\partial\varepsilon_{k,s}}\right) =$$
$$\frac{1}{(2\pi)^2}\int_0^\pi d\theta \sin\theta\cos^2\theta \int_0^\infty \frac{\hbar^2k^4}{m^2} dk\delta\left(\varepsilon_F - \varepsilon_s^0 - \frac{\hbar^2k^2}{2m}\right)$$
$$= \frac{1}{(2\pi)^2}\cdot\frac{2}{3}\int_0^\infty dk \frac{\hbar^2k^4}{m^2}\frac{m}{\hbar^2 k}\delta(k-k_{\mathrm{F}_s})$$
$$= \frac{1}{6\pi^2}\frac{k_{\mathrm{F}_s}^3}{m} = \frac{n_s^0}{m}, \tag{D.34}$$

which will be used to find the electron distribution functions when including spin-flip.

D.4.2 Spin-Flip in the Boltzmann Transport Equation

We include spin-flip in the BTE by introducing the term $(f_s - f_{-s})/\tau_s^{\mathrm{sf}}$ on the RHS of Eq. (7.34), such that the linearized BTE for a steady-state is

$$v_z\frac{\partial f_s}{\partial z} + \vec{F}_{\mathrm{tot}}^s \cdot \frac{\partial f_{\mathrm{FD}}(\varepsilon_{k,s}-\mu_0)}{\partial\vec{p}} = -\frac{f_s - \langle f_s\rangle_{\hat{p}}}{\tau_{\mathrm{el}}} + \frac{f_s - f_{-s}}{\tau_s^{\mathrm{sf}}}, \tag{D.35}$$

with τ_s^{sf} as the spin-flip rate for spin s flipping to spin $-s$.

The solution ansatz for $f_s(z,\vec{k})$ is the same as for inelastic scattering, in Eq. (7.33), i.e.

$$f_s(z,\vec{k}) = f_{\mathrm{FD}}\left(\varepsilon_{k,s}-\mu_s(z)\right) + \left(-\frac{\partial f_{\mathrm{FD}}(\varepsilon_{k,s}-\mu_0)}{\partial\varepsilon_{k,s}}\right)\cos\theta g_s^{(1)}(z,k). \tag{D.36}$$

With f_s from Eq. (D.36) it is necessary to calculate the term

$$f_s - f_{-s} = f_{\mathrm{FD}}(\varepsilon_{k,s}-\mu_s(z)) - f_{\mathrm{FD}}(\varepsilon_{k,-s}-\mu_{-s}(z)) - \frac{\partial f_{\mathrm{FD}}(\varepsilon_{k,s}-\mu_0)}{\partial\varepsilon_{k,s}}\cos\theta g_s^{(1)}$$
$$- \left(-\frac{\partial f_{\mathrm{FD}}(\varepsilon_{k,-s}-\mu_0)}{\partial\varepsilon_{k,-s}}\right)\cos\theta g_{-s}^{(1)}$$
$$\approx f_{\mathrm{FD}}(\varepsilon_{k,s}-\mu_0) - f_{\mathrm{FD}}(\varepsilon_{k,-s}-\mu_0) - \frac{\partial f_{\mathrm{FD}}(\varepsilon_{k,s}-\mu_0)}{\partial\varepsilon_{k,s}}\left(\mu_s(z)-\mu_0+\cos\theta g_s^{(1)}\right)$$
$$- \left(-\frac{\partial f_{\mathrm{FD}}(\varepsilon_{k,-s}-\mu_0)}{\partial\varepsilon_{k,-s}}\right)\left(\mu_{-s}(z)-\mu_0+\cos\theta g_{-s}^{(1)}\right), \tag{D.37}$$

where it is assumed that $\mu_0 \gg \mu_s(z) - \mu_0$.

It is important in the case of spin-flip that the Fermi energy lies at different k_{F_s}, i.e.

$$\frac{\partial f_{\mathrm{FD}}(\varepsilon_{k,s} - \mu_0)}{\partial \varepsilon_{k,s}} \neq \frac{\partial f_{\mathrm{FD}}(\varepsilon_{k,-s} - \mu_0)}{\partial \varepsilon_{k,-s}}, \tag{D.38}$$

such that it is necessary to do the integrations of the BTE over energies explicitly.

By using Eq. (D.37) and inserting f_s from Eq. (D.36) in the BTE in Eq. (D.35) the result is

$$\begin{aligned}
&v\cos\theta\left(-\frac{\partial f_{\mathrm{FD}}}{\partial \varepsilon_{k,s}}\right)\left(\frac{\partial \mu_s}{\partial z} - F^s_{\mathrm{tot}} + \cos\theta\frac{\partial g^{(1)}_s}{\partial z}\right) \\
&\quad = \left(-\frac{\partial f_{\mathrm{FD}}}{\partial \varepsilon_{k,s}}\right)\left(\frac{-\cos\theta g^{(1)}_s}{\tau_{\mathrm{el}}}\right) + \frac{1}{\tau^{\mathrm{sf}}_s}\left(f_{\mathrm{FD}}(\varepsilon_{k,s} - \mu_0) - f_{\mathrm{FD}}(\varepsilon_{k,-s} - \mu_0)\right) \\
&\qquad + \frac{1}{\tau^{\mathrm{sf}}_s}\Bigg(\left(-\frac{\partial f_{\mathrm{FD}}}{\partial \varepsilon_{k,s}}\right)\left(\mu_s(z) - \mu_0 + \cos\theta g^{(1)}_s\right) \\
&\qquad - \left(-\frac{\partial f_{\mathrm{FD}}}{\partial \varepsilon_{k,-s}}\right)\left(\mu_{-s}(z) - \mu_0 + \cos\theta g^{(1)}_{-s}\right)\Bigg).
\end{aligned} \tag{D.39}$$

By using Eqs. (D.33), (2.14) and (2.16), the integration over all momentum vectors, $\int \frac{d^3k}{(2\pi)^3}$, of Eq. (D.39) is

$$\begin{aligned}
\frac{1}{6\pi^2\hbar}k^2_{\mathrm{F}_s}\frac{\partial g^{(1)}_s}{\partial z} =& \frac{1}{\tau^{\mathrm{sf}}_s}\Bigg(\int \frac{d^3k}{(2\pi)^3}\left(f_{\mathrm{FD}}(\varepsilon_{k,s} - \mu_0) - f_{\mathrm{FD}}(\varepsilon_{k,-s} - \mu_0)\right) \\
&+ \int \frac{d^3k}{(2\pi)^3}\left(\left(-\frac{\partial f_{\mathrm{FD}}}{\partial \varepsilon_{k,s}}\right)(\mu_s(z) - \mu_0) - \left(-\frac{\partial f_{\mathrm{FD}}}{\partial \varepsilon_{k,-s}}\right)(\mu_{-s}(z) - \mu_0)\right)\Bigg) \\
=& \frac{1}{\tau^{\mathrm{sf}}_s}\left(n^0_s - n^0_{-s} + d_s(\varepsilon_{\mathrm{F}})(\mu_s(z) - \mu_0) - d_{-s}(\varepsilon_{\mathrm{F}})(\mu_{-s}(z) - \mu_0)\right),
\end{aligned} \tag{D.40}$$

since all terms proportional to $\cos\theta$ integrates to zero.

A multiplication of Eq. (D.39) with $\cos\theta$ and then an integration over all momentum vectors, gives the relation

$$\begin{aligned}
\frac{1}{6\pi^2\hbar}k^2_{\mathrm{F}_s}\left(\frac{\partial \mu_s(z)}{\partial z} - F^s_{\mathrm{tot}}\right) =& \int \frac{d^3k}{(2\pi)^3}\cos^2\theta\Bigg(\left(-\frac{\partial f_{\mathrm{FD}}}{\partial \varepsilon_{k,s}}\right)g^{(1)}_s\left(\frac{1}{\tau^{\mathrm{sf}}_s} - \frac{1}{\tau_{\mathrm{el}}}\right) \\
&- \left(-\frac{\partial f_{\mathrm{FD}}}{\partial \varepsilon_{k,-s}}\right)\frac{g^{(1)}_{-s}}{\tau^{\mathrm{sf}}_s}\Bigg) \\
=& \frac{1}{3}d_s(\varepsilon_{\mathrm{F}})\left(\frac{1}{\tau^{\mathrm{sf}}_s} - \frac{1}{\tau_{\mathrm{el}}}\right)g^{(1)}_s - \frac{1}{3}d_{-s}(\varepsilon_{\mathrm{F}})\frac{g^{(1)}_{-s}}{\tau^{\mathrm{sf}}_s},
\end{aligned} \tag{D.41}$$

by using the integrals in Eqs. (D.32) and (D.33). The calculation to find the full solutions for $\mu_s(z)$ and $\mu_{-s}(z)$ from Eqs. (D.40) and (D.41) would require a lot of algebraic manipulations, since the equations are coupled.

We assume now that the time between spin-flipping scattering events is much longer than the time between elastic scattering events, i.e. $\frac{1}{\tau_{\rm el}} \gg \frac{1}{\tau_s^{\rm sf}}$, where $\tau_s^{\rm sf}$ is a characteristic time for scattering which flips the spin from s to $-s$. By keeping only the lowest order terms in Eq. (D.40) then

$$\frac{\partial g_s^{(1)}}{\partial z} = \frac{3}{\tau_s^{\rm sf} v_{{\rm F}_s}} \left(\mu_s(z) - \frac{d_{-s}(\varepsilon_{\rm F})}{d_s(\varepsilon_{\rm F})} \mu_{-s}(z) \right). \tag{D.42}$$

We further approximate the term $d_{-s}/d_s \sim 1 + \Delta_{\rm ex}/(2\varepsilon_{\rm F}) + \mathcal{O}((\frac{\Delta_{\rm ex}}{2\varepsilon_{\rm F}})^2) \approx 1$. In this approximation Eq. (D.42) reduces to

$$\frac{\partial g_s^{(1)}}{\partial z} \approx \frac{3}{\tau_s^{\rm sf} v_{{\rm F}_s}} (\mu_s(z) - \mu_{-s}(z)). \tag{D.43}$$

By neglecting the terms $\sim \frac{1}{\tau_s^{\rm sf}}$ in Eq. (D.41) it reads

$$\frac{\partial \mu_s(z)}{\partial z} - F_{\rm tot}^s(z) = -\frac{1}{\tau_{\rm el} v_{{\rm F}_s}} g_s^{(1)}. \tag{D.44}$$

We now combine Eq. (D.43) with the spatial derivative of Eq. (D.44) such that

$$\frac{\partial^2 \mu_s(z)}{\partial z^2} = \frac{\partial F_{\rm tot}^s}{\partial z} - \frac{3}{\tau_{\rm el} \tau_s^{\rm sf} v_{{\rm F}_s}^2} (\mu_s(z) - \mu_{-s}(z)), \tag{D.45}$$

which gives the differential equation for the difference between the spin chemical potentials

$$\frac{\partial^2 \left(\mu_s(z) - \mu_{-s}(z) \right)}{\partial z^2} + \frac{1}{\lambda_{\rm sf}^2} \left(\mu_s(z) - \mu_{-s}(z) \right) = \frac{\partial F_s}{\partial z}, \tag{D.46}$$

where we defined the constant

$$\frac{1}{\lambda_{\rm sf}^2} = \frac{3}{\tau_{\rm el}} \left(\frac{1}{\tau_s^{\rm sf} v_{{\rm F}_s}^2} + \frac{1}{\tau_{-s}^{\rm sf} v_{{\rm F}_{-s}}^2} \right). \tag{D.47}$$

A check for the differential equation in Eq. (D.46) is by checking the limit of no spin-flipping scattering events, i.e. when $1/\lambda_{\rm sf}^2 \to 0$ which is equivalent with letting $1/\tau_s^{\rm sf} \to 0$ in Eq. (D.47). In this limit Eq. (D.46) reduces to

$$\frac{\partial^2 \left(\mu_s(z) - \mu_{-s}(z) \right)}{\partial z^2} = \frac{\partial F_s}{\partial z}, \tag{D.48}$$

which is the same as the case of inelastic scattering, with spin chemical potential from the differential Eq. (7.37).